DEVELOPMENT OF ENZYME-BASED BIOSENSORS FOR THE DETECTION OF ORGANOPHOSPHATE NEUROTOXINS

Except where reference is made to the work of others, the work described in this dissertation is my own or was done in collaboration with my advisory committee. This dissertation does not include proprietary, restricted or classified information.

_____

Sheetal Paliwal

Certificate of Approval:

_____	_____
Jeffrey Fergus Associate Professor Materials Engineering	Aleksandr Simonian, Chair Professor Materials Engineering
_____	_____
Barton Prorok Associate Professor Materials Engineering	William Moar Professor Entomology
_____	_____
Vitaly Vodyanoy Professor Anatomy, Physiology and Pharmacology	George T. Flowers Dean Graduate School

DEVELOPMENT OF ENZYME-BASED BIOSENSORS FOR THE DETECTION OF ORGANOPHOSPHATE NEUROTOXINS

Sheetal Paliwal

A Dissertation

Submitted to

the Graduate Faculty of

Auburn University

in Partial Fulfillment of the

Requirements for the

Degree of

Doctor of Philosophy

Auburn, Alabama
December 19, 2008

DEVELOPMENT OF ENZYME-BASED BIOSENSORS FOR THE DETECTION OF ORGANOPHOSPHATE NEUROTOXINS

Sheetal Paliwal

_____
Signature of Author

_____
Date of Graduation

VITA

Sheetal Paliwal, daughter of Sri. Hansraj Paliwal and Smt. Savita Paliwal, was born on March 8, 1980, in Hyderabad, India. She graduated from Ratna Junior College, Hyderabad, India in May 1997. She joined MJCET, Osmania University, Hyderabad, India in November 1997 and graduated with a Bachelor of Engineering in Mechanical Engineering in May 2001. She graduated with a Masters in Industrial Engineering from Arizona State University in May 2003. She joined the doctoral program in Materials Engineering at Auburn University in August 2003 under the guidance of Dr. Simonian. She is married to Sai Vamshidhar Nudurupati, son of Sri. Saibaba Nudurupati and Smt. Sarada Nudurupati.

DISSERTATION ABSTRACT

DEVELOPMENT OF ENZYME-BASED BIOSENSORS FOR THE DETECTION OF ORGANOPHOSPHATE NEUROTOXINS

Sheetal Paliwal

Doctor of Philosophy, December 19, 2008
(M.S, Arizona State University, 2003)
(B.E, MJCET, Osmania University, 2001)

183 Typed pages

Directed by Aleksandr Simonian

Elevated concerns of ecological safety and environmental pollution have facilitated massive research in the area of chemical and biological agent detection. Large numbers of anthropogenic chemicals were introduced in the environment within last 50 years, which posed a serious threat to the natural ecological balance. The series of unfortunate events in the past could have been avoided or minimized by the availability of adequately selective and sensitive detectors, capable of discriminating between common use pesticides and chemical warfare agents. Organophosphates (OPs) in particular are more of a concern because of their toxicity and inhibition of esterase enzymes which are involved in nerve transmission. They have been an integral part of agricultural industry for past decades owing to their specificity. In addition, to their wide usage, they have also been exploited for the development of chemical warfare agents. Consequently, there is an emergent need for rapid and sensitive detection methods.

Enzyme-based studies have been investigated in an effort to develop simple, rapid, user-friendly and sensitive detection of OPs. The methods described have been developed using OPH, an enzyme capable of hydrolyzing OPs. A rapid detection method using a fiber-optic waveguide and a portable fluorimeter Analyte 2000 was developed. Immobilization of OPH was accomplished using avidin-biotin chemistry. Change in fluorescence intensity was observed upon hydrolysis of substrate by OPH, concentration as low as 0.05μM paraoxon (PX) was qualitatively measured. A novel detection method for *p*-nitrophenol and *p*-nitrophenyl substituent OPs based on fluorescence quenching of coumarin1, a dye similar in structure to some OPs have also been developed. Decrease in fluorescence intensity of coumarin1 was proportional to paraoxon concentration in the range of 0.7–170 μM.

To preserve OPH activity and stability, encapsulation using lysozyme-mediated silica nanoparticles was accomplished and detection limit for PX was found to be 20μM. To improve site accessibility and sensor sensitivity, orientation-specific immobilization of OPH was achieved using site-specific antibodies and different variants of OPH. Finally, the potential use of carbon nanotubes for the electrochemical biosensing of OPs has been exploited OPH was covalently immobilized on the surface of these nanotubes and a detection limit of 2.3 μM was obtained for PX. Results demonstrated that the immobilized enzyme retained a significant degree of enzymatic activity, and displayed remarkable stability with only 8% decrease in signal over a period of 10 days.

ACKOWLEDGEMENTS

I would like to express my earnest gratitude to Dr. Aleksandr Simonian for his continuous support and guidance throughout the course of my degree. I would like to acknowledge my committee members, Dr. William Moar, Dr. Jeffrey Fergus, Dr. Vitaly Vodyanoy, and Dr. Bart Prorok for their valuable time and support. My sincere gratitude to Dr. Holly Ellis for acting as an external reader. I would like to extend my special thanks to Maj. Leamon Viveros, who spent effortless hours helping me understand concepts underlying this work and his continued support for all these years. I sincerely acknowledge Dr. James Wild, Dr. Melinda Wales and Dr. Janet Grimsley for providing me the enzyme without which this work was not possible. My nanotube work would not be possible without gracious help from Dr. Dhriti Nepal. Appreciation goes to my entire research group for their help and support. I am deeply indebted to my family, who went far beyond their extremities to provide me with all comforts. I thank them for all the sacrifices they have made and their devotion. The unconditional love and support of my siblings, Richa and Mitrank helped me accomplish this degree. My parents-in law, deserve a special mention for their immense support and affection. Words fail to express my appreciation to my husband, Vamshi whose commitment and persistence have helped me realize my aspirations. His endless love and patience kept me focused and always steered me in right direction. I consider myself fortunate to have him as my life partner. Thanks to one and all. Finally, thanks to Lord Sri Sairam for his grace and blessings.

Style manual or journal used	Sensors and Actuators B
Computer software used	Microsoft Office XP, Endnote X and OriginPro 8.0

TABLE OF CONTENTS

LIST OF TABLES

LIST OF FIGURES

1. INTRODUCTION AND LITERATURE REVIEW

1.1 INTRODUCTION TO BIOSENSORS

A biosensor is an analytical device that recognizes the presence of the species of interest and converts it into an electrical signal. Typically, a biosensor is comprised of three major elements, the target analyte, the biosensing element; which is capable of recognizing the target analyte and finally a transducer which is in close proximity with the biosensing element (Figure 1-1). These devices are capable of rapid and selective detection of any biological or chemical threat agents. Biosensors demonstrate the ability of generating analytical solutions for both laboratory and field testing. These systems find applications in environmental monitoring, food safety, agricultural product safety, biological and chemical warfare, clinical diagnostics, process control and biomedical research to mention a few. These systems must possess several criteria which include but are not limited to:

1. Sensitive and Specific
2. Potential for continuous monitoring
3. Rapid in response
4. Inexpensive
5. User-friendly
6. Stable and reproducible
7. Easy to manufacture

8. Compact and portable

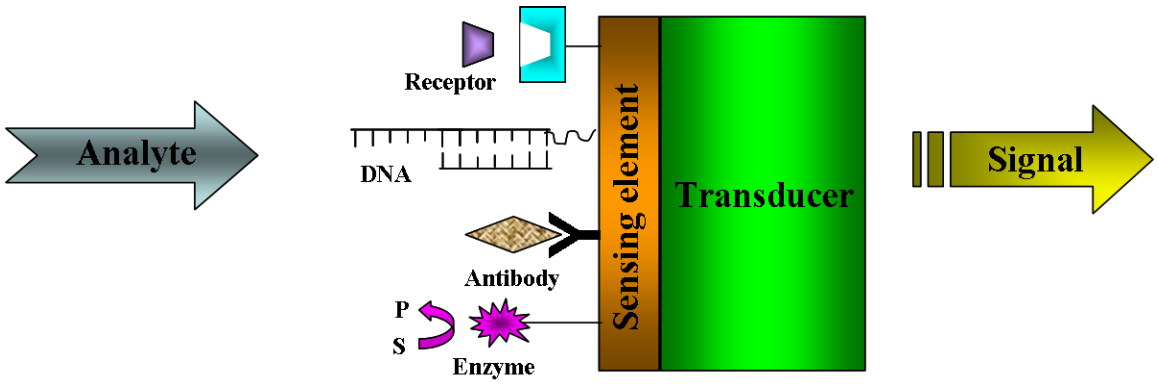

Figure 1-1: Schematic of a biosensor setup

The first biosensor, a glucose sensor was developed by Clark and Lyons in 1962 [1]. Since then there has been enormous advancement in the area of biosensor technology. In this research study, I will be particularly focusing attention on enzyme-based biosensors, wherein the biosensing element is an enzyme that reacts selectively with its substrate.

1.2 CLASSIFICATION OF BIOSENSORS

Biosensors can be classified based on either the biosensing element or the transducer (Figure 1-2). Biosensors based on the biorecognition element can be subdivided into three categories based on their mechanism of action.

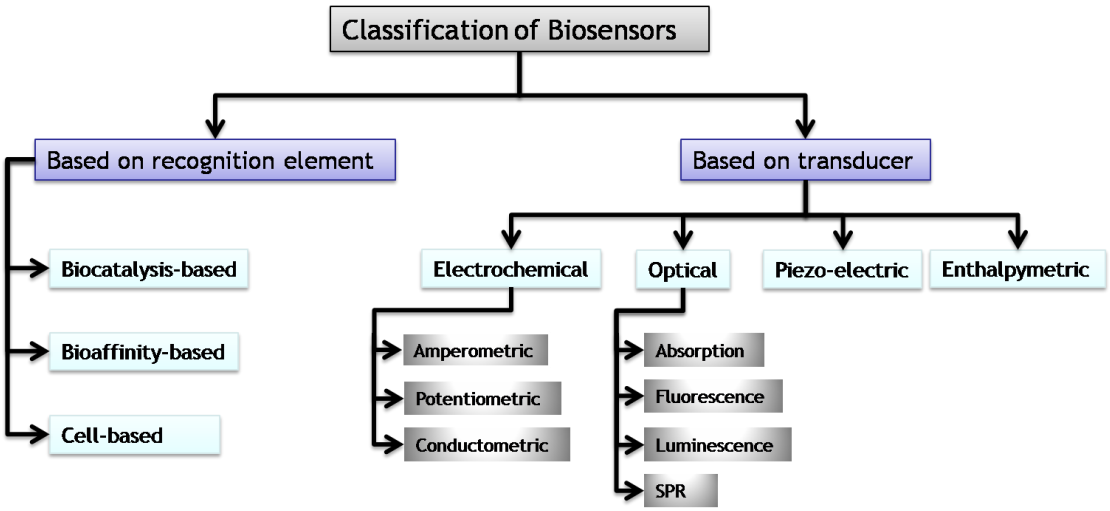

Figure 1-2: Classification of biosensor systems

1.2.1 Biocatalysis-based Biosensors

These biosensors use enzymes as their biosensing element. There are two mechanisms of action for these systems; the first involves the catalytic conversion of the analyte by the enzyme. This catalysis action can be explained using the following equation:

$$S + E \underset{k_{-1}}{\overset{k_1}{\longleftrightarrow}} ES \xrightarrow{k_2} E + P$$

where S = substrate

E = Enzyme

ES = enzyme-substrate complex

P = product

k_1 = rate of enzyme-substrate complex formation

k_{-1} = rate of enzyme-substrate complex dissociation

k_2 = rate of dissociation of enzyme-substrate complex to products

The second mechanism involves detection using the inhibition of the enzymatic activity by the target analyte. The advantage of enzyme-based systems is that they are simple in design and easy to operate.

1.2.2 Bioaffinity-based Biosensors

These biosensors employ antibodies as their biosensing element. The mechanism of action is based on the interaction between an antibody and an antigen. Though these systems are more specific and sensitive than enzyme-based systems, they face limitations in that they are complex and require multi-step assay configurations. The other drawback is the ease of availability and the cost associated with monoclonal antibodies.

1.2.3 Microbe-based Biosensors

These biosensors utilize microorganisms as their biosensing element. Their mechanism is based either on the respiratory or the metabolic functions of the microorganism. These systems are relatively inexpensive and are more susceptible to harsh conditions of pH and temperature than enzyme-based systems.

Biosensors based on the type of transducers can be categorized into four different kinds.

1.2.4 Electrochemical Transducers

1.2.4.1 Potentiometric

These sensors are based on the measurement of potential between the reference electrode and working electrode at zero current. The concentration of the target analyte bears a logarithmic relation with the generated potential. The main advantage of these

transducers is their wider detection limits, however the requirement of a very stable reference electrode have limited their application.

1.2.4.2 Amperometric

These sensors are based detection of the current generated due to the oxidation or reduction of the analyte at the working electrode. The working electrode is maintained at a fixed potential with respect to the reference electrode. The concentration of analyte present in the sample is linearly proportional to the current produced.

1.2.4.3 Conductometric

These sensors are based on the measurement of the change in the electrical conductivity of the solution due to a change in the ionic strength.

1.2.5 Optical Transducers

Optical sensor systems have been the oldest and the most used transducers for biosensor development. These can employ several types of optical biosensors, which are described below.

1.2.5.1 Absorption

These sensors involve the measurement of intensity of absorbed or reflected light. Their principle is based on the Lambert-Beer law, where the absorbance is linearly proportional to the concentration of the analyte present.

1.2.5.2 Fluorescence

These sensors involve the measurement of fluorescence response upon excitation. Some of these systems are based on the principle of total internal reflection (TIR).

1.2.5.3 Luminescence

These sensors involve the measurement of luminescence response upon UV excitation. Two different kinds of luminescence may occur: chemiluminescence, which is determined by a chemical reaction or bioluminescence, determined by living organisms.

1.2.5.4 Surface Plasmon Resonance (SPR)

It is based on the principle of total internal reflection (TIR). SPR occurs at a certain angle of incidence due to the creation of an evanescent wave at the surface. The intensity of light decreases exponentially away from the surface. This particular angle at which TIR occurs is known as the SPR angle and is dependent on the refractive index of the substance. The refractive index near the sensor surface changes when a macromolecule is bound. The change in the refractive index causes a change in the SPR angle which in turn can be correlated to amount of substance bound. The sensor system which will be used for this study is Spreeta™ manufactured by Texas Instruments. It is a fully integrated device which consists of a light-emitting diode, a polarizer, a thermistor and linear photodiode detector array mounted on an integrated circuit. The flow cell is made of Teflon and rubber gaskets are used for sealing. The sensing surface is made of gold and various solutions of different concentrations can be introduced on the surface and a peristaltic pump can be used to control the flow rate.

SPR-based method of detection is simple, fast and sensitive. In addition, the system permits continuous monitoring of the formation of ligand-analyte complex and the dissociation of analyte from immobilized ligand. Other advantages of SPR-based sensing include: no modification to the analyte, allows both qualitative and quantitative analyses, can determine stoichiometry and mechanism of interaction and is highly reproducible. Though it offers a range of merits, SPR sensors have their own demerits such as; dependence of sensitivity on the optical thickness of the adsorbed layer, difficulty in measuring small molecules, measurement of one analyte at a time, generation of artifacts and mass transport effects.

1.2.6 Piezo-electric Transducers

These biosensors are based on the generation of electricity from a vibrating crystal. The oscillating frequency is linearly dependent on the change in mass of adsorbed material at the crystal surface. The crystals are referred to as quartz crystal microbalances (QCM). Some examples of these sensors is the surface acoustic wave (SAW), shear horizontal surface acoustic wave (SH-SAW), thickness shear mode (TSM) and flexure plate wave (FPW) sensors.

1.2.7 Enthalpymetric Transducers

These sensors are also referred to as thermal or calorimetric biosensors. Most of the biochemical reactions involve the generation or absorption of heat. These sensors are based on the measurement of heat which can be related to the amount of analyte present.

1.3 ENZYME

An enzyme is a proteinaceous biological catalyst, capable of accelerating any chemical reaction by converting the target substrate/reactant into specific products (Figure 1-3). The "lock and key" model was introduced by Fisher [2] to understand the action of enzymes. Also, enzymes speed up the rate of chemical reactions because they lower the amount of energy required to activate the reactants (Figure 1-4). These protein molecules display high specificity and do not get utilized in the course of the enzymatic reaction. Therefore, when working with enzymes in solution, it is very difficult to recover the active enzyme from their reaction mixture. The effective way to proceed is to physically secure or immobilize these protein molecules to solid supports.

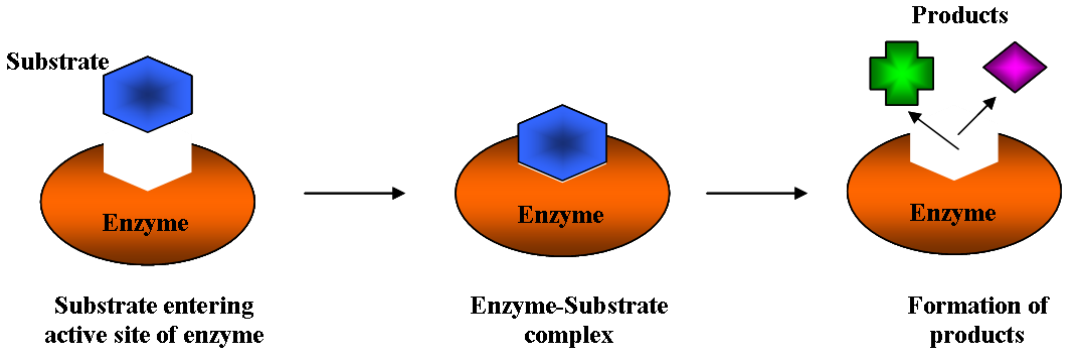

Figure 1-3: Schematic of enzyme action

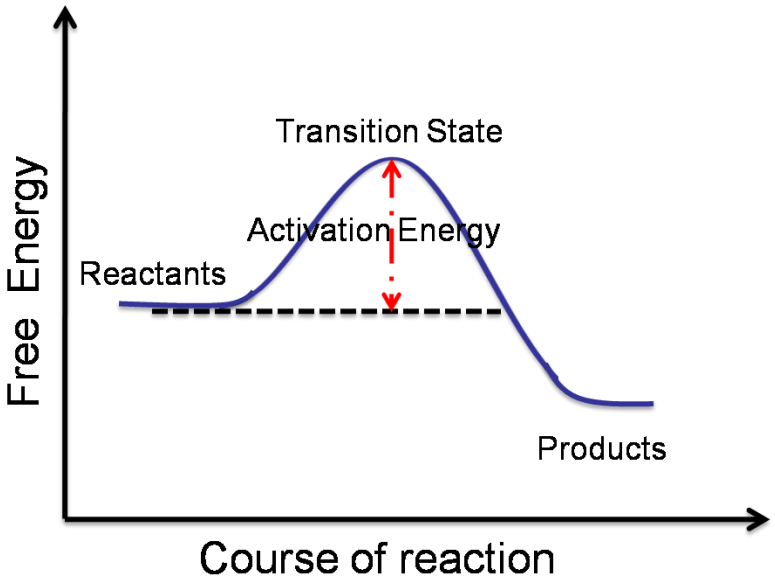

Figure 1-4: Gibbs free energy diagram for an enzymatic reaction

1.4 IMMOBILIZATION OF ENZYMES

For the successful operation of any biosensor it is very important that the sensing element and the transducer are in close contact with each other. Quantitation of the analyte is achieved by coupling the biorecognition element with the transducer. This purpose is served through proper choice of an immobilization technique. Immobilization of an enzyme is a very critical process involved in biosensor design. Some of the advantages of immobilization include: repeated use over time, easier recovery of enzyme, increased enzyme stability, easier separation of product and enzyme and many more. Enzymes undergo changes in both physical and chemical properties during immobilization; therefore, several factors need to be considered for each immobilization method such as the decrease in stability of the enzyme, loss of catalytic activity which can occur due to conformational changes within the enzyme and weak attachment of the enzyme to the solid support. For successful development of biosensors based on

immobilized enzymes, several different approaches have been investigated. Some of the common techniques are discussed below:

1.4.1 Physical adsorption

This is the oldest and the simplest method for enzyme immobilization. The adsorption of the enzyme to the solid support can be either due to electrostatic attraction, hydrophobic interaction, van der Waal's forces or hydrogen bonding [3]. Under suitable conditions of pH and ionic strength, the enzyme is brought in contact with the support. After a brief period of incubation, the surface with the adsorbed enzyme is obtained (Figure 1-5). Unreacted and loosely bound enzyme is removed by extensive washing. Significant amount of binding is observed even though the enzyme is bound to the support through weak interactions. This method of immobilization does not lead to any deactivation of enzyme and is very simple and easy to use. However, since the enzyme is weakly bound to the surface, it can easily exude upon repeated use.

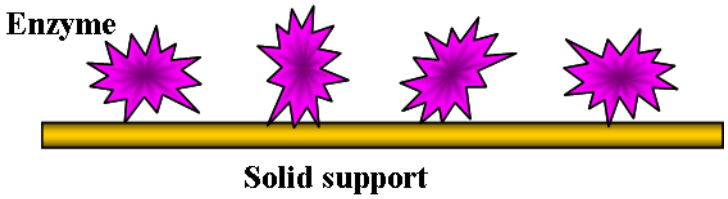

Figure 1-5: Physical binding of enzyme to solid support

1.4.2 Cross linking

Immobilization of enzymes can also be achieved by cross-linking the enzyme, either to other enzyme molecules to form a three dimensional complex or to functional groups on an insoluble support matrix (Figure 1-6). Two most common cross linking techniques that have been frequently used in past and still in use are the avidin-biotin system and crosslinking using gluteraldehyde.

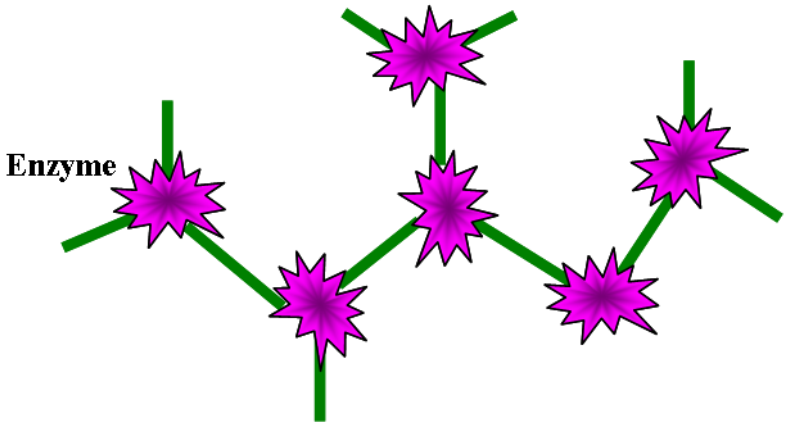

Figure 1-6: Schematic of enzyme immobilization using a crosslinker

1.4.2.1 Avidin-Biotin System

Avidin is a basic glycoprotein found in chicken egg whites. It assumes a tetrameric structure with two-fold symmetry and has four identical subunits connected through disulfide bridges. Its molecular weight can range from 66-69 kDa and the isoelectric point (pI) is approximately 10. This protein is readily soluble in aqueous solutions and is highly stable over a wide pH and temperature ranges. The most characteristic feature of avidin is its ability to form a stable complex with biotin and its derivatives in each subunit. The association constant for the avidin-biotin complex is around 10^{15} M^{-1} at pH 5 (Figure 1-7). Biotin is a naturally occurring vitamin found in

every living cell. It is a small molecule with a molecular weight of 244.31 g/mol. Biotin is comprised of 49.16% carbon, 19.65% oxygen, 13.12% sulfur, 11.47% nitrogen and 6.6% of hydrogen. The molecular formula for biotin is $C_{10}H_{16}N_2O_3S$ and is known by the chemical name cis-hexahydro-2-oxo-1H-thieno[3,4] imidazole-4-pentanoic acid [4].

The exceptionally strong affinity between avidin and biotin is due to the hydrophobic interactions between biotin and the aromatic amino acid residues (tryptophan and phenylalanine) present in the binding pocket of avidin [5]. The avidin-biotin interaction is the strongest non-covalent bond known between a protein and ligand. The bond formation between the two is very rapid and is susceptible to wide ranges of pH, temperature, organic solvents and denaturing agents. The complex is shown to be unaffected by treatments with 8M guanidine.HCl and by pH values in range of 2-13. Neutravidin and streptavidin are two homologous versions of avidin. Neutravidin is the deglycosylated form of avidin whereas streptavidin was isolated from the bacterium *Streptomyces avidinii*. Both have a molecular weight of ~60kDa, isoelectric point (pI) ~6 and have similar binding affinity toward biotin. The key advantage of using streptavidin and neutravidin over avidin is their ability to significantly reduce non-specific interactions.

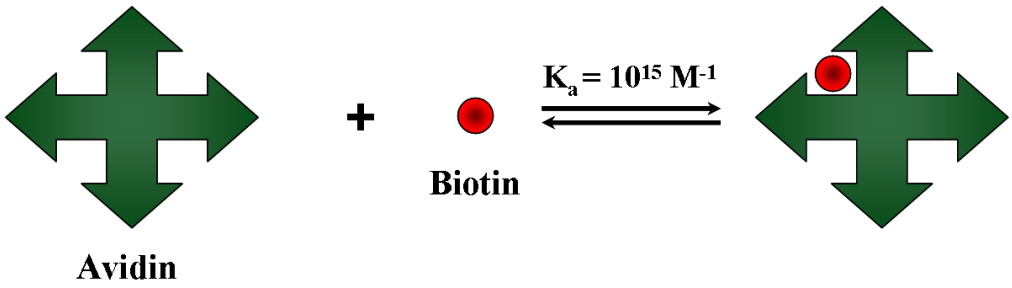

Figure 1-7: Schematic of specific binding between avidin and biotin

1.4.2.2 Crosslinking using gluteraldehyde

The most commonly used cross linking agent for immobilizing enzymes is gluteraldehyde. The aldehyde groups present on gluteraldehyde reacts covalently with the amino groups on the enzyme to form a stable imine linkage.

1.4.3 Covalent immobilization

Covalent attachment to solid supports is the most common and extensively used immobilization method for enzyme-based systems. This attachment is achieved by first activating the surface of the support followed by coupling the enzyme to the activated surface. Any unbound or unreacted enzyme can be removed by washing. The benefit of this method of immobilization is that it provides firm and stable binding of enzyme to the support. Lysine residues are invariably present on most enzyme surfaces and are a common means of covalent attachment. These residues are exposed on the enzyme surface and are the most reactive. Activation of surface of support with carboxyl groups (COOH) can lead to the formation of covalent (peptide) bond between the amine group on the enzyme and the carboxyl group on the support (Figure 1-8). Other reactive groups

present on enzymes, which may be used for chemical binding are the hydroxyl (OH) and sulfhydryl (SH) groups.

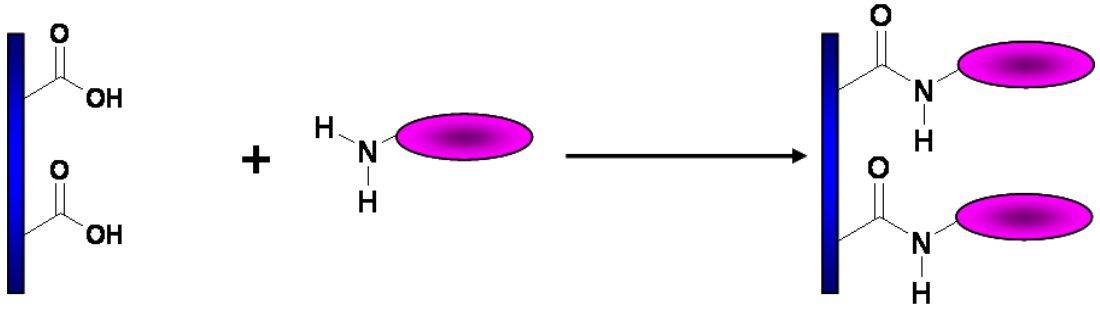

Figure 1-8: Covalent immobilization by amide bond formation

1.4.4 Entrapment

Entrapment is based on confining the enzymes within a polymer matrix, wherein the enzyme is not chemically bound to the gel matrix (Figure 1-9). The most common matrices used for entrapment include polyacrylamide, silicon rubber, polyvinyl alcohol, starch or silica gel [6]. In this immobilization method, the enzyme solution is mixed with a monomer and a cross linking reagent. To start polymerization, a catalyst is added and after a fixed amount of time, the liquid solution starts to form a solid mass. The solid matrix is washed extensively to remove any enzyme that has not been trapped within the gel. The polymer matrix is semi-permeable and allows free passage small molecules but restricts entry of large molecules. The enzyme is properly entrapped and does not diffuse out of the three dimensional structure of the matrix. This is a very simple method for immobilization of any enzyme but the major limitation with this method is that, since the gel pore size is small, large substrates cannot be enzymatically catalyzed. Also, leakage of smaller molecular weight enzymes has been another drawback with these systems [7].

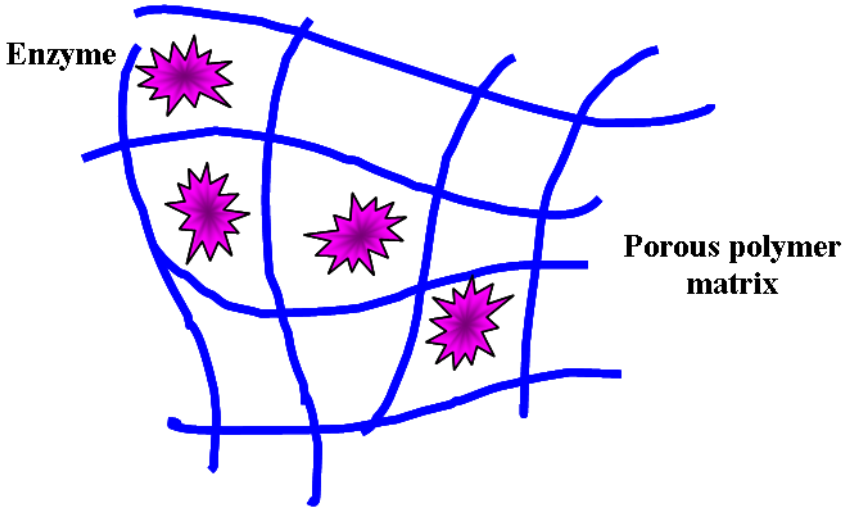

Figure 1-9: Schematic of enzyme entrapped in a porous polymer matrix

1.4.5 Encapsulation

This method of immobilization involves encapsulating the enzymes in a semi-permeable membrane. This immobilization method is very similar to the enzyme entrapment except for the fact that the porosity of the membrane can be controlled [8]. Membrane materials like nylon, epoxy resins, butyl rubber and cellulose nitrate have been reportedly used as support materials. Three different procedures like phase separation (coacervation), interfacial polymerization and liquid drying have been used for encapsulation of enzymes [9].

1.5 BIORECOGNITION ELEMENT - ORGANOPHOSPHORUS HYDROLASE

1.5.1 Enzymes for OP detection

Several enzymes have been utilized for the development of OP detection biosensors. These include acetylcholinesterase (AChE), butyrylcholinesterase (BChE), urease, glucose oxidase (GOx), organophosphorus acid anhydrolase (OPAA) and

organophosphorus hydrolase (OPH). The cholinesterases, urease and GOx have been mostly used in inhibition-based systems [10-14]. Although very sensitive, these systems face limitations with respect to poor specificity, longer incubation times and interference from other substances including heavy metals and carbamates [15-17] . To overcome the drawbacks of the inhibition-based systems, focus has been shifted towards catalytic-based systems based on OPAA (E.C. 3.1.8.2) [18] and OPH (E.C.3.1.8.1) [19]. OPAA is an enzyme capable of effectively detoxifying the P-F bond (G agents) of OPs which includes the two most harmful neurotoxins, sarin and soman [18, 20]. Though highly specific towards G agents, OPAA is not effective towards other class of organophosphates (P-O, P-S and P-CN). In contrast, OPH is a broad range enzyme capable of hydrolyzing P-O, P-F, P-CN, and P-S bonds of organophosphate neurotoxins. This makes OPH the most attractive alternative, as it is capable of hydrolyzing many more OP compounds than OPAA.

1.5.1.1 AChE-based biosensors

Various studies have been reported in the literature which discusses irreversible inhibition of AChE by OPs. The underlying concept of these biosensors is the quantitative measurement of enzyme activity before and after incubation with the OP compound. Almost all of the systems suggested by various researchers either differ in the technique used for enzyme immobilization or the transducer for response measurement. Marty and coworkers [21] used three different approaches for immobilization of AChE and compared their effect on biosensor characteristics and detection limits. The enzyme was also non-covalently incorporated into an amine-derivatized polymer,

polyethyleneimine (PEI) for detection of dichlorvos [22]. AChE-based sensors have been actively applied in areas of food and environmental monitoring. A cost-effective and high sample throughput kit has been designed for the analysis of pesticides in agricultural samples [23]. Disposable screen printed electrodes (SPE) were developed by Dario et al., [24] for the detection of carbaryl and methyl parathion in complex food matrices. AChE has also been used in combination with enzymes such as choline oxidase and BChE for development of OP sensors [25]. In a recent study, quantum dots immobilized with AChE has been described for improved and sensitive electrochemical detection of trichlorfon [26]. Commercial detection kits including the Agri-Screen® Ticket developed by Neogen Corporation [27] and Organophosphate/Carbamate (OP/C) Screen Kit by Abraxis [28] based on cholinesterase inhibition are also available. Rapid and sensitive detection systems have been developed utilizing AChE, however, these systems are single-use and therefore lack selectivity.

1.5.1.2 OPAA-based biosensors

OPAA is a single polypeptide enzyme with a molecular weight of 60kDa [29] and was first isolated from a halophilic bacterial isolate, JD6.5. OPAA demonstrates high catalytic activity towards DFP and has shown to be highly selective towards G-type agents. It has been incorporated into biosensing systems using different approaches. Simonian et al., [20] covalently attached OPAA onto a porous silica gate insulator of a pH-sensitve field effect transistor yielding a highly sensitive system, while, Letant [30] and his team immobilized OPAA onto luminescent porous silicon devices, showing retention of enzymatic activity up to six months. OPAA has also been incorporated into

Langmuir-Blodgett (LB) films for studying the molecular interaction between OPAA and DFP at the air-water interface using techniques such as circular dichroism and fluorescence infrared reflection absorption spectroscopy for sensor applications [31]. Fluorine selective electrodes have also shown to be effective for the detection of these substrates [32]. To prevent exposure from chemical warfare agents, a topical skin protectant containing OPAA was formulated by Braue and coworkers [33].

1.5.1.3 Immuno-based biosensors

Biosensors based on immunosensing have been widely used as an alternative to chromatographic techniques. These sensors are based on the specific interaction between the organophosphate with its respective antibody and have shown to be simple, rapid and highly sensitive. Catalytic antibodies have been increasingly used because of their ability to destroy a pesticide catalytically than just physically binding to it. Vayron et al., [34, 35] synthesized a hapten monoclonal antibody for the detoxification of VX and its less toxic analog phenylphosphonothioate (PhX). Biosensors based on heterogeneous competitive enzyme immunoassay has been developed using anti-carbaryl antibodies labeled with horseradish peroxidase which were assayed both in direct and indirect format with a detection limit of 26ng/L [36]. An immunosensor for soman detection based on the principle of indirect competitive Enzyme Linked Immuno-sorbent Assay (ELISA) with a detection limit of 1.6nM has been developed by Erhard and coworkers [37]. Though proven to be highly sensitive, these sensors face limitations such as irreversible binding, extensive sample handling and difficulty in availability and the cost associated with developing monoclonal antibodies towards specific analytes.

1.5.1.4 OPH-based biosensors

OPH is a 72kDa homodimeric metalloenzyme capable of degrading a large variety of organophosphorus-containing compounds by hydrolyzing the phosphorus-ester bonds between the phosphorus center and an electrophilic leaving group (Figure 1-10). This makes OPH a suitable recognition element for the detection of these substrates. OPH operates near the limits of diffusion with some substrates and can be altered to enhance its specificity towards a variety of OP compounds [19, 38-41].

OPH was first found in *Pseudomonas diminuta*, and then in *Flavobacterium sp.*, both soil microbes [42]. The active site of the homodimeric enzyme contains two divalent metal ions that are vital for its catalytic activity. These metal ions are embedded within a cluster of histidine residues [43]. Each subunit is composed of eight strands of parallel β-pleated sheets in an α, β-barrel structure [44]. The native enzyme contains Zn^{2+} ions but can be replaced with Mn^{2+}, Co^{2+}, Cd^{2+} or Ni^{2+} with altered activity [45]. Replacement of Zn^{2+} ions with Co^{2+} results in an enhanced enzymatic activity, for instance the k_{cat} of the enzyme with Co^{2+} ions for paraoxon is 4700 sec^{-1} in comparison to 2100sec^{-1} for the Zn^{2+} enzyme [46].

The gene encoding OPH, *opd*, has been expressed in various systems including *Escherichia coli* [38], *Drosophila melanogaster* [47], *Streptomyces lividans*, insect cells [48], and many more. It also has been found in a variety of organisms such as squid, protozoa, mammals, yeast, fungi and soil bacteria [42, 47]. OPH is also known as phosphotriesterase, parathion hydrolase, paraoxonase, DFPase, somanase, sarinase, phosphorothiolase and parathion aryl esterase [38, 39]. Upon incubation with chelating agents such as EDTA, 1,10-phenanthroline, and 8-hydroxyquinone-5-sulfonic acid, OPH

loses its catalytic activity. However its activity can be regained upon incubation with a buffer containing Mn^{2+}, Co^{2+}, Cd^{2+} or Ni^{2+} [49]. It has been shown that OPH can retain partial activity (12%) even after interaction with *o*-phenanthroline when dialyzed against a buffer containing 1mM Zn^{2+} [23].

OPH has been studied extensively over the last 15 years [19, 38, 50] and several genetically engineered variants have been produced in an effort to improve its catalytic ability [41, 50]. The variants have been designed to have different catalytic activities for different substrates, and thus, offer potentially additional recognition elements that could lead to an array of biosensors with a capacity to identify and distinguish substrates based on differing selectivity or activity as a part of a decision matrix. Further combination with another enzyme, AChE in the next generation of sensors will allow discrimination between different classes of neurotoxins, organophosphates and carbamates.

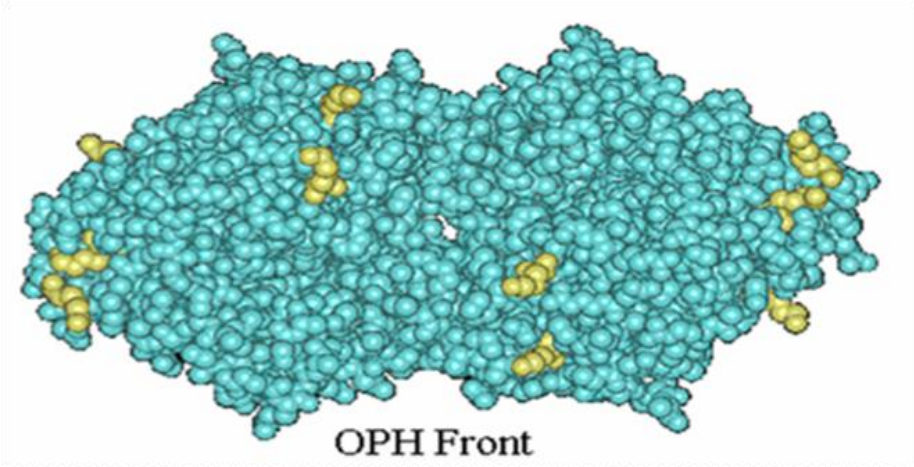

Figure 1-10: Front view of OPH enzyme

To overcome the drawbacks associated with other enzyme systems and for direct detection of organophosphates, immobilized OPH has been widely used. This has been

achieved using a variety of techniques and each technique has helped achieve improved sensor characteristics and lower detection limits. A layer-by layer approach for the construction of highly sensitive biosensors has been described in the literature which involves sandwiching strong positively charged chitosan with weak positively charged OPH between layers of negatively charged (CdSe)ZnS quantum dots [51, 52]. Langmuir-Blodgett deposition technique has been utilized for covalently immobilization of OPH on a silanized quartz slide using diethylthiocarbamoyl chloride (DCC) and finally labeling with a fluorophore for rapid, reproducible and sensitive detection of OPs [53, 54]. To broaden the horizon of sensor applications, discriminative detection of neurotoxins has been attempted by analysis of multi-component samples containing both carbamates and OPs. This was accomplished by integrating AChE and OPH into the system by crosslinking to silanized silica gels and analyzing real-world samples for the presence of these analytes [55].

OPH-based neurotoxin detection methods were pioneered in 1996 in Texas A&M University [56] and were based on the measurement of pH upon OP hydrolysis [17, 57, 58]. Another interesting approach was illustrated by Simonian and co-authors [59] which discusses enhancement or quenching of fluorescence based on the distance between the gold nanoparticle and fluorophore. Here, OPH was labeled with functionalized gold nanoparticles and then incubated with a fluorophore which also happens to be a competitive inhibitor of the enzyme.

For wider applicability and increased substrate specificity, different genetic mutants of OPH have been designed. In one approach, modification of OPH has increased the kinetic efficiency of the enzyme by three orders of magnitude for

detoxification of soman [60], while in another structural change resulted in a 25-fold improved hydrolysis of methyl parathion [61]. To reduce costs associated with enzyme purification and prevent resistance due to mass transfer of analyte, researchers have shown interest in the use of whole cell-based sensors [62, 63]. Chen et al. [64] developed a biosensor using *Moraxella* Sp. that expresses OPH on their cell surface. These cells were introduced on the carbon paste electrode and the sensor system retained enzyme activity for 45 days when placed at 4ºC. To preserve enzymatic activity and protect the enzyme from harsh environments, OPH has been encapsulated or incorporated: in a porous silica matrix using a sol-gel method [65], into a poly(carbamoyl sulfonate) (PCS) prepolymer matrix [66], in pH-sensitve hydrogels [67], and into nafion [68, 69].

Recent advances in the area of carbon nanotechnology have also found potential applications in the area of organophosphate biosensing. Enzyme-modified carbon nanotubes have been incorporated into biosensors for OP detection. OPH was physically adsorbed onto multi-walled carbon nanotubes (MWNT) and the conjugate was deposited onto a glassy carbon electrode using nafion. Detection limits as low as 0.15µM and 0.8µM were observed for paraoxon and methyl parathion respectively [70]. Simultaneous sensing of methanol and OPs has been achieved using OPH/MWNT conjugate incorporated onto graphite-ink screen printed electrodes [71]. OPH has also been integrated into paints and coatings allowing for spontaneous and effective surface decontamination [72]. For efficient wider area decontamination, researchers have also incorporated OPH into fire fighting foams which is known to reduce the volatilization of contaminants [73].

Biosensors for the determination of OP pesticides have been a subject of several reviews. Biosensors based on electrochemical-based enzyme systems have been extensively discussed by Trojanowicz [74] and Anzai [75] while Singh [76] and D'Souza [77] concentrated on the use of microbial organisms for the degradation of these compounds. Since OPH is the most utilized enzyme for direct detection of OPs, Mulchandani et al. [78], have discussed the application of this enzyme for optical, amperometric and potentiometric sensors, and Raushel in his reviews have described the properties and catalytic abilities of OPH [79] and OPAA [80] for the hydrolysis of OP compounds. Martinez [81] have focused his attention on the specific use of screen-printed electrodes for monitoring applications while Dzyadevych et al. [82] reviewed biosensors based on ion-selective field-effect transistors.

Detection of OP's can be an awkward, error-fraught process, as commonly used, gas chromatography equipment are not often available in the field. Furthermore, the present portable equipment is inaccurate and non-specific. As a result of these problems, many studies have investigated novel approaches to try and improve the specificity and the sensitivity of OP detection. It must be recognized that cost, portability and low levels of false positives will be necessary requirements for any new sensor that is to be developed.

1.6 TARGET ANALYTE- ORGANOPHOSPHATES

Organophosphates (OPs) contain a central phosphorus atom with a double bond to sulfur or oxygen, R_1 and R_2 groups that are either ethyl or methyl in structure, and a leaving group which is specific to the individual organophosphate (Figure 1-11). OPs can

be found as part of insecticides, herbicides, and nerve gases. Some less-toxic organophosphates have been used as solvents, plasticizers, and extreme pressure (EP) additives. Due to their toxic nature they have also been exploited for the development of chemical warfare agents including sarin, soman, and O-ethyl-S-[2(diisopropylamino)ethyl] methylphosphonothiolate (VX) (Figure 1-12).

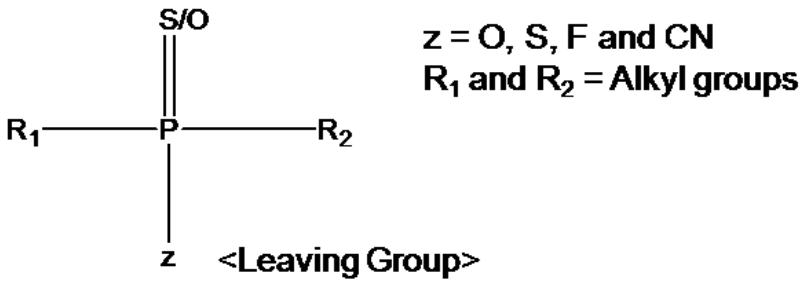

Figure 1-11: General Structure of Organophosphates

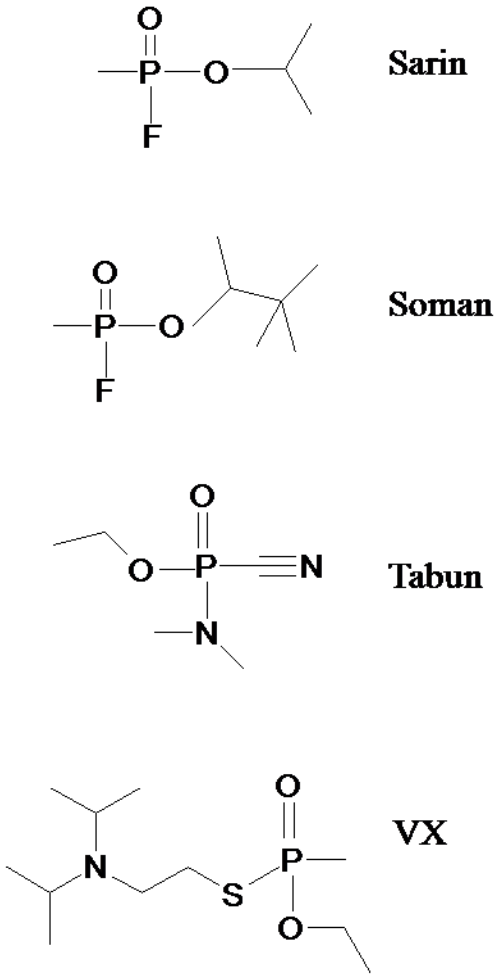

Figure 1-12: Chemical structures of some nerve agents

Commonly used OP pesticides include chlorpyrifos, malathion, guthion, parathion, coumaphos, diazinon, fensulfothion, methyl parathion and cyanophos [83] and their structures are shown in Figure 1-13. Because these compounds pose adverse health threats or injury to non-target organisms when they are used, accurate monitoring of these compounds in different environments is necessary.

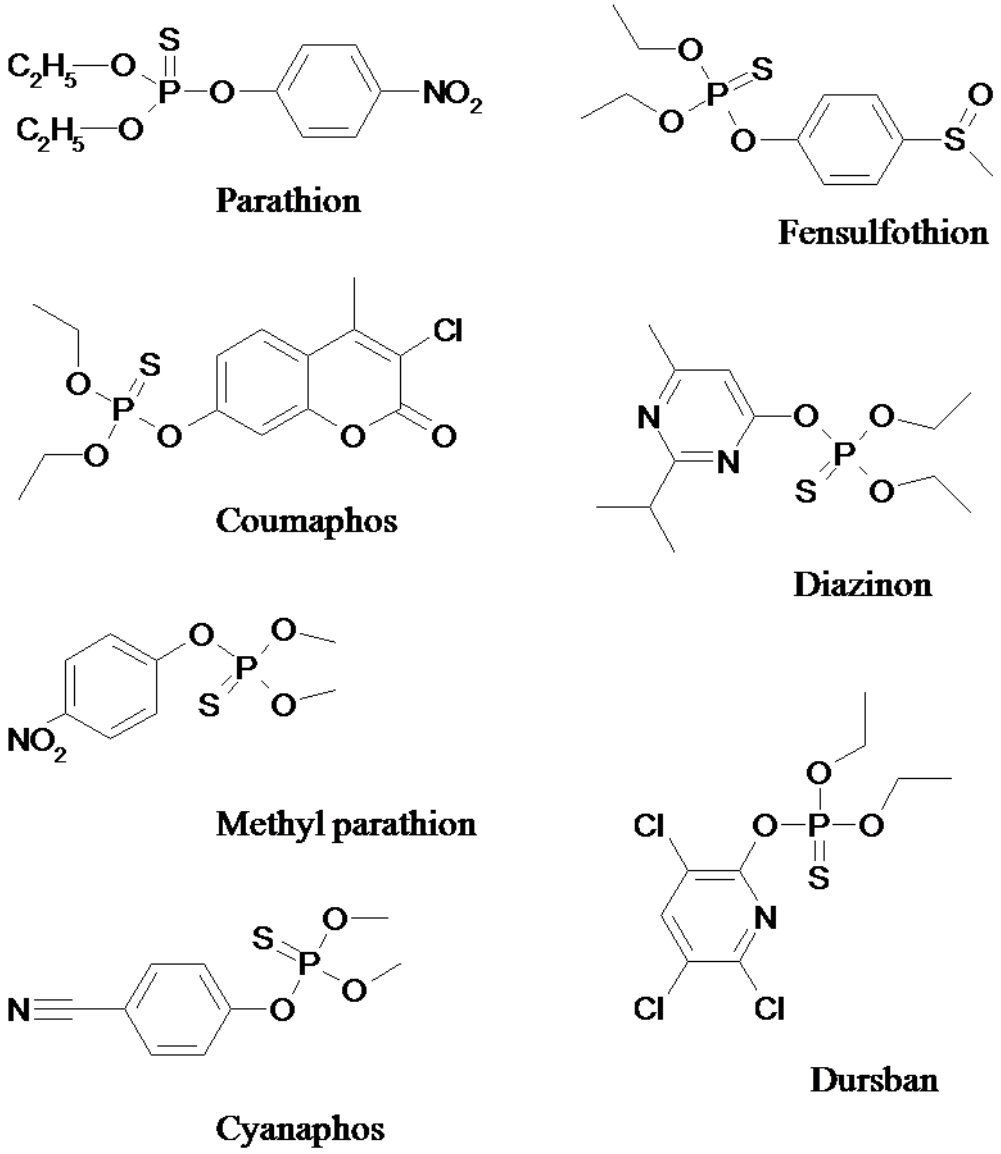

Figure 1-13: Chemical structures of some common organophosphates

1.6.1 Facts about OPs

Each year OPs poison thousands of humans throughout the world, causing hundreds of deaths [84]. Organophosphates were first synthesized in the early 1800s but their mechanism of action was not understood until the 1930s [85]. OPs have achieved enormous commercial success as a key component in the arsenal of agricultural

pesticides and herbicides, and are currently an integral element of modern agriculture.. Accordingly, they are used to control numerous insect pests including moths, ants, cockroaches, termites, fruit flies and similar insects, fleas, locusts, caterpillars and ticks. OPs do not bioaccumulate due to their rapid break down in the environment, have a high catalytic rate and are susceptible to microbial hydrolysis. For this reason, they have been preferred over the more persistent chlorinated hydrocarbons for insecticide/pesticide use. Even though OPs are generally considered safer than the organochlorines and chlorinated hydrocarbons, they can be highly toxic to humans and other mammals and may be carcinogenic [86] . For example, parathion has an oral LD_{50} in rats of about 2–30 mg kg^{-1} which is more toxic than dichloro-diphenyl-trichloroethane (DDT) (oral LD_{50} in rats = 87 mg kg^{-1}) [87]. Also, malathion, one of the earliest and a wide-spectrum OP has an oral LD_{50} of 480 mg kg^{-1} in rats [88]. The wide usage of OP insecticides for agricultural purposes and their presence in water, food and environment presents a potential hazard to non-target organisms. The inherent toxicity of these compounds has posed a major threat for their use. Owing to the toxicity of these compounds, EPA has placed then in the first priority group to be reviewed under the Food Quality Protection Act (FQPA). Approximately 60 million pounds of OP pesticides are applied to 38 million acres of U.S. agricultural crops annually [89]. Nonagricultural use accounts for about 17 million pounds per year, which includes usage such as malathion in the manufacture of flea powders, dichlorvos for polychlorovinyl resin pet collars and pest strips [90]. The amount of OP pesticide usage as a percentage of total insecticide usage has increased from 58% in 1980 to 70% in 2001.

In December 2000, EPA banned the use of diazinon and chlorpyrifos in United States because of health concerns for humans and wildlife. This decision of EPA was greatly influenced by the FQPA, a cumulative risk assessment which evaluates exposure based on the common mechanism of toxicity. However, both OPs were continually used until their stockpiles ran out and they are still known to be legally available for certain uses [91]. Azinphos methyl (trade name: Guthion), one of the most toxic OPs with an oral LD_{50} of 4.4 mg kg^{-1} was ordered to be cancelled for certain uses in 2000 by EPA. This decision was based on the health risks posed by azinphos methyl to farm workers, pesticide applicators and aquatic ecosystems. However, very recently EPA has announced its final decision for a complete phase out of azinphos methyl for all uses by 2012 [92]. Data compiled by the National Water Quality Assessment Program (NAWQA) provides a very good summary of the occurrence and concentrations of all pesticides (including organophosphates) collected from streams, ground water sites, agricultural areas, urban areas and major aquifers [93]. Another study conducted by NAWQA, National Stream Quality Accounting Network (NASQAN) and U.S. Geological Survey (USGS) in U.S. from 1992 to 97 evaluated the occurrence and distribution of 11 OPs in surface and ground water samples. The analysis concluded that OPs (specifically diazinon, chlorpyrifos and malathion) were detected more often and at higher concentrations in surface water than in ground water. Diazinon was the most commonly detected OP in surface water with percent detections ranging from 22 to 100% of samples and chlorpyrifos and malathion from 0 to 91% and 0 to 43%, respectively. Chlorpyrifos was the most widely distributed OP in surface water with concentrations ranging from 0 to 0.3 $\mu g\ L^{-1}$[94].

1.6.2 Toxicology of OPs

OP triesters, phosphonates, phosphonofluoridates and phosphonothioates comprise a broad class of chemical neurotoxins targeting cholinesterases and various neurotoxic esterases. OPs work by inhibiting cholinesterases (ChE), enzymes of the nervous system important for nerve transmission. The enzymes are inhibited by binding to the OP compound which, upon hydrolysis, leaves a stable, phosphorylated and largely unreactive enzyme. This inhibition results in the accumulation of acetylcholine [95] at the neuron/neuron and neuron/muscle (neuromuscular) junctions or synapses, causing headache, rapid twitching of voluntary muscles and abdominal cramps [96, 97]. The severity of the symptoms depends on the degree of acetylcholinesterase inhibition, and the more severe effects include muscle paralysis which can lead to severe difficulty in breathing, and eventually death by respiratory failure. In addition to AChE, OPs inhibit a number of other enzymes, including plasma pseudocholinesterase, neuropathy target esterase (NTE), A-esterases (tissue esterases capable of hydrolyzing OP esters) and carboxy-esterases, as well as other esterases and proteases [98-100].

In addition to the symptoms from acute exposure, long-term exposure to low doses may lead to the development of cancer, genetic diseases, and other dangerous effects [95, 101-103]. Some OP neurotoxins are associated with an organophosphate-induced delayed neurotoxicity (OPIDN) in humans and susceptible species [104, 105]. OPIDN is characterized by distal degeneration of sensory and motor axons that occurs after a delay of about 8–21 days following OP poisoning [106]. Recovery from this complex and poorly understood disease is usually rare and there is no specific treatment.

1.6.3 Hydrolysis of OPs by OPH

In the catalytic process of OPs by OPH, two protons are released during each hydrolysis reaction, and direct neurotoxin detection is thus possible via measurement of the pH change associated with enzyme activity (Figure 1-14). The stoichiometric production of hydrogen ions offers an opportunity to detect the activity of the enzyme on a substrate by the change in pH.

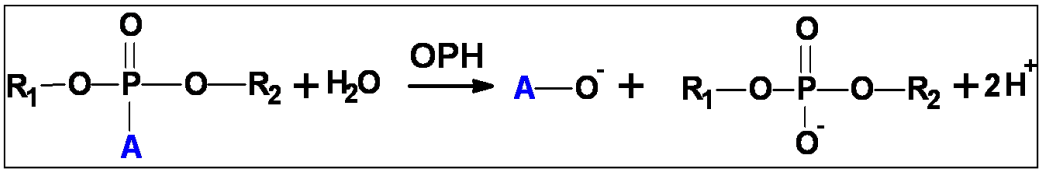

Figure 1-14: Catalytic reaction of OPH. "A" =R O, R S, F or CN leaving group

OPH is capable of hydrolyzing a wide variety of OPs with P-O (phosphotriester), P-S (OP-thioate), P-F (phosphorofluoridates) and P-CN bond cleavage. The OP hydrolysis products are known to have reduced toxicity as compared to their reactants [46]. Hydrolysis of parathion by OPH leads to the formation of two water-soluble products, *p*-nitrophenol and diethylthiophosphoric acid which can be readily degraded by microbial enzymes [107]. This hydrolysis reduces the toxicity of parathion by 120-fold and the resultant metabolites can be further exploited by other microorganisms as a source of carbon, energy and phosphorus [108].

OPH has been shown to hydrolyze OPs such as parathion, coumaphos, orthene, DFP, sarin, malathion, demeton-S, VX, acephate, soman, tabun, mipafox, diazinon, tetriso (analogue of VX), 4-nitrophenyl ethyl phenyl phosphinate (NPEPP). Paraoxon has shown to be the fastest and the best substrate of OPH with a k_{cat} of 2100 sec^{-1} [44, 109] and demeton-S, a poor substrate with a k_{cat} of 1.2 sec^{-1} [39].

Lewis et al. [110] described three possible mechanisms for hydrolysis of organophosphates by OPH. In the actual hydrolysis reaction mechanism, during the interaction of an OP with the enzyme, a base at the active site activates a water molecule which attacks the phosphorus atom of the substrate yielding the degraded metabolites. Hydrolysis of organophosphates with P-O bond results in the formation of *p*-nitrophenol, which has an absorption maximum between 400-405 nm. Hydrolysis of organophosphates with P-S bond results in the formation of free thiol groups which can be characterized using Ellman's reagent, 5,5'-Dithio-(bis-2-nitrobenzoic acid) (DTNB). The free thiol groups upon reaction with DTNB form a chromogenic product 5'-thiol-2-nitrobenzoate anions. This product has an absorption maximum between 405-420 nm and an extinction coefficient of 13,600 $M^{-1}cm^{-1}$ at pH 7.2.

Previously a suggested method for disposal of OP pesticides was chemical hydrolysis by sodium hydroxide. Other methods for the treatment of pesticide waste involved the use of whole cells. However these methods proved to be unproductive because the cells could be easily subjected to chemical shock, overloading, catabolite repression or metabolite inhibition [111]. Therefore, improved and reliable methods need to be developed for detoxification of these pesticides and their empty containers so as to minimize their adverse effect on the environment. Owing to their high toxicity and because of their constant use as pesticides in agriculture, there is an increasing need for an effective biosensor system capable of selective detection.

1.7 REFERENCES

1. L.C. Clark and C. Lyons, Electrode Systems for Continuous Monitoring in Cardiovascular Surgery, Annals of the New York Academy of Sciences 102 (1962) pp. 29-45.
2. C.E. Ophardt, Role of Enzymes in Biochemical Reactions, Available from: http://www.elmhurst.edu/~chm/vchembook/571lockkey.html.
3. M.M.F. Choi, Progress in Enzyme-Based Biosensors Using Optical Transducers, Microchimica Acta 148 (2004) pp. 107-132.
4. Pierce, Avidin-Biotin Chemistry: A Handbook, Available from: http://www.piercenet.com/Objects/View.cfm?ID=E82B5AEB-A192-4548-83BF-9229E3397C6C&type=Page.
5. V.C.-M. Yang and T.T. Ngo, Biosensors and Their Applications, Springer, 2000.
6. P.W. Carr and L.D. Bowers, Immobilized Enzymes in Analytical and Clinical Chemistry: Fundamentals and Applications, John Wiley & Sons, New York, 1980.
7. J.M. Engasser and C. Horvath, Applied Biochemistry and Bioengineering (Immobilized Enzyme Principles), vol. 1, Academic Press, New York, 1976.
8. F.X. Hasselberger, Uses of Enzymes and Immobilized Enzymes, Nelson Hall, 1978.
9. R.F. Taylor, Protein Immobilization: Fundamentals and Applications, Marcel Dekker Inc, 1991.

10. H.Y. No, Y.A. Kim, Y.T. Lee, and H.S. Lee, Cholinesterase-Based Dipstick Assay for the Detection of Organophosphate and Carbamate Pesticides, Analytica Chimica Acta 594 (2007) pp. 37-43.

11. S.V. Dzyadevych, V.N. Arkhypova, C. Martelet, N. Jaffrezic-Renault, J.M. Chovelon, A.V. El'skaya, and A.P. Soldatkin, Potentiometric Biosensors Based on Isfets and Immobilised Cholinesterases, International Journal of Applied Electromagnetics and Mechanics 23 (2006) pp. 229-244.

12. P. Skladal, Detection of Organophosphate and Carbamate Pesticides Using Disposable Biosensors Based on Chemically Modified Electrodes and Immobilized Cholinesterase, Analytica Chimica Acta 269 (1992) pp. 281-287.

13. R.B. Shi and K. Stein, Flow Injection Analysis of Paraoxon with the Use of an Immobilized Acetylcholinesterase Reactor, Analytica Chimica Acta 324 (1996) pp. 21-27.

14. N.A. Pchelintsev and P.A. Millner, A Novel Procedure for Rapid Surface Functionalisation and Mediator Loading of Screen-Printed Carbon Electrodes, Analytica Chimica Acta 612 (2008) pp. 190-197.

15. S. Xu, A. Wu, H. Chen, Y. Xie, Y. Xu, L. Zhang, J. Li, and D. Zhang, Production of a Novel Recombinant Drosophila Melanogaster Acetylcholinesterase for Detection of Organophosphate and Carbamate Insecticide Residues, Biomolecular Engineering 24 (2007) pp. 253-261.

16. A.L. Simonian, B.D. diSioudi, and J.R. Wild, An Enzyme Based Biosensor for the Direct Determination of Diisopropyl Fluorophosphate, Analytica Chimica Acta 389 (1999) pp. 189-196.

17. A.W. Flounders, A.K. Singh, J.V. Volponi, S.C. Carichner, K. Wally, A.S. Simonian, J.R. Wild, and J.S. Schoeniger, Development of Sensors for Direct Detection of Organophosphates.: Part Ii: Sol-Gel Modified Field Effect Transistor with Immobilized Organophosphate Hydrolase, Biosensors and Bioelectronics 14 (1999) pp. 715-722.

18. T.C. Cheng and J.J. Calomiris, A Cloned Bacterial Enzyme for Nerve Agent Decontamination, Enzyme and Microbial Technology 18 (1996) pp. 597-601.

19. D.P. Dumas, H.D. Durst, W.G. Landis, F.M. Raushel, and J.R. Wild, Inactivation of Organophosphorus Nerve Agents by the Phosphotriesterase from Pseudomonas-Diminuta, Archives of Biochemistry and Biophysics 277 (1990) pp. 155-159.

20. A.L. Simonian, J.K. Grimsley, A.W. Flounders, J.S. Schoeniger, T.C. Cheng, J.J. DeFrank, and J.R. Wild, Enzyme-Based Biosensor for the Direct Detection of Fluorine-Containing Organophosphates, Analytica Chimica Acta 442 (2001) pp. 15-23.

21. S. Andreescu, L. Barthelmebs, and J.L. Marty, Immobilization of Acetylcholinesterase on Screen-Printed Electrodes: Comparative Study between Three Immobilization Methods and Applications to the Detection of Organophosphorus Insecticides, Analytica Chimica Acta 464 (2002) pp. 171-180.

22. A. Vakurov, C.E. Simpson, C.L. Daly, T.D. Gibson, and P.A. Millner, Acetylcholinesterase-Based Biosensor Electrodes for Organophosphate Pesticide Detection I. Modification of Carbon Surface for Immobilization of Acetylcholinesterase, Biosensors & Bioelectronics 20 (2004) pp. 1118-1125.

23. B.M. Kim, A.M.A. El-Aty, T.E. Hwang, L.T. Jin, Y.S. Kim, and J.H. Shim, Development of an Acetylcholinesterase-Based Detection Kit for the Determination of Organophosphorus and Carbamate Pesticide Residues in Agricultural Samples, Bulletin of the Korean Chemical Society 28 (2007) pp. 929-935.

24. M. Del Carlo, M. Mascini, A. Pepe, G. Diletti, and D. Compagnone, Screening of Food Samples for Carbamate and Organophosphate Pesticides Using an Electrochemical Bioassay, Food Chemistry 84 (2004) pp. 651-656.

25. G. Palleschi, M. Bernabei, C. Cremisini, and M. Mascini, Determination of Organophosphorus Insecticides with a Choline Electrochemical Biosensor, Sensors and Actuators B-Chemical 7 (1992) pp. 513-517.

26. X.H. Li, Z.H. Xie, H. Min, C.X. Li, M.C. Liu, Y.Z. Xian, and L.T. Jin, Development of Quantum Dots Modified Acety1cholinesterase Biosensor for the Detection of Trichlorfon, Electroanalysis 18 (2006) pp. 2163-2167.

27. N. Corporation, Available from: http://www.neogen.com/FoodSafety/AS_Index.asp.

28. Abraxis, Available from: http://www.abraxiskits.com/product_pesticides.htm.

29. J.J. Defrank and T.C. Cheng, Purification and Properties of an Organophosphorus Acid Anhydrase from a Halophilic Bacterial Isolate, Journal of Bacteriology 173 (1991) pp. 1938-1943.

30. S.E. Letant, S.R. Kane, B.R. Hart, M.Z. Hadi, T.C. Cheng, V.K. Rastogi, and J.G. Reynolds, Hydrolysis of Acetylcholinesterase Inhibitors - Organophosphorus

Acid Anhydrolase Enzyme Immobilization on Photoluminescent Porous Silicon Platforms, Chemical Communications (2005) pp. 851-853.

31. J.Y. Zheng, C.A. Constantine, L. Zhao, V.K. Rastogi, T.C. Cheng, J.J. DeFrank, and R.M. Leblanc, Molecular Interaction between Organophosphorus Acid Anhydrolase and Diisopropylfluorophosphate, Biomacromolecules 6 (2005) pp. 1555-1560.

32. S.C. Kim and N.T. Lee, Detoxification of Sarin, an Acetylcholinesterase Inhibitor, by Recombinant Organophosphorus Acid Anhydrolase, Journal of Biochemistry and Molecular Biology 34 (2001) pp. 440-445.

33. E.H. Braue Jr., S.T. Hobson, C. Govardhan, and N. Khalaf, Active Topical Skin Protectants Containing Opaa Enzymes and Clecs (2002) Available from: http://www.freepatentsonline.com/6410604.html.

34. P. Vayron, P.Y. Renard, F. Taran, C. Creminon, Y. Frobert, J. Grassi, and C. Mioskowski, Toward Antibody-Catalyzed Hydrolysis of Organophosphorus Poisons, Proceedings of the National Academy of Sciences of the United States of America 97 (2000) pp. 7058-7063.

35. P. Vayron, P.Y. Renard, A. Valleix, and C. Mioskowski, Design and Synthesis of an Alpha,Alpha-Difluorophosphinate Hapten for Antibody-Catalyzed Hydrolysis of Organophosphorus Nerve Agents, Chemistry-a European Journal 6 (2000) pp. 1050-1063.

36. M.A. GonzalezMartinez, S. Morais, R. Puchades, A. Maquieira, A. Abad, and A. Montoya, Monoclonal Antibody-Based Flow-through Immunosensor for Analysis of Carbaryl, Analytical Chemistry 69 (1997) pp. 2812-2818.

37. M.H. Erhard, A. Jungling, T. Schoneberg, L. Szinicz, and U. Losch, A Homogeneous Immunological Detection System for Soman Using the Invitro Protection of Acetylcholinesterase by a Monoclonal-Antibody, Archives of Toxicology 67 (1993) pp. 220-223.

38. C.S. McDaniel, L.L. Harper, and J.R. Wild, Cloning and Sequencing of a Plasmid-Borne Gene (Opd) Encoding a Phosphotriesterase, Journal of Bacteriology 170 (1988) pp. 2306-2311.

39. K. Lai, N.J. Stolowich, and J.R. Wild, Characterization of P-S Bond Hydrolysis in Organophosphorothioate Pesticides by Organophosphorus Hydrolase, Archives of Biochemistry and Biophysics 318 (1995) pp. 59-64.

40. D.P. Dumas, J.R. Wild, and F.M. Raushel, Diisopropylfluorophosphate Hydrolysis by a Phosphotriesterase from Pseudomonas-Diminuta, Biotechnology and Applied Biochemistry 11 (1989) pp. 235-243.

41. B.D. Di Sioudi, C.E. Miller, K.H. Lai, J.K. Grimsley, and J.R. Wild, Rational Design of Organophosphorus Hydrolase for Altered Substrate Specificities, Chemico-Biological Interactions 120 (1999) pp. 211-223.

42. S.R. Caldwell, J.R. Newcomb, K.A. Schlecht, and F.M. Raushel, Limits of Diffusion in the Hydrolysis of Substrates by the Phosphotriesterase from Pseudomonas-Diminuta, Biochemistry 30 (1991) pp. 7438-7444.

43. S.B. Hong and F.M. Raushel, Metal-Substrate Interactions Facilitate the Catalytic Activity of the Bacterial Phosphotriesterase, Biochemistry 35 (1996) pp. 10904-10912.

44. J.M. Kuo, M.Y. Chae, and F.M. Raushel, Perturbations to the Active Site of Phosphotriesterase, Biochemistry 36 (1997) pp. 1982-1988.

45. M.Y. Chae, G.A. Omburo, P.A. Lindahl, and F.M. Raushel, Antiferromagnetic Coupling in the Binuclear Metal Cluster of Managanese-Substituted Phosphotriesterase, Journal of the American Chemical Society 115 (1993) pp. 12173-12174.

46. K.H. Lai, K.I. Dave, and J.R. Wild, Bimetallic Binding Motifs in Organophosphorus Hydrolase Are Important for Catalysis and Structural Organization, Journal of Biological Chemistry 269 (1994) pp. 16579-16584.

47. J.P. Phillips, J.H. Xin, K. Kirby, C.P. Milne, P. Krell, and J.R. Wild, Transfer and Expression of an Organophosphate Insecticide-Degrading Gene from Pseudomonas in Drosophila-Melanogaster, Proceedings of the National Academy of Sciences of the United States of America 87 (1990) pp. 8155-8159.

48. G.A. Omburo, J.M. Kuo, L.S. Mullins, and F.M. Raushel, Characterization of the Zinc-Binding Site of Bacterial Phosphotriesterase, Journal of Biological Chemistry 267 (1992) pp. 13278-13283.

49. M.M. Benning, J.M. Kuo, F.M. Raushel, and H.M. Holden, Three Dimensional Structure of Phosphotriesterase - an Enzyme Capable of Detoxifying Organophosphate Nerve Agents, Biochemistry 33 (1994) pp. 15001-15007.

50. K.H. Lai, J.K. Grimsley, B.D. Kuhlmann, L. Scapozza, S.P. Harvey, J.J. DeFrank, J.E. Kolakowski, and J.R. Wild, Rational Enzyme Design: Computer Modeling and Site-Directed Mutagenesis for the Modification of Catalytic Specificity in Organophosphorus Hydrolase, Chimia 50 (1996) pp. 430-431.

51. X.J. Ji, J.Y. Zheng, J.M. Xu, V.K. Rastogi, T.C. Cheng, J.J. DeFrank, and R.M. Leblanc, (Cdse)Zns Quantum Dots and Organophosphorus Hydrolase Bioconjugate as Biosensors for Detection of Paraoxon, Journal of Physical Chemistry B 109 (2005) pp. 3793-3799.

52. C.A. Constantine, K.M. Gattas-Asfura, S.V. Mello, G. Crespo, V. Rastogi, T.C. Cheng, J.J. DeFrank, and R.M. Leblanc, Layer-by-Layer Biosensor Assembly Incorporating Functionalized Quantum Dots, Langmuir 19 (2003) pp. 9863-9867.

53. J. Orbulescu, C.A. Constantine, V.K. Rastogi, S.S. Shah, J.J. DeFrank, and R.M. Leblanc, Covalent Immobilization of Organophosphorus Hydrolase for Detection of Toxic Organophosphorus Compounds, Analytical Chemistry 78 (2006) pp. 7016-7021.

54. X.H. Cao, S.V. Mello, R.M. Leblanc, V.K. Rastogi, T.C. Cheng, and J.J. DeFrank, Detection of Paraoxon by Immobilized Organophosphorus Hydrolase in a Langmuir-Blodgett Film, Colloids and Surfaces a-Physicochemical and Engineering Aspects 250 (2004) pp. 349-356.

55. A.L. Simonian, E.N. Efremenko, and J.R. Wild, Discriminative Detection of Neurotoxins in Multi-Component Samples, Analytica Chimica Acta 444 (2001) pp. 179-186.

56. E.I. Rainina, E.N. Efremenco, S.D. Varfolomeyev, A.L. Simonian, and J.R. Wild, The Development of a New Biosensor Based on Recombinant E-Coli for the Direct Detection of Organophosphorus Neurotoxins, Biosensors & Bioelectronics 11 (1996) pp. 991-1000.

57. M.J. Schoning, M. Arzdorf, P. Mulchandani, W. Chen, and A. Mulchandani, A Capacitive Field-Effect Sensor for the Direct Determination of Organophosphorus Pesticides, Sensors and Actuators B-Chemical 91 (2003) pp. 92-97.

58. A.L. Simonian, A.W. Flounders, and J.R. Wild, Fet-Based Biosensors for the Direct Detection of Organophosphate Neurotoxins, Electroanalysis 16 (2004) pp. 1896-1906.

59. A.L. Simonian, T.A. Good, S.S. Wang, and J.R. Wild, Nanoparticle-Based Optical Biosensors for the Direct Detection of Organophosphate Chemical Warfare Agents and Pesticides, Analytica Chimica Acta 534 (2005) pp. 69-77.

60. C.M.H. Cho, A. Mulchandani, and W. Chen, Altering the Substrate Specificity of Organophosphorus Hydrolase for Enhanced Hydrolysis of Chlorpyrifos, Applied and Environmental Microbiology 70 (2004) pp. 4681-4685.

61. C.M.H. Cho, A. Mulchandani, and W. Chen, Functional Analysis of Organophosphorus Hydrolase Variants with High Degradation Activity Towards Organophosphate Pesticides, Protein Engineering Design & Selection 19 (2006) pp. 99-105.

62. A. Mulchandani, I. Kaneva, and W. Chen, Biosensor for Direct Determination of Organophosphate Nerve Agents Using Recombinant Escherichia Coli with Surface-Expressed Organophosphorus Hydrolase. 2. Fiber Optic Microbial Biosensor, Analytical Chemistry 70 (1998) pp. 5042-5046.

63. A. Mulchandani, P. Mulchandani, S. Chauhan, I. Kaneva, and W. Chen, A Potentiometric Microbial Biosensor for Direct Determination of Organophosphate Nerve Agents, Electroanalysis 10 (1998) pp. 733-737.

64. P. Mulchandani, W. Chen, A. Mulchandani, J. Wang, and L. Chen, Amperometric Microbial Biosensor for Direct Determination of Organophosphate Pesticides Using Recombinant Microorganism with Surface Expressed Organophosphorus Hydrolase, Biosensors & Bioelectronics 16 (2001) pp. 433-437.

65. D. Yu, J. Volponi, S. Chhabra, C.J. Brinker, A. Mulchandani, and A.K. Singh, Aqueous Sol-Gel Encapsulation of Genetically Engineered Moraxella Spp. Cells for the Detection of Organophosphates, Biosensors & Bioelectronics 20 (2005) pp. 1433-1437.

66. S. Gaberlein, F. Spener, and C. Zaborosch, Microbial and Cytoplasmic Membrane-Based Potentiometric Biosensors for Direct Determination of Organophosphorus Insecticides, Applied Microbiology and Biotechnology 54 (2000) pp. 652-658.

67. M. Zourob, K.G. Ong, K.F. Zeng, F. Mouffouk, and C.A. Grimes, A Wireless Magnetoelastic Biosensor for the Direct Detection of Organophosphorus Pesticides, Analyst 132 (2007) pp. 338-343.

68. A. Mulchandani, P. Mulchandani, W. Chen, J. Wang, and L. Chen, Amperometric Thick Film Strip Electrodes for Monitoring Organophosphate Nerve Agents Based on Immobilized Organophosphorus Hydrolase, Analytical Chemistry 71 (1999) pp. 2246-2249.

69. C.H. Lei, M.M. Valenta, K.P. Saripalli, and E.J. Ackerman, Biosensing Paraoxon in Simulated Environmental Samples by Immobilized Organophosphorus Hydrolase in Functionalized Mesoporous Silica, Journal of Environmental Quality 36 (2007) pp. 233-238.

70. R.P. Deo, J. Wang, I. Block, A. Mulchandani, K.A. Joshi, M. Trojanowicz, F. Scholz, W. Chen, and Y.H. Lin, Determination of Organophosphate Pesticides at a Carbon Nanotube/Organophosphorus Hydrolase Electrochemical Biosensor, Analytica Chimica Acta 530 (2005) pp. 185-189.

71. M. Trojanowicz, A. Mulchandani, and M. Mascini, Carbon Nanotubes-Modified Screen-Printed Electrodes for Chemical Sensors and Biosensors, Analytical Letters 37 (2004) pp. 3185-3204.

72. C.S. McDaniel, J. McDaniel, M.E. Wales, and J.R. Wild, Enzyme-Based Additives for Paints and Coatings, Progress in Organic Coatings 55 (2006) pp. 182-188.

73. K.E. LeJeune and A.J. Russell, Biocatalytic Nerve Agent Detoxification in Fire Fighting Foams, Biotechnology and Bioengineering 62 (1999) pp. 659-665.

74. M. Trojanowicz, Determination of Pesticides Using Electrochemical Enzymatic Biosensors, Electroanalysis 14 (2002) pp. 1311-1328.

75. J.I. Anzai, Use of Biosensors for Detecting Organophosphorus Agents, Yakugaku Zasshi-Journal of the Pharmaceutical Society of Japan 126 (2006) pp. 1301-1308.

76. B.K. Singh and A. Walker, Microbial Degradation of Organophosphorus Compounds, Fems Microbiology Reviews 30 (2006) pp. 428-471.

77. S.F. D'Souza, Microbial Biosensors, Biosensors and Bioelectronics 16 (2001) pp. 337-353.

78. A. Mulchandani, W. Chen, P. Mulchandani, J. Wang, and K.R. Rogers, Biosensors for Direct Determination of Organophosphate Pesticides, Biosensors & Bioelectronics 16 (2001) pp. 225-230.

79. E. Ghanem and F.M. Raushel, Detoxification of Organophosphate Nerve Agents by Bacterial Phosphotriesterase, Toxicology and Applied Pharmacology 207 (2005) pp. 459-470.

80. F.M. Raushel, Bacterial Detoxification of Organophosphate Nerve Agents, Current Opinion in Microbiology 5 (2002) pp. 288-295.

81. O.D. Renedo, M.A. Alonso-Lomillo, and M.J.A. Martínez, Recent Developments in the Field of Screen-Printed Electrodes and Their Related Applications, Talanta 73 (2007) pp. 202-219.

82. S.V. Dzyadevych, A.P. Soldatkin, A.V. El'skaya, C. Martelet, and N. Jaffrezic-Renault, Enzyme Biosensors Based on Ion-Selective Field-Effect Transistors, Analytica Chimica Acta 568 (2006) pp. 248-258.

83. D.P. Dumas, S.R. Caldwell, J.R. Wild, and F.M. Raushel, Purification and Properties of the Phosphotriesterase from Pseudomonas-Diminuta, Journal of Biological Chemistry 264 (1989) pp. 19659-19665.

84. C.S. Rao, V. Venkateswarlu, T. Surender, M. Eddleston, and N.A. Buckley, Pesticide Poisoning in South India: Opportunities for Prevention and Improved Medical Management, Tropical Medicine & International Health 10 (2005) pp. 581-588.

85. K.D. Katz, Toxicity, Organophosphate, Available from: http://www.emedicine.com/med/byname/Toxicity--Organophosphate.htm.

86. G.A.H.C. Chemical Terms, Available from: http://frontierassoc.net/greenaffordablehousing/Tools/ChemicalTerms.shtml.

87. Insecticides, Available from: http://users.rcn.com/jkimball.ma.ultranet/BiologyPages/I/Insecticides.html.

88. Extension Toxicology Network, Malathion, Available from: http://pmep.cce.cornell.edu/profiles/extoxnet/haloxyfop-methylparathion/malathion-ext.html.

89. Center for Disease Control and Prevention, Report on Organophosphate Pesticides: Dialkyl Phosphate Metabolites, Available from: http://www.cdc.gov.

90. G.W. Ware, The Pesticide Book Thomson Publications 1993.

91. W. Foshee, Pest-Control Knowledge: More Important Than Ever Before, Available from: http://www.aces.edu/dept/extcomm/newspaper/diazinon.html.

92. E.P. Agency, Azinphos-Methyl Phaseout, Available from: http://www.epa.gov/pesticides/reregistration/azm/phaseout_fs.htm.

93. Pesticides in Surface and Ground Water of the United States: Summary of Results of the National Water Quality Assessment Program (Nawqa), Available from: http://ca.water.usgs.gov.

94. E.H. Hopkins, D.J. Hippe, E.A. Frick, and G.R. Buell, Organophosphorus Pesticide Occurence and Distribution in Surface and Ground Water of the United States, Available from: http://ga.water.usgs.gov/publications/ofr00-187.pdf.

95. R. Stephens, A. Spurgeon, I.A. Calvert, J. Beach, L.S. Levy, J.M. Harrington, and H. Berry, Neuropsychological Effects of Long-Term Exposure to Organophosphates in Sheep Dip, The Lancet 345 (1995) pp. 1135-1139.

96. C. Smulders, T.J.H. Bueters, S. Vailati, R. van Kleef, and H.P.M. Vijverberg, Block of Neuronal Nicotinic Acetylcholine Receptors by Organophosphate Insecticides, Toxicological Sciences 82 (2004) pp. 545-554.

97. F.M. Dyro, Organophosphates, Available from: www.emedicine.com.

98. J.E. Chambers and S.F. Oppenheimer, Organophosphates, Serine Esterase Inhibition, and Modeling of Organophosphate Toxicity, Toxicological Sciences 77 (2004) pp. 185-187.

99. E.B. Sener, E. Ustun, S. Kocamanoglu, and A. Tur, Prolonged Apnea Following Succinylcholine Administration in Undiagnosed Acute Organophosphate Poisoning, Acta Anaesthesiologica Scandinavica 46 (2002) pp. 1046-1048.

100. Extoxnet, Report on Cholinesterase Inhibition, Toxicology Information Briefs, Available from: http://extoxnet.orst.edu/tibs/cholines.htm.

101. B. Eskenazi, A. Bradman, and R. Castorina, Exposures of Children to Organophosphate Pesticides and Their Potential Adverse Health Effects, Environmental Health Perspectives 107 (1999) pp. 409-419.

102. G.A. Jamal, S. Hansen, and P.O.O. Julu, Low Level Exposures to Organophosphorus Esters May Cause Neurotoxicity, Toxicology 181-182 (2002) pp. 23-33.

103. Pesticide Action Network Uk, Organophosphate Insecticides, Available from: http://www.pan-uk.org.

104. M.A. Brown and K.A. Brix, Review of Health Consequences from High-, Intermediate- and Low-Level Exposure to Organophosphorus Nerve Agents, Journal of Applied Toxicology 18 (1998) pp. 393-408.

105. C.N. Pope, D. Tanaka, and S. Padilla, The Role of Neurotoxic Esterase (Nte) in the Prevention and Potentiation of Organophosphorus-Induced Delayed Neurotoxicity (Opidn), Chemico-Biological Interactions 87 (1993) pp. 395-406.

106. C.N. Pope, M.L. Chapman, D. Tanaka, and S. Padilla, Phenylmethylsulfonyl Fluoride Alters Sensitivity to Organophosphorus-Induced Delayed Neurotoxicity in Developing Animals, Neurotoxicology 13 (1992) pp. 355-364.

107. W.W. Mulbry, J.S. Karns, P.C. Kearney, J.O. Nelson, C.S. McDaniel, and J.R. Wild, Identification of a Plasmid-Borne Parathion Hydrolase Gene from Flavobacterium Sp by Southern Hybridization with Opd from Pseudomonas-Diminuta, Applied and Environmental Microbiology 51 (1986) pp. 926-930.

108. C.M. Serdar, D.T. Gibson, D.M. Munnecke, and J.H. Lancaster, Plasmid Involvement in Parathion Hydrolysis by Pseudomonas-Diminuta, Applied and Environmental Microbiology 44 (1982) pp. 246-249.

109. D.P. Dumas and F.M. Raushel, Chemical and Kinetic Evidence for an Essential Histidine in the Phosphotriesterase from Pseudomonas-Diminuta, Journal of Biological Chemistry 265 (1990) pp. 21498-21503.

110. V.E. Lewis, W.J. Donarski, J.R. Wild, and F.M. Raushel, Mechanism and Stereochemical Course at Phosphorus of the Reaction Catalyzed by a Bacterial Phosphotriesterase, Biochemistry 27 (1988) pp. 1591-1597.

111. D.M. Munnecke, Enzymatic-Hydrolysis of Organophosphate Insecticides, a Possible Pesticide Disposal Method, Applied and Environmental Microbiology 32 (1976) pp. 7-13.

2. RESEARCH OBJECTIVES

The primary objective of this research was to develop methods for the detection of OPs. Numerous analytical advances have been made in the area of biosensors for the detection of organophosphates. But the drawbacks associated with these techniques, demands an urgent need for an improved biosensor system. The proposed biosensor addresses those drawbacks and an improvement to the existing detection technologies. New detection strategies and biomaterials have been developed for improved future analytical applications. Several different detection platforms have been suggested in this research. The specific goal was to develop a system that is capable of:

- Faster response time
- Selective detection of organophosphates
- High sensitivity of detection
- Easy to use and inexpensive system

This dissertation deals in particular, with the development of enzyme-based biosensors for the detection of neurotoxic compounds. OPH was used as the biorecognition element for all biosensor systems. Paraoxon has been used as a model substrate for all analysis. Application of these sensors for detection of other substrates has also been investigated. Development and evaluation of methodologies such as immobilization and encapsulation of proteins and the modification of surfaces has been attempted in the following work and is strongly related to advance biomaterials

development which directly influences the research and development for model systems, biosensors and smart devices. The major objectives of this research were:

1. To develop simple, rapid and sensitive sensor platforms for the detection of neurotoxic OPs
2. To optimize the factors associated with enzyme immobilization, which includes but are not limited to, the retention of enzymatic activity and stability upon immobilization

2.1 DISSERTATION ORGANIZATION

Biosensor development is a multidisciplinary effort and requires performance of experiments in different areas such as biochemistry and surface chemistry, materials and chemical engineering and biophysics. To be consistent, each chapter is organized in the similar manner, providing introduction, experimental results, conclusions and references. Chapter 1 describes the characteristics of OP neurotoxins and the need for their detection. It also includes the literature review of the biosensor technology and the existing techniques for OP detection. Chapter 2 provides an insight on the research goals and objectives. Chapter 3 details a fiber-optic fluorescence biosensor using a four-channel fluorimeter, Analyte 2000. OPH was immobilized using avidin-biotin chemistry. The change in fluorescence of a pH-sensitive fluorophore, carboxynaphthofluorescein (CNF) was a direct measure of the concentration of analyte present in the sample. The lowest detection limit for paraoxon was 0.5µM. Since *p*-nitrophenyl (*p*NP)-substituent OPs are more frequently used than the non-*p*NP counterparts, a more specific detection strategy

based on the fluorescence resonance energy transfer (FRET) between Coumarin1 and *p*NP was developed, which is described in Chapter 4.

Immobilization of enzymes with total retention of its activity in different matrices with good diffusion properties for substrates is a crucial factor for the development of biosensors. Therefore, in order to achieve this purpose, a simple method for encapsulation of OPH within silica nanoparticles is described in Chapter 5. As indicated in the conclusions of Chapter 3, that higher sensitivity of detection can be obtained by through optimization of binding chemistry on sensor surface. One such approach is OPH immobilization though site-specific binding which can be achieved using OPH antibodies. In all the preceding chapters (Chapters 3, 4 and 5), OPH has been immobilized in a random fashion and as enzymatic activity is a direct consequence of the manner the enzyme is immobilized on the surface, Chapter 6 provides a detailed insight on orientation-specific attachment of OPH using antipeptide antibodies on sensor surfaces. Therefore, this study addresses the issue of orientation of OPH to achieve higher sensitivity. In addition, an effort towards the improvement in the efficiency of immobilized enzyme has been presented in Chapter 7. It describes a study on the orientation-specific attachment of OPH to a gold surface using SPR. This strategy has provided an opportunity for optimization of active site accessibility and thus sensitivity of detection using variants of the enzyme.

Due to their high surface area for immobilization of biomolecules and excellent electrical properties, carbon nanotubes (CNTs) have been incorporated for detection of OPs. CNTs not only provided a support for the immobilization of OPH but also enabled amplification of the electrochemical signal of *p*-nitrophenol because of their ability to

promote fast electron transfer. Therefore, Chapter 8 details the purification, functionalization and characterization of the OPH-immobilized CNTs and their application for electrochemical biosensing of OPs. Chapter 9 and 10 presents an overall summary and conclusions of this research and the proposed future work respectively.

3. A FLUORESCENCE-BASED BIOSENSOR FOR THE DETECTION OF ORGANOPHOSPHATE PESTICIDES AND CHEMICAL WARFARE AGENTS

3.1 INTRODUCTION

In this chapter, the development of an OPH enzyme-based biosensor system for direct and real-time detection of nerve agents using the Analyte 2000 is described. The great advantage of this approach over antibody-based affinity analysis is the kinetic nature of the assay and possibility to use the same waveguide for multiple analyses; most immunoassay systems can be used only one time as they are unable to operate once a target analyte is bound. Classically, they should be replaced with new biosensor element. In contrast, enzyme-based systems are capable of analyzing great numbers of samples with the same waveguide, until the activity of the immobilized enzyme drops to very low levels (usually due to enzyme attrition). This makes analyses more cost and operationally efficient and allows using the system in field applications.

The pH-reporter fluorophore used in this project is a carboxynaphthofluorescein (CNF), a pH-sensitive fluorophore (Figure 3-1a). CNF has two absorption maxima, at 512 and 598 nm, and its emission spectral peaks are observed at 563 and 668 nm, respectively. CNF is available with a succinimidyl ester conjugation motif that can form a very stable amide bond with the protein or target of interest. Given an aqueous solution with a starting pH of 9.0, CNF fluorescence intensity will decrease as the pH decreases

(Figure 3-1b). Even though the absorption wavelength for CNF is not well matched with the light source wavelength of the Analyte 2000, there is a large enough absorption cross section at 635 nm for useful excitation to occur.

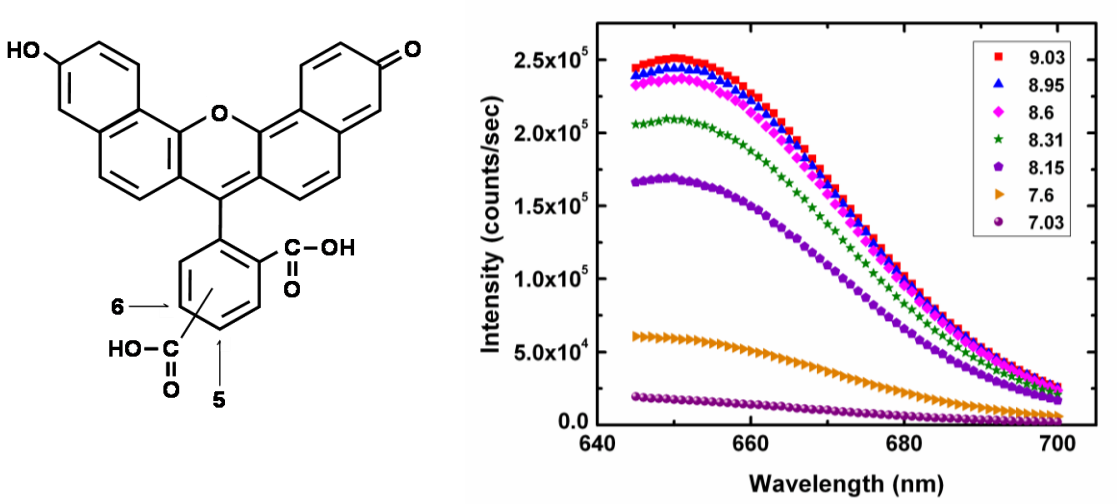

Figure 3-1: (a) Carboxynaphthofluorescein structure and (b) emission spectra at different pHs with excitation at 635 nm

3.2 EXPERIMENTAL

3.2.1 Reagents and enzymes

Wild-type and variants of OPH (E.C.3.1.8.1) were isolated from a recombinant *Escherichia coli* strain using published procedures [1, 2] .CHES and phosphate buffers were obtained from Sigma Chemical Co. (St. Louis, MO). Organophosphate compounds were purchased from Chem. Service Inc. (West Chester, PA). Neutravidin and biotinylated albumin was purchased from Pierce Biotechnology Inc. (Rockford, IL). CNF and biotin–XX–SE were purchased from Molecular Probes (Eugene, OR). All other reagents were purchased from Fisher Scientific (Hampton, NH). All water used in the

preparation of reagents and for rinsing waveguides and other surfaces was Type I water prepared in a Millipore system and determined to be ≤18.2mΩ.

3.2.2 Analyte 2000

The Analyte 2000™ is a four-channel, single-wavelength fluorescent detection platform, and each channel includes an optical waveguide in a cuvette housing, a fiber-optic cable transmitting the excitation light to the waveguide and a coaxial cable carrying the electrical signal back from the photodiode. The main unit houses four sets of opto-electronics for the four channels consisting of the laser diodes, the amplifiers and the analog-to-digital converters. A motherboard with an onboard microprocessor controls the four channels and sends information to a laptop computer through an RS232 connection. A proprietary software package displays the real-time signal from up to four individual waveguides in graphic and numerical formats and provides for running automated assay protocols. The 40mm long polystyrene waveguides terminate in a convex lens. Light is launched down the center of the waveguide where an aspheric surface focuses the light into the sensing portion so as to maximize the evanescent energy that excites the fluorophores. Emitted light is recovered by the waveguide and passed through absorptive and dichroic filters to remove extraneous excitation light. The beam is then focused onto a photodiode for detection (Figure 3-2). Avidin may be adsorbed directly to the surface as is commonly used with microtiter plates and seems to have worked well in many immunoassay studies using these waveguides [3].Our current process has evolved after a multitude of variations of the adsorption was attempted.

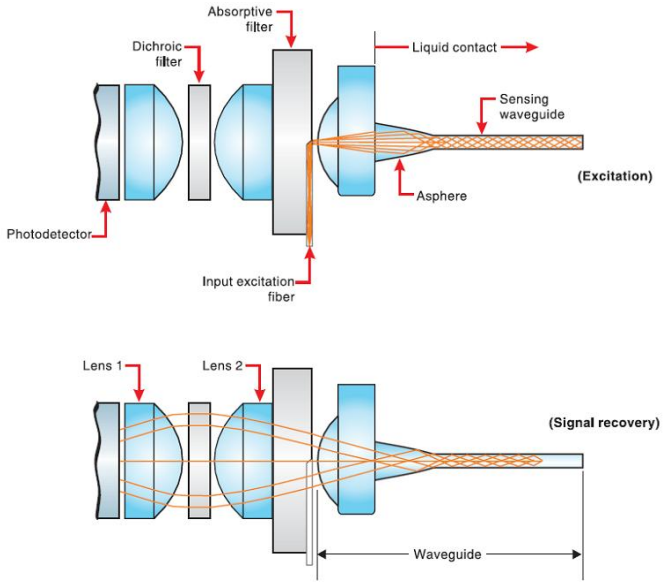

Figure 3-2: Light path of the polystyrene waveguide (photo from Research International website, www.resrchintl.com)

3.2.3 Waveguide Preparation

Each polystyrene waveguide (Research International) was washed in 50% ethanol in an ultrasound cleaner for 5 min. The tip of the waveguide was dipped in black enamel paint and allowed to dry to minimize back-reflected laser light. The waveguide was then placed in a plasma cleaner chamber (REFLEX Analytical Corporation, Ridgewood, New Jersey) and the air is exchanged with industrial grade (99.9%) nitrogen (BOC Edwards, Wilmington, MA). After a vacuum was applied, nitrogen was allowed to flow slowly to maintain low pressure and the production of plasma around the guide for 6 min. The chamber was allowed to reach room pressure with nitrogen. The waveguide was quickly transferred to a plain capillary tube to be used as a reaction chamber with 1 mg/mL Neutravidin in phosphate buffer (20 mM, pH 8.3). Each capillary tube holds a minimum of 80µL of solution around the waveguide. The waveguide was incubated in the

Neutravidin overnight. All incubations for waveguide preparation are performed at 4ºC. The waveguide was rinsed with water, allowed to dry, then was incubated with biotin–XX–SE (0.5 mg/mL biotin in DMF + water; DMF: water = 1:10) overnight and rinsed again. The waveguides were ultimately incubated in 1 mg/mL OPH or bovine serum albumin (as a reference channel) in phosphate buffer (20 mM, pH 8.3) with 20mM $CoCl_2$ overnight followed by a 2 h incubation (minimum) with 100µg/mL CNF. During the incubations, periodic moving of the waveguide in and out of the capillary tubes mixed the solutions. The incubation waveguides were intensively rinsed with Type I water and stored in the storage buffer. Once the waveguide was prepared, it was placed in the waveguide holder. The system was turned on and the signal was monitored on a PC using the Research International proprietary software.

3.2.4 Calculations

The relative change in intensity $[(I_1–I_5/I_1) \times 100]$ is calculated to obtain the calibration graphs. The change is calculated after 5 s of the injection of the sample for PX. This time interval varies with the kind of substrate depending on its hydrolysis by the OPH enzyme. The activity of soluble OPH with paraoxon was measured in an aqueous solution according to a published protocol [4] . The activity of immobilized enzyme on the waveguide was measured in a cuvette in a spectrophotometer. Minor modifications to the referenced procedure were made to accommodate the waveguide. The waveguide with immobilized enzyme was placed in 4mL of 50mM CHES buffer in a cuvette with a stir bar. The reaction was initiated with the addition of substrate and measured over 2 min.

Samples tested on the Analyte 2000 were prepared in 1 and 0.5mM CHES buffer with 120mM NaCl, 2.7mM KCl and 20mM $CoCl_2$. A non-buffered preparation was also made with the identical salts. The 3mL samples are introduced into the Analyte cuvettes by injection with a syringe. The signal was monitored for 30 s and the measurement cell was rinsed with buffer. After the signal stabilizes (<5 pA change per second), another sample was introduced.

3.3 RESULTS AND DISCUSSION

3.3.1 Analytical characteristics of immobilized enzyme detection

In a pilot study, a mixture of CNF, OPH and 1mM CHES buffer was introduced in the cuvette of the spectrofluorimeter QM-1 (Photon Technologies International, Lawrenceville, NJ). After obtaining a baseline, paraoxon was added and fluorescence intensity was monitored. CNF is a pH-sensitive fluorophore with the longest available excitation wavelength. The peak absorption wavelength is 598 nm and the peak emission wavelength is 668 nm. Although not at its peak, the pH probe is still amply excited at 635 nm (required by the Analyte), showing a 34% signal loss due to the longer excitation wavelength (Figure 3-3).

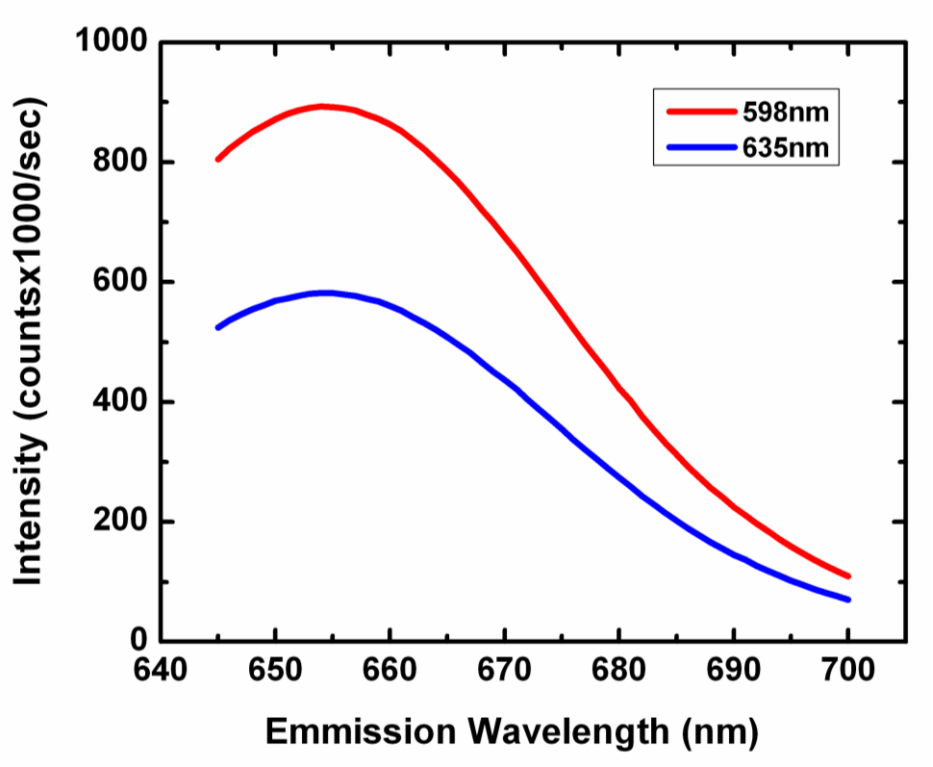

Figure 3-3: Carboxynaphthofluorescein (CNF) excitation at optimal wavelength (598 nm) and red laser wavelength (635 nm) obtained in cuvette of the spectrofluorometer QM-1

Bovine serum albumin, a protein of similar size to OPH (68 kDa), was employed in the preparation of a reference waveguide. The biotinylated albumin was bound to avidin, and subsequently, incubated with CNF in the same manner as the OPH waveguide. There was no detectable signal upon adding paraoxon (data not shown). The multi-channel capability of the Analyte allows the direct comparison of one to three waveguides prepared with enzyme and one BSA reference, when a single sample may be injected into multiple separate measurement units containing individual waveguides. The simultaneous analyses on reference and enzyme waveguides using the identical sample offer a valuable comparison which clearly differentiates the actual enzymatic action as

opposed to minute pH differences between the buffer and sample preparations as seen on the reference BSA waveguide. When a sample of paraoxon was introduced to an OPH/CNF-coated waveguide and a BSA reference waveguide, a characteristic pattern was seen (Figure 3-4).

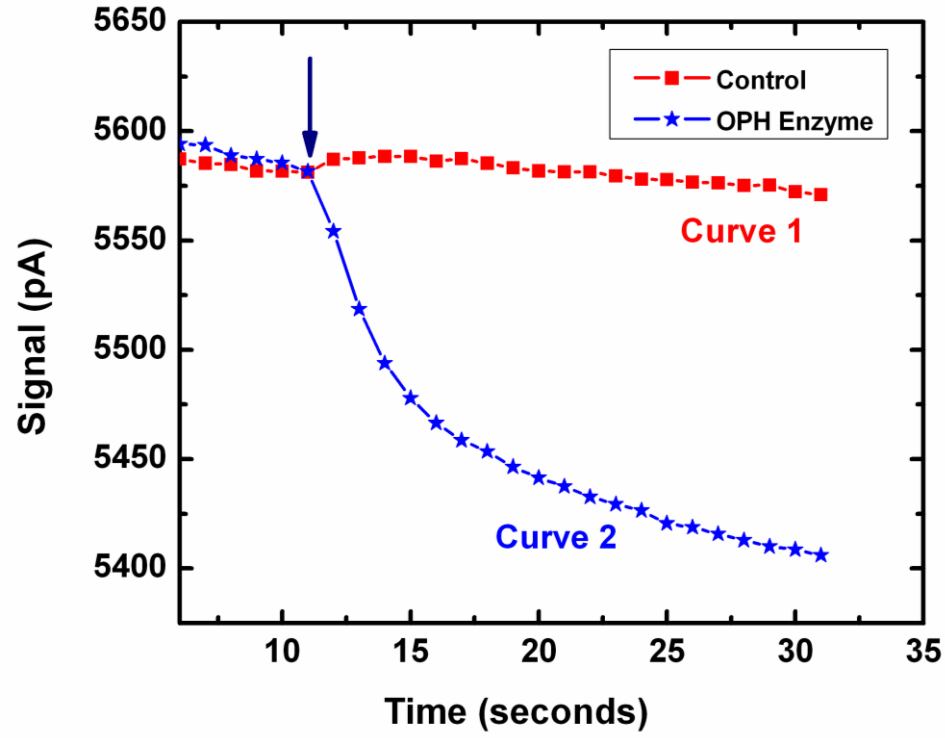

Figure 3-4: Example of typical signal response to introduction of substrate (vertical arrow) to a two-channel system of the Analyte 2000 (has up to four channels). Curve 1 corresponds to the waveguide with OPH and CNF and Curve 2 obtained from the reference waveguide with BSA and CNF. CHES 1mM, pH 9.0

There was a small rapid initial change upon addition of sample, which may be caused by a small difference of buffer pH. It was critical to observe the control waveguide as it provided information as to how much the OPH waveguide was

influenced by sample pH bias. The steep slope observed following substrate introduction was markedly different from that of the reference due to the changes that occur as the maximum velocity of the reaction is reached. The slope appeared to increase with substrate concentration as is expected. While the signal change from the reference channel was negligible, a significant change in working channel signal was observed. As the substrate in the reaction cuvette was exhausted, diffusion transports additional substrate to the surface of the waveguide. However, with immobilized enzymes, this process is much slower than in a homogenous soluble enzyme preparation. This prevents the OPH waveguide from reaching the rapid equilibrium seen in the reaction chamber on the spectrofluorimeter. As the signal returned to the slope of signal degradation, it remained slightly higher for a long time. Given enough time, the slope of the signal would reflect that all substrate was eliminated from the ports and the tubing. Determination of substrate concentration has been established as 95% of signal change over 30 s.

3.3.2 Buffer selection

The influence of the buffer capacity of the solution on sensor response is a well-documented limitation of any pH measurement-based biosensor [5]. On one hand, it is necessary to minimize buffer capacity to maximize the pH change available from enzymatic hydrolysis of the analyte and on the other hand, it is necessary to provide some solution pH control to minimize background pH drift caused by sample addition and to maintain the pH required for enzyme activity. A high salt concentration helps stabilize

buffer by providing ionic strength; however, in aqueous water solutions, salts alone do not stabilize the pH throughout prolonged experiments.

Based on previous work [5] , a buffer strength of 1mM was shown to represent a compromise between a satisfactory signal and the ability of an open system (subject to CO_2 absorption) to maintain constant pH. The independent control pH measurements were performed on the reference channel with a waveguide containing only BSA and CNF, but not OPH, indicated negligible changes in bulk pH associated with analyte hydrolysis. The buffer strengths tested were sufficient to compensate the acidic product generated by the immobilized enzyme once it diffused into the bulk. NaCl and KCl are added to provide ionic stability and as cobalt is a vital cofactor for OPH, $CoCl_2$ was added to prevent depletion of cobalt from the immobilized enzyme. This buffer, 1mM CHES, pH 9.0, 200mM NaCl, 2.7mM KCl, 20mM $CoCl_2$, was used as the main buffer for the fluorimetric assays in this study. Since environmental samples may not have a buffer of measurable strength, other buffer concentrations were evaluated to avoid big signal changes on sample introduction. CHES (0.5 mM) and Type I water with salts but no buffer were tested and sensitivity curves were evaluated in comparison to the 1mM buffer (Figure 3-5).

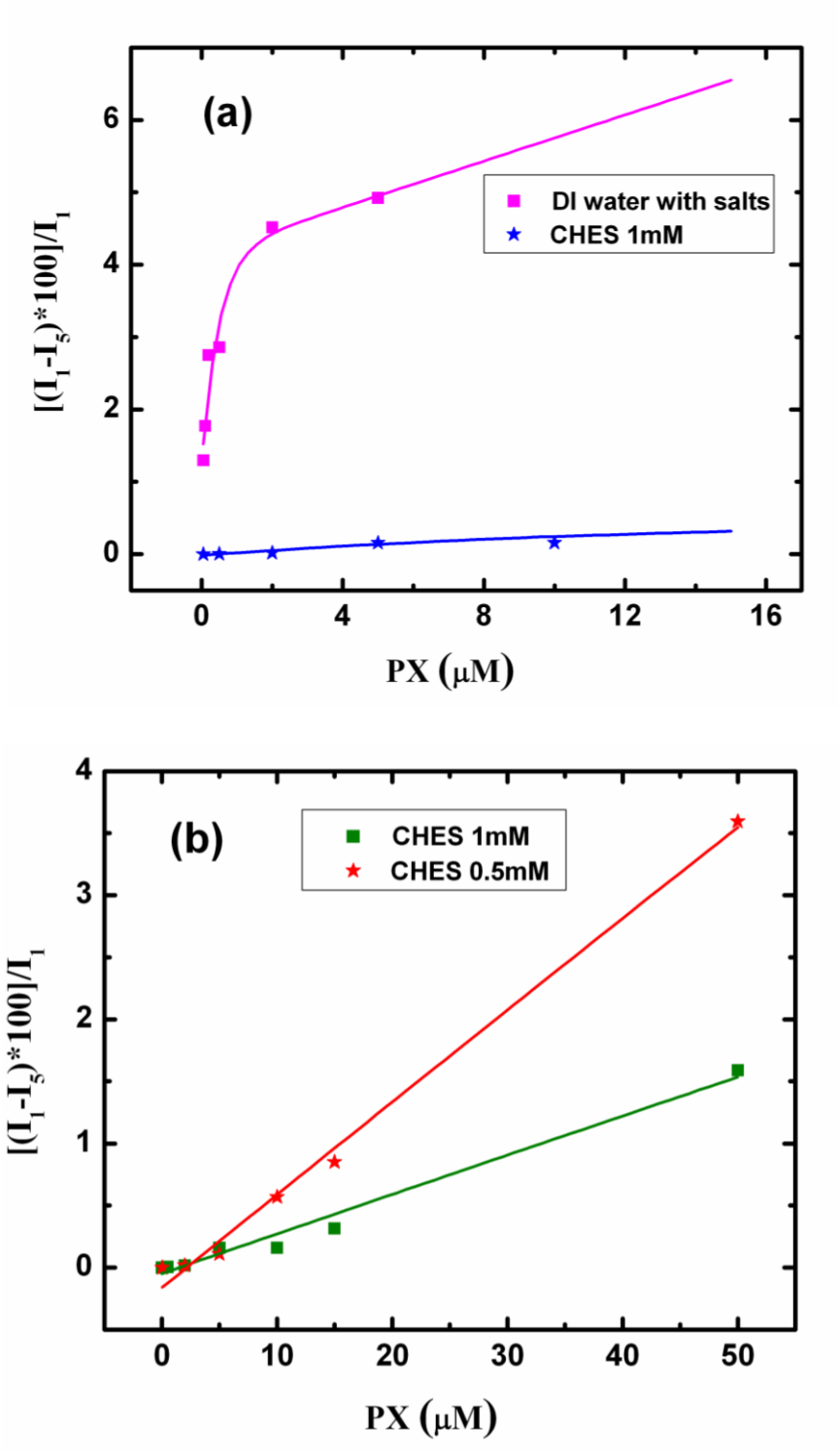

Figure 3-5: (a) Comparison of CHES 1mM and DI water with salt buffers with PX. (b) Comparison of CHES 1mM and CHES 0.5mM buffers with PX

3.3.3 Enzyme immobilization quantitation and activity

Experiments were conducted to determine the amount of enzyme immobilized on the waveguides. Each incubation cuvette holds 100µL of solution and 20µL is displaced by the waveguide. A ratio of enzyme concentration was determined by the activity of the solution after incubation and compared to the known concentration of the enzyme before incubation. The immobilized enzyme on one waveguide had the equivalent activity of approximately 10 ng soluble OPH. These studies indicate that an average of 7.78 ng of enzyme was immobilized on the waveguides. The coefficient of variation for this analysis was high and additional evaluations are in progress.

3.3.4 Reaction pH

CNF shows a change in fluorescence intensity over the pH range of ~6–10, easily covering the pH 7.5–9.5 range of optimal OPH activity. Samples were prepared in a buffer of pH of 9.0. This allows for a large signal drop should it occur. Paraoxon samples of 7mM and greater saturated the amount of CNF present and decreased the fluorescence signal below a point where no changes are discernable, which prevents measurement of the actual extent of pH change by this method and only provides information that a large amount of substrate was present.

Varying concentrations of paraoxon were assayed to establish the sensitivity of the system. The data in Figure 3-6 shows the relative stability of the control waveguide and the increasing signal change from the OPH waveguides. The reference waveguide was invaluable to distinguish the effects of sample pH changes versus other interfering substances.

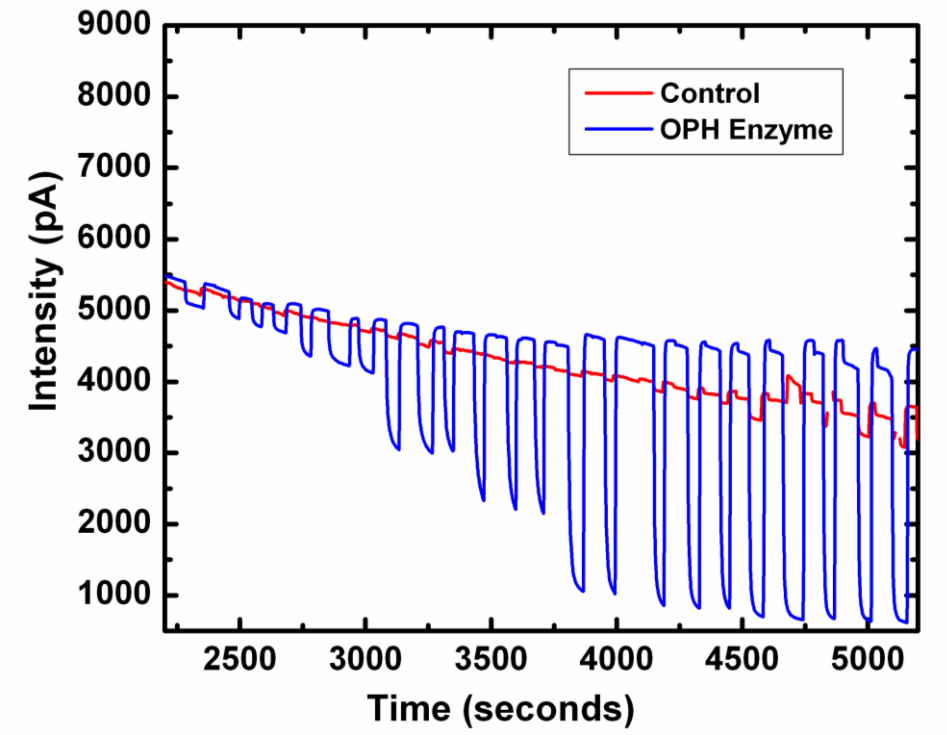

Figure 3-6: Signal responses to increasing amounts of paraoxon (5–50 µM)

An important aspect of this system is signal decay, which was evident on all waveguides over time. Newly prepared waveguides generally have a high initial signal (12,000–24,000 pA) that falls rapidly after the laser is turned on. The decay rate decreases and reaches a rate where the reactions are discernable. Thus, it was necessary to allow new waveguides to stabilize before the samples are introduced. The rate of <5 pA/s change was established as acceptable and allows for determination of calibration data. If the lasers are turned off between measurements, the decay was reduced for this time. This suggests that photobleaching might be a contributor to the signal decay. The calibration curve in Figure 3-7 shows sensitivity as low as to 1µM paraoxon in 1mM CHES. The storage stability was very good, and the waveguide retained about 80% of the starting activity after storage for 4 weeks in PBS with 50mM $CoCl_2$.

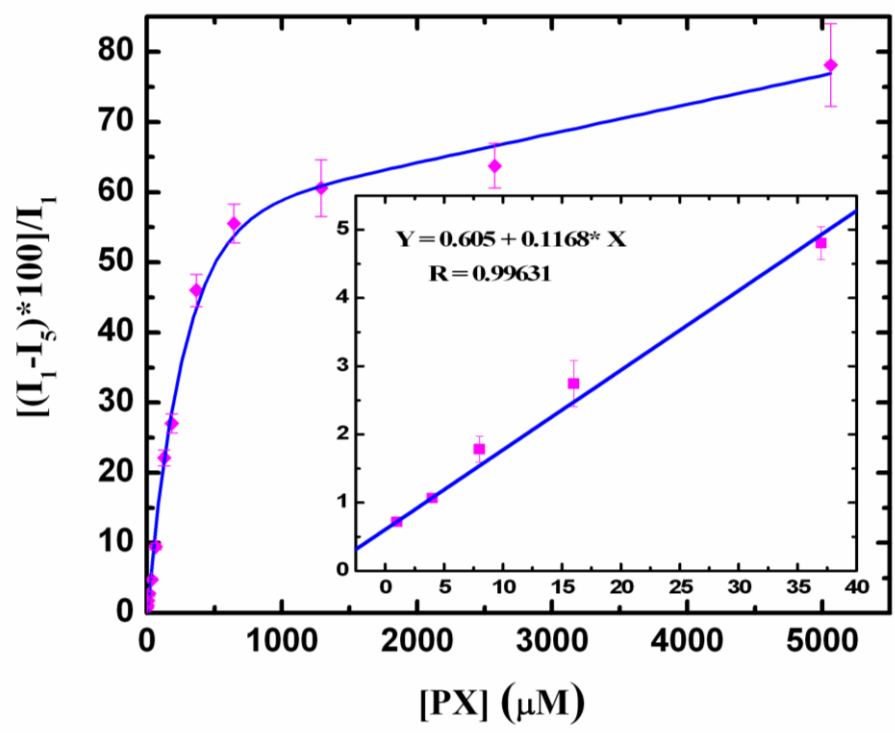

Figure 3-7: Calibration curve for paraoxon with CHES 1 mM, pH 9.0, buffer

In order to validate this sensor for other OP neurotoxins, another substrate was tested on the same set of waveguides as used for paraoxon. Diisopropyl phosphorofluoridate (DFP) is an OP with a P F bond, which is seen in G-type nerve agents, such as soman and sarin. As such, it is commonly used as a surrogate for these compounds. The reaction with OPH is similar to paraoxon with the fluorine becoming the leaving group. The raw data using revealed the characteristic signal drop from OPH enzymatic activity and increasing signal change in response to increases in substrate concentration (Figure 3-8a). A linear detection range for DFP in 1mM CHES buffer was 2–400 µM (Figure 3-8b).

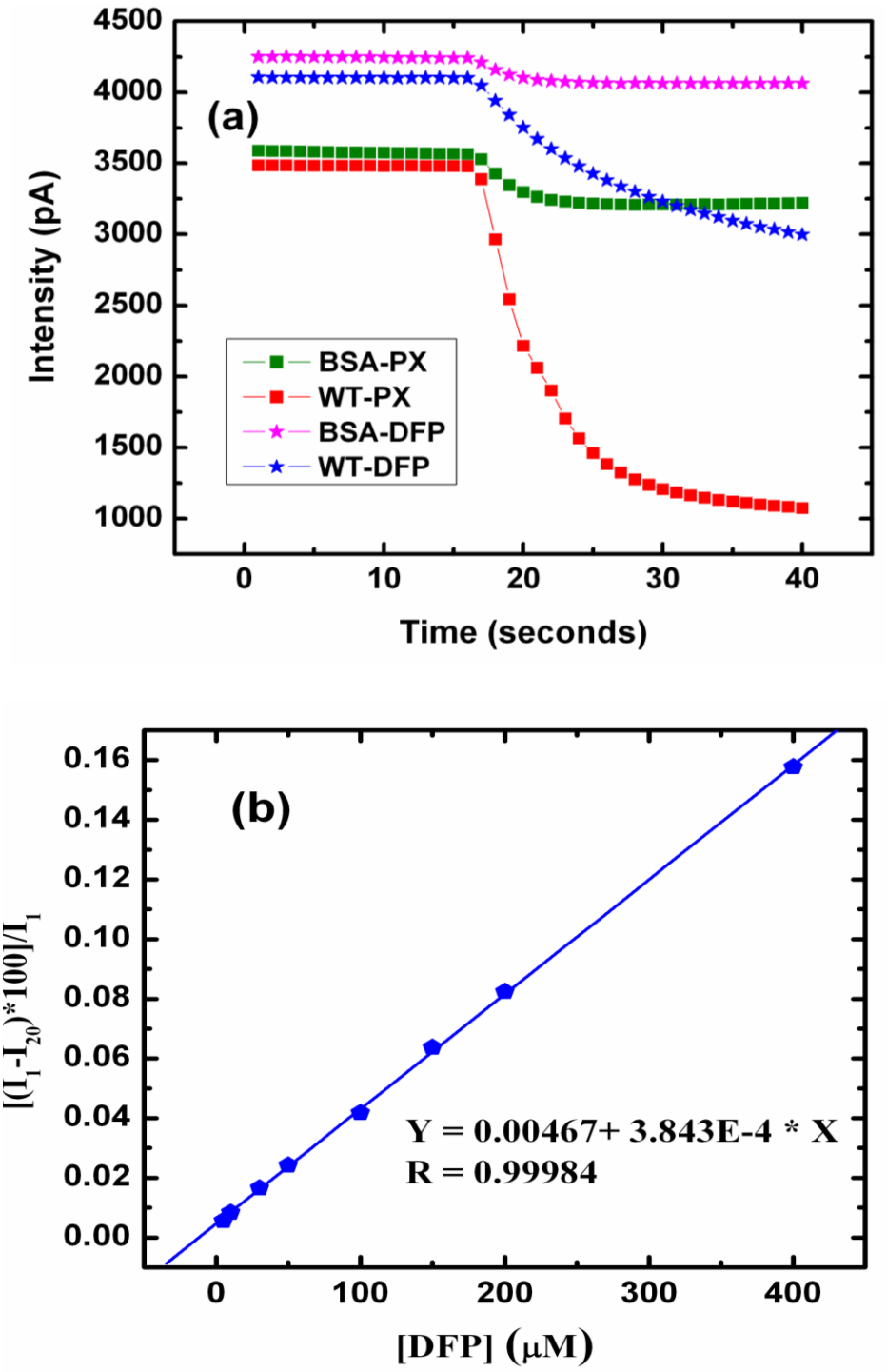

Figure 3-8: (a) System responses to the sample contained similar concentrations (50 µM) of PX and DFP. Two control channels with BSA and two working channels with OPH. (b) Calibration graph for DFP with CHES 1 mM, pH 9.0, buffer

As previously stated, the Analyte 2000 spectrofluorimeter was mostly used for immunological methods. We have now demonstrated that it can be used successfully for the enzymatic detection of a chemical. The system was able to make a real-time evaluation of the substrate hydrolysis and produce quantitative information at a wide range of concentrations. This approach provides a measurement of products from the catalytic reaction that is directly proportional to the substrate concentration based on the fluorescence spectral intensity change. The reference channel allows for a measurement of pH changes from the buffer solution and the sample solution and eliminates incidental change.

From these data, we can conclude that the measurement of OPs by this method is linear from 1 to 3000 µM (data not shown for higher concentrations) in a 1mM buffer. In lower concentration buffers or in water, OPs are directly detectable as low as 0.05µM. Whether this is practical for an assay will depend on the origin of the sample. In some cases, such as in food preparation, concentrating samples may be considered to increase the detectable range. It would allow for this particular array to be used in more types of monitoring. Comparison studies with a spectrofluorimeter revealed that up to 34% of the potential signal was lost by not using the optimum excitation and emission wavelengths for CNF. If the wavelengths were changed on the Analyte 2000 or on another platform with adjustable excitation/emission wavelengths, the signal to noise ratio would be much greater and better characteristics could be achieved.

3.3.5 Confirmation of Binding chemistry using SPR

Surface Plasmon resonance was used to confirm the successful immobilization of OPH on the waveguides. The binding events were similar to the ones used on the waveguides (Figure 3-9).

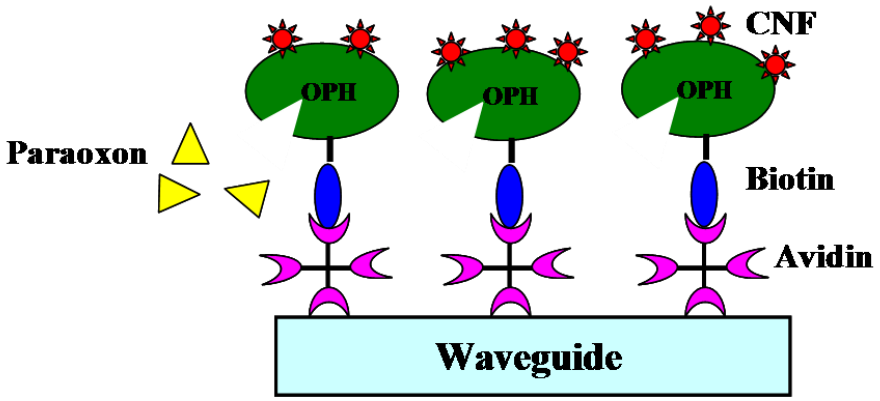

Figure 3-9: Binding sequence on the SPR sensor surface

The gold sensor surface was cleaned with piranha solution followed by rinsing and sonication with Milli-Q water. The sensor was then initialized in air and water, followed by in-situ cleaning with NaOH-TritonX. After establishing a baseline with CHES, Neutravidin was non-specifically adsorbed on the gold surface. BSA and PBS-Tween was used to block the remaining sites, followed by specific immobilization of biotinylated OPH only on the working channel. The real-time binding events on the sensor surface are shown in Figure 3-10a. Known concentrations of paraoxon were introduced to determine the activity of the immobilized OPH. Paraoxon, 0.6-64 µM, was circulated across the surface at a flow rate of 105µl/min for 2 min. Activity was measured by collecting 200 µl of the flow through, measuring the absorbance of p-nitrophenol thus formed at 405nm, after the two minute circulation. A calibration graph

was obtained by plotting the absorbance of p-nitrophenol measured at 405nm versus the paraoxon concentration (Figure 3-10b).

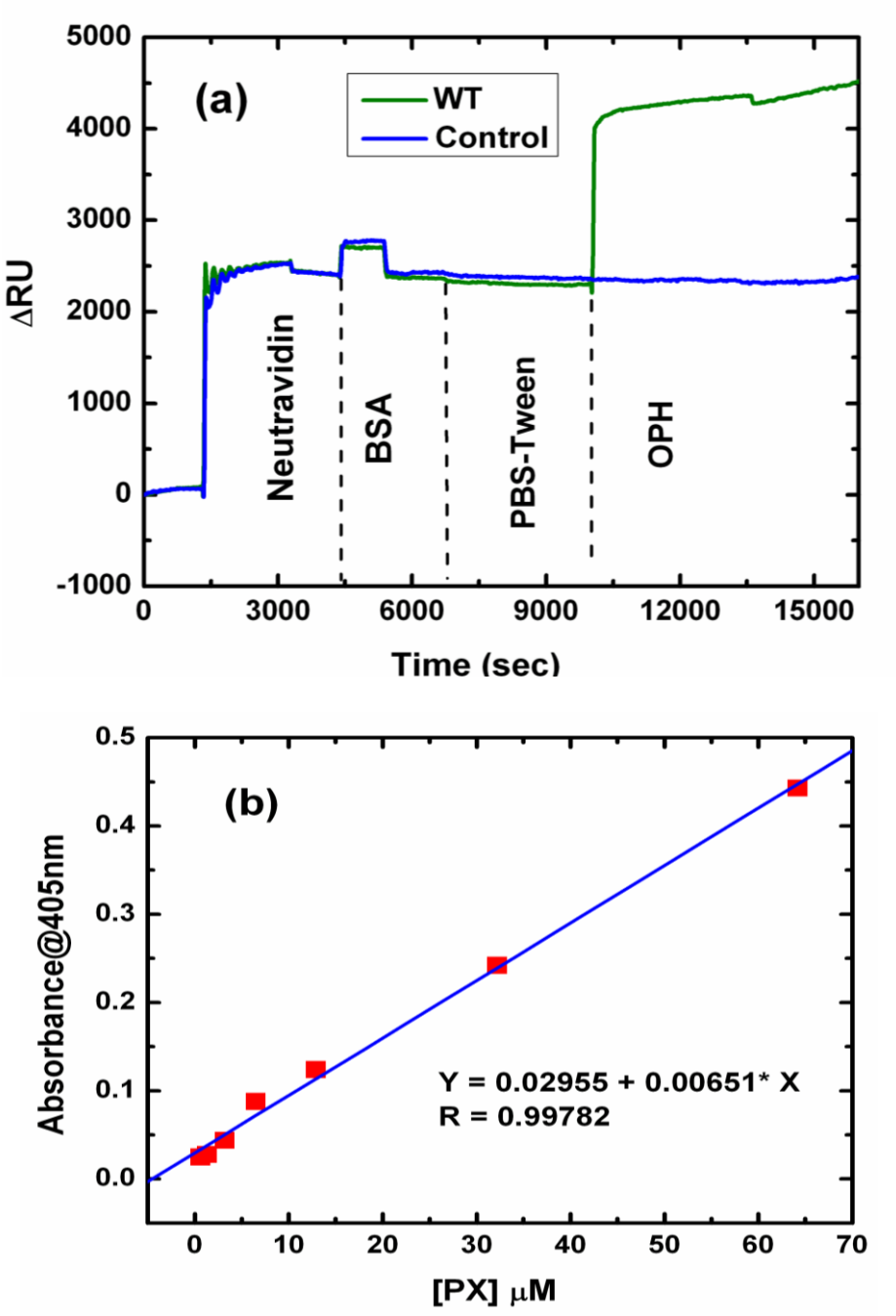

Figure 3-10: (a) Real-time SPR sensorgram of the binding events on the sensor surface (b) Calibration graph for 0.6-64 µM PX

3.4 CONCLUSION

The study demonstrated the direct detection of OP neurotoxins based on the OPH enzyme conjugated with reporter CNF fluorophore and anchored on the optical waveguide of portable fluorimeter Analyte 2000. Because of the rational design of the recognition (OPH) and reporter (CNF) molecules, OP samples as low as 0.05µM were qualitatively detected, with quantitative detection range of 1–800 µM. This biosensor assay system has the potential to be directly connected to a laptop computer and information may be immediately distributed to enact an appropriate response. This could also be used to provide continual remote monitoring and notification. The obvious improvement of the system parameters may be achieved by alteration of excitation light source to the appropriate wavelength of reporter fluorophore dye and optimization of coupling chemistry. With those improvements in the mind, the Analyte 2000 shows promise to be applied in numerous other enzymatic assays. Using CNF as an indicator, any reaction occurring in the 7–10 pH region could feasibly be measured. Other pH-sensitive dyes, such as seminapthofluorescein and seminaphthorhodafluors (SNARF dyes, Molecular Probes Inc.), should be evaluated on this system. Application of FRET approaches may be useful. Considering the portability of the instrument, a niche of environmental, food safety or bedside healthcare detection is possible.

3.5 REFERENCES

1. J. Kulys and E.J. Dcosta, Printed Amperometric Sensor Based on Tcnq and Cholinesterase, Biosensors & Bioelectronics 6 (1991) pp. 109-115.

2. G. Palleschi, M. Bernabei, C. Cremisini, and M. Mascini, Determination of Organophosphorus Insecticides with a Choline Electrochemical Biosensor, Sensors and Actuators B-Chemical 7 (1992) pp. 513-517.

3. G. Voirin, D. Gehriger, O.M. Parriaux, and B.A. Usievich, Si3n4/Sio2/Si Waveguide Grating for Fluorescent Biosensors, Integr. Opt. Devices III, Proc. SPIE 3620 (1999) pp. 109-116.

4. C.S. McDaniel, L.L. Harper, and J.R. Wild, Cloning and Sequencing of a Plasmid-Borne Gene (Opd) Encoding a Phosphotriesterase, Journal of Bacteriology 170 (1988) pp. 2306-2311.

5. A.L. Simonian, A.W. Flounders, and J.R. Wild, Fet-Based Biosensors for the Direct Detection of Organophosphate Neurotoxins, Electroanalysis 16 (2004) pp. 1896-1906.

4. FLUORESCENCE-BASED SENSING OF p-NITROPHENOL AND p-NITROPHENYL SUBSTITUENT ORGANOPHOSPHATES

4.1. INTRODUCTION

A novel detection method for organophosphate neurotoxins has been described, based on the fluorescence quenching of a Coumarin derivative. These dyes are similar in structure to some organophosphates (OPs), and they fluoresce in the blue–green region of the spectra. This methodology has been utilized for the detection of organophosphates whose hydrolysis product is *p*-nitrophenol by using an enzyme, organophosphorus hydrolase (OPH). Coumarin1 in the presence of *p*-nitrophenol results in a quenching of fluorescence, providing a direct measure of the concentration of *p*-nitrophenol present in the sample. The decrease in fluorescence intensity is proportional to the paraoxon concentration in the range of 7.0×10^{-7}–1.7×10^{-4} M. The specificity of this sensing application for *p*-nitrophenyl substituent OPs has also been demonstrated. OPs are a class of synthetic organic pesticides which generally have a short residual life and can cause numerous acute and chronic health effects. They have been an integral part of the agricultural industry for the past several decades due to their target specificities and selectable toxicities. The toxic nature of these compounds can be attributed to the species–specific inhibition of acetylcholinesterase (AChE), an important enzyme responsible for the regeneration of neural synaptic function. In addition to their wide agricultural and urban usage, they have also been exploited for the development of

neurological chemical warfare agents. Currently available technologies for OP detection include sol–gel thin films, screen printed electrodes, acoustic patterning, gas chromatography–mass spectrometry, and various other intricate techniques that have limited field applicabilities. This optically-based approach promises much simpler and more direct detection capabilities.

p-Nitrophenol, the degradation product of some of the OPs, is corrosive and acutely toxic by oral route [1]. This class of compounds has also been found as environmental contaminants in fresh water and in the atmosphere, acute exposure to which causes headaches, nausea and cyanosis [2]. Therefore, detection of these compounds is a matter of environmental and health concern. *p*-Nitrophenyl (*p*NP)-substituent organophosphates, which include ethyl parathion, methyl parathion, paraoxon, and fenitrothion, are more extensively used than their non-*p*NP counterparts [3]. Malathion and diazinon (*p*NP-substituent OPs) were ranked number one and three, respectively, as the most commonly used organophosphate insecticides active ingredients by EPA [4]. The extensive usage of these pesticides generates large volumes of pesticide-containing waste. Typical pesticide concentrations can range from 1 to 10,000 ppm and improper disposal can be hazardous to the environment [5].

Fluorescence-based methods can be used to detect very low concentrations of an analyte or a molecule of interest. Fluorescent probes enable researchers to detect individual components of complex systems, such as living cells, with exceptional sensitivity and selectivity. Coumarin compounds are derivatives of 1,2-benzopyrone which display high fluorescence quantum yield in the blue–green region upon photoexcitation. Previously, the fluorescence properties of coumarin derivatives

combined with substrates have been used to investigate enzymatic process [6]. In a recent study the fluorescence properties of 7-isothiocyanato-4-methylcoumarin have been utilized by Orbulescu et al. for development of a highly sensitive biosensor for the detection of low concentrations of paraoxon [7].

The present study reports the development of a new sensor for the direct detection of *p*-nitrophenol and *p*-nitrophenol substituent organophosphorus neurotoxins. In this system, detection is based on the fluorescence quenching of coumarin1, competitive inhibitor of an OP-hydrolyzing enzyme, organophosphorus hydrolase (OPH, E.C. 3.1.8.1). OPH is a 72 kDa homodimeric enzyme which catalyzes the hydrolysis of the P–O, P–S, P–F, and P–CN bonds of OP-neurotoxins. This makes OPH a suitable recognition element for the detection of these substrates. OPH operates near the limits of diffusion with some substrates and can be altered to enhance its specificity towards a variety of OP-substrates [8-13]. The kinetic evaluation of OPH with the fluorescence compounds coumarin and coumarin1 determined these compounds to be competitive inhibitors of the enzyme. While Orbulescu et al. [7] focused on the surface characterization of the OPH-based biosensor, this current study concentrated upon the sensing element, OPH, and the potential of using an untethered dye as the reporter. In addition, our analysis demonstrated the applicability of this method beyond paraoxon to other *p*-nitrophenol OPs.

4.2. EXPERIMENTAL

4.2.1. Materials

The enzyme, organophosphorus hydrolase, was purified as previously described [51]. Paraoxon was purchased from Chem-Service, Inc. (West Chester, PA) and coumarin dyes were obtained from Sigma (Aldrich, St. Louis, MO) and were diluted in ethanol for use. Water used for preparation of aqueous solutions was from a Millipore Direct-Q Water system (resistivity, 18MΩcm^{-2}).

4.2.2. Instrumentation

All fluorescence intensities were measured using a Photon Technology International (PTI) Quantum Master Fluorescence spectrophotometer equipped with a xenon lamp. The excitation and emission spectra were evaluated for both dyes; buffer without coumarin dye was used as a control. Coumarin and coumarin1 were first prepared in 95% ethanol and then at the required concentrations as solutions in 20mM 2-(*N*-cyclohexylamino)ethane sulfonic acid (CHES), pH9.0. The total reaction volume for the fluorescent assays was 3 ml.

4.2.3. Procedures

The fluorescent compounds coumarin and coumarin1 were selected for evaluation based on their structural similarity with some organophosphates (Figure 4-1). A one molar solution of both coumarin and coumarin1 were made in 95% ethanol. The solutions were stored at room temperature and used within 1–4 days. Both compounds were stable under these conditions. Due to their limited solubility in aqueous solutions, all kinetic

assays with these compounds were done in 1% ethanol. Control assays without inhibitors were also performed in 1% ethanol. Kinetic assays were performed in 20mM CHES, pH 9.0 with 7×10^{-14} mol OPH. The catalytic rates (k_{cat}) for the enzyme in the presence and absence of potential inhibitors were determined by evaluating velocity of a constant enzyme concentration with variable concentrations of substrate. Three final concentrations of coumarin (5, 10, and 20 mM) and coumarin1 (1.25, 2, and 5 mM) were used. All assays were performed in a 1 ml total volume and the reaction was initiated by the addition of paraoxon. Change in absorbance per minute (ΔAmin−1) was monitored at 400 nm. Measurements of ΔAmin−1 were converted to μmol product per second using the molar extinction coefficient for the product, *p*-nitrophenol, of 17,000M^{-1} cm^{-1}. The K_i values for coumarin and coumarin1 were 4.7 and 0.3 mM, respectively.

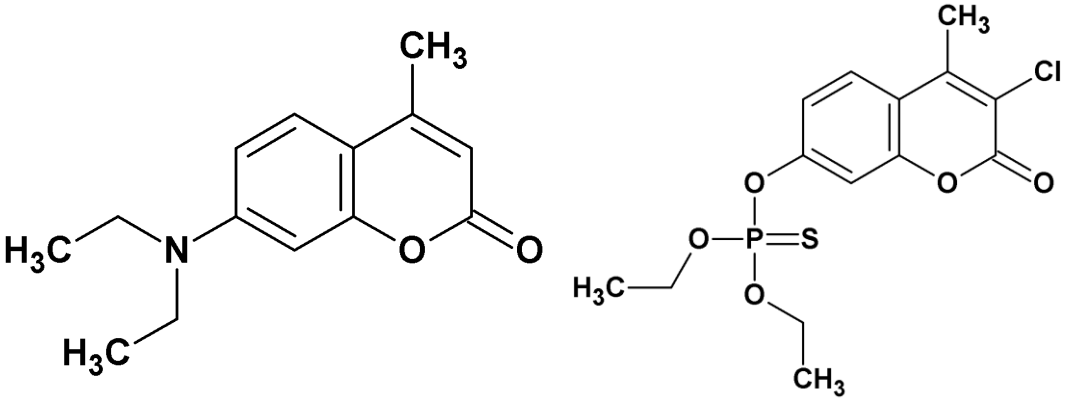

Figure 4-1: (a) Coumarin1, the fluorescent compound and competitive inhibitor selected as the Reporter in this study. (b) Coumaphos, an OP insecticide commonly used for control of a wide variety of livestock insects.

4.3. RESULTS AND DISCUSSION

Kinetic evaluation determined that both coumarin and coumarin1 behave as competitive inhibitors of OPH; however, comparison of the emission spectra relative to the buffer control demonstrated that the coumarin emission peak coincided with the Raman peak of water. Since the emission peak of coumarin1 was distinct, it was selected as the fluorescent reporter for sensor development. The excitation and emission peaks of coumarin1 were observed at 343 and 465 nm, respectively.

4.3.1. Fluorescence measurements for p-nitrophenol

The fluorescence intensity of coumarin1 was measured following the addition of varying concentrations of *p*-nitrophenol. As expected the system showed fluorescence quenching with increasing concentration of *p*NP (Fig. 4-2a). A calibration graph was obtained for *p*-nitrophenol and the minimum detection limit was found to be 1.8 µM (Fig. 4-2b). When the fluorescence changes of *p*NP in the absence of OPH was tested (Fig. 4-2c), the system showed a similar response as in the presence of OPH. This demonstrated that OPH is not required for detection of *p*-nitrophenol alone.

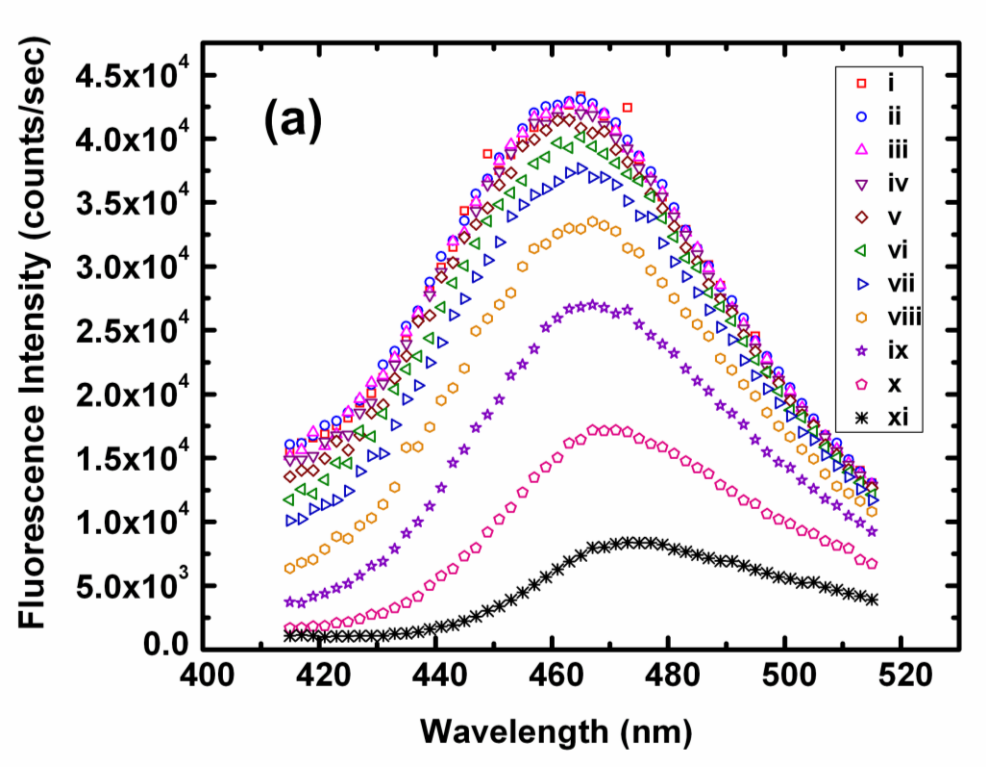
(a)
Fluorescence Intensity (counts/sec)
4.5x10^4
4.0x10^4
3.5x10^4
3.0x10^4
2.5x10^4
2.0x10^4
1.5x10^4
1.0x10^4
5.0x10^3
0.0
400
420
440
460
480
500
520
Wavelength (nm)
i
ii
iii
iv
v
vi
vii
viii
ix
x
xi

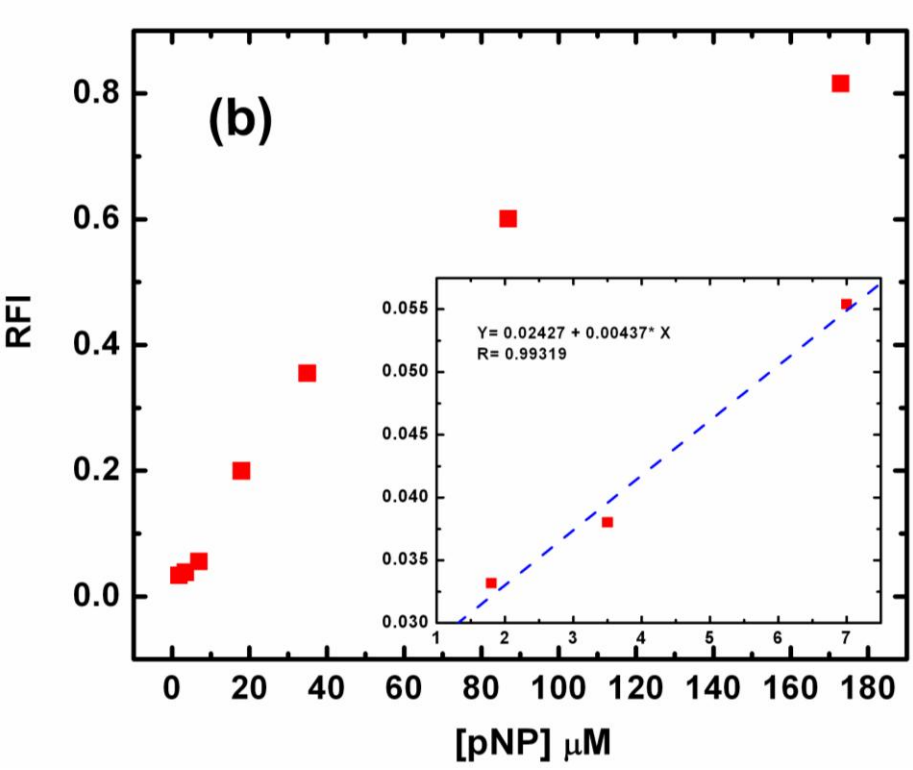
(b)
RFI
0.8
0.6
0.4
0.2
0.0
0
20
40
60
80
100
120
140
160
180
[pNP] μM
Y= 0.02427 + 0.00437* X
R= 0.99319
0.055
0.050
0.045
0.040
0.035
0.030
1
2
3
4
5
6
7

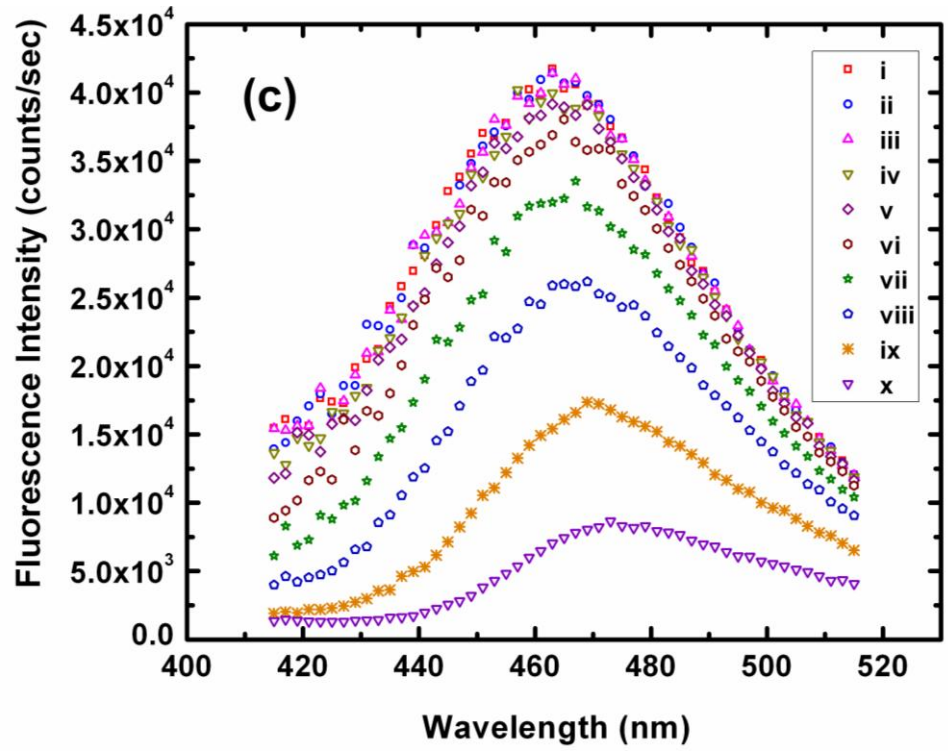

Figure 4-2: (a) Fluorescence of coumarin1 (C1) at *p*-nitrophenol (*p*NP) concentrations from 0.4×10^{-6} to 0.173×10^{-3} M. (i) C1, (ii) C1 +WT, (iii) 0.4µM, (iv) 0.7µM, (v) 1.8µM, (vi) 3.5µM, (vii) 7µM, (viii) 18µM, (ix) 35µM, (x) 87µM, and (xi) 173µM. (b) Calibration curve with *p*-nitrophenol. Relative fluorescence intensity change (RFI) is plotted as a function of added *p*-nitrophenol (*p*NP) concentration. (c) Fluorescence of Coumarin1 at *p*-nitrophenol (*p*NP) concentrations from 0.4×10^{-6} to 0.173×10^{-3} M in absence of OPH; (i) C1, (ii) 0.4µM, (iii) 0.7µM, (iv) 1.8µM, (v) 3.5µM, (vi) 7µM, (vii) 18µM, (viii) 35µM, (ix) 87µM, and (x) 173µM. All the experiments were conducted in the absence/presence of OPH in 20mM CHES buffer, pH 9.0. [Coumarin1] = 2.33×10^{-8} M. Coumarin1 was excited at 343 nm. Coumarin1: OPH= 1:1.

4.3.2. Fluorescence measurements for paraoxon

As paraoxon is hydrolyzed, a chromogenic, *p*-nitrophenol (*p*NP) and a colorless product, diethyl phosphate are released. The hydrolytic generation of *p*-nitrophenol leads to quenching of the coumarin1 fluorescence. The relative concentrations of coumarin1 and OPH were standardized for all assays at a 1:1 molar ratio. If the amount of coumarin1 was in excess in solution, the background fluorescence reduced the detection limit for the OP compound, as demonstrated in Figure 4-3. The fluorescence intensity of coumarin1 was measured and used as a background signal level. OPH was added and the intensity of fluorescence was measured again (FI_0). Equimolar concentration of OPH and coumarin1 were used for all the experiments.

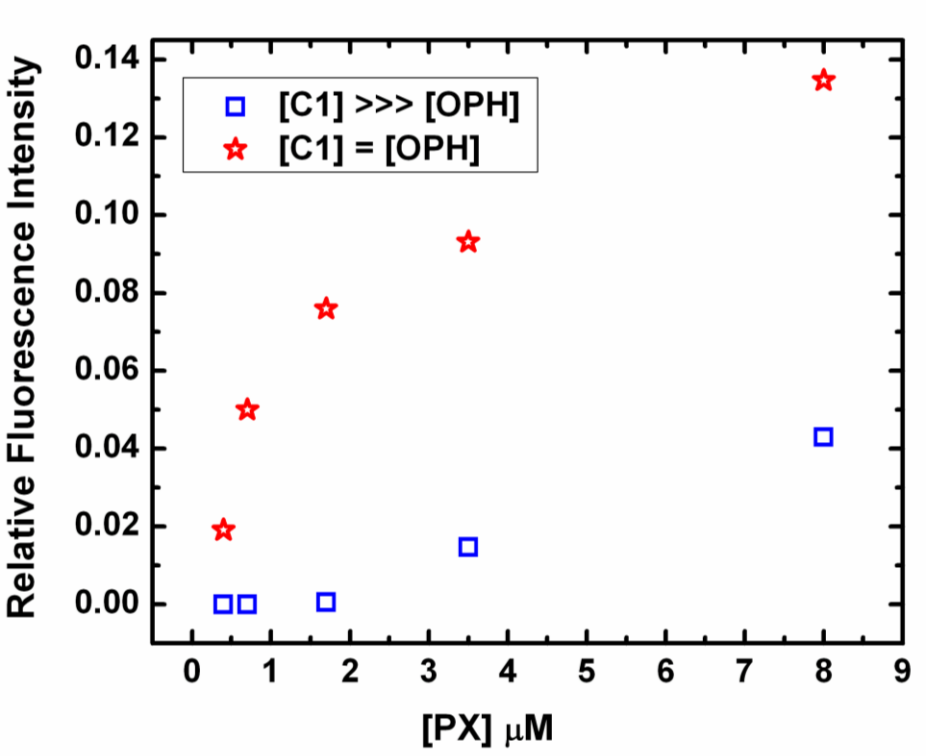

Figure 4-3: Calibration curve showing differences in sensitivity of PX detection when the concentration of coumarin1 is made equal to and greater than the

concentration of OPH in working solution. 20mM CHES buffer, pH 9.0. Coumarin1:OPH = 1:1 and 14:1.

Control experiments were performed to monitor for fluorescence intensity changes in the absence of OPH (Figure 4-4a). Paraoxon was added in a concentration series and fluorescence intensities (FI_n) were again measured (Figure 4-4b).

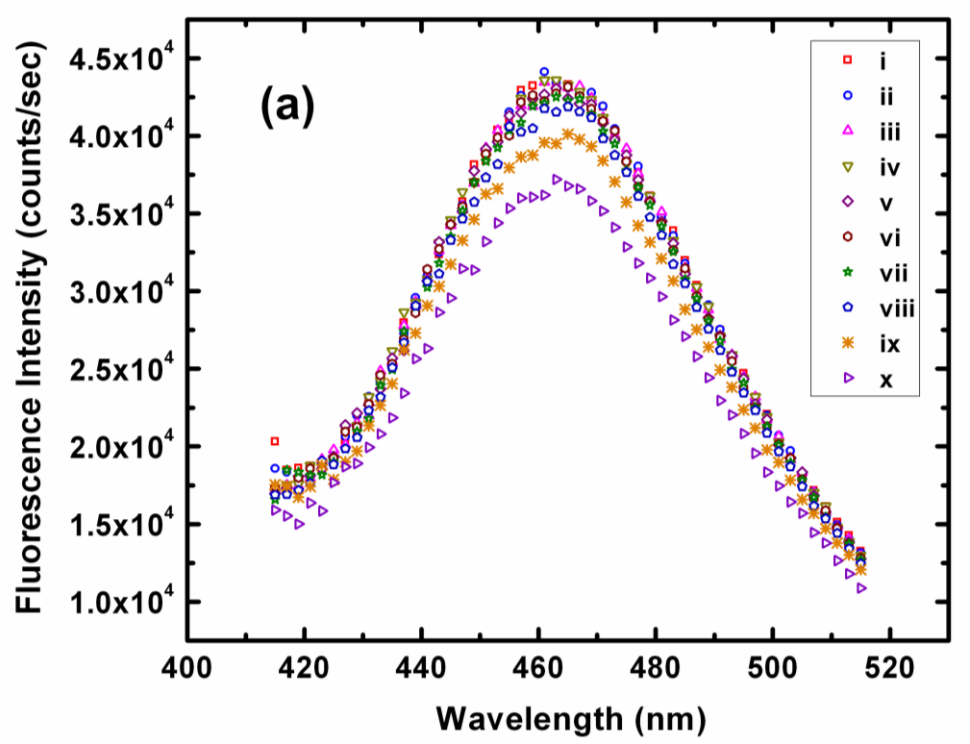

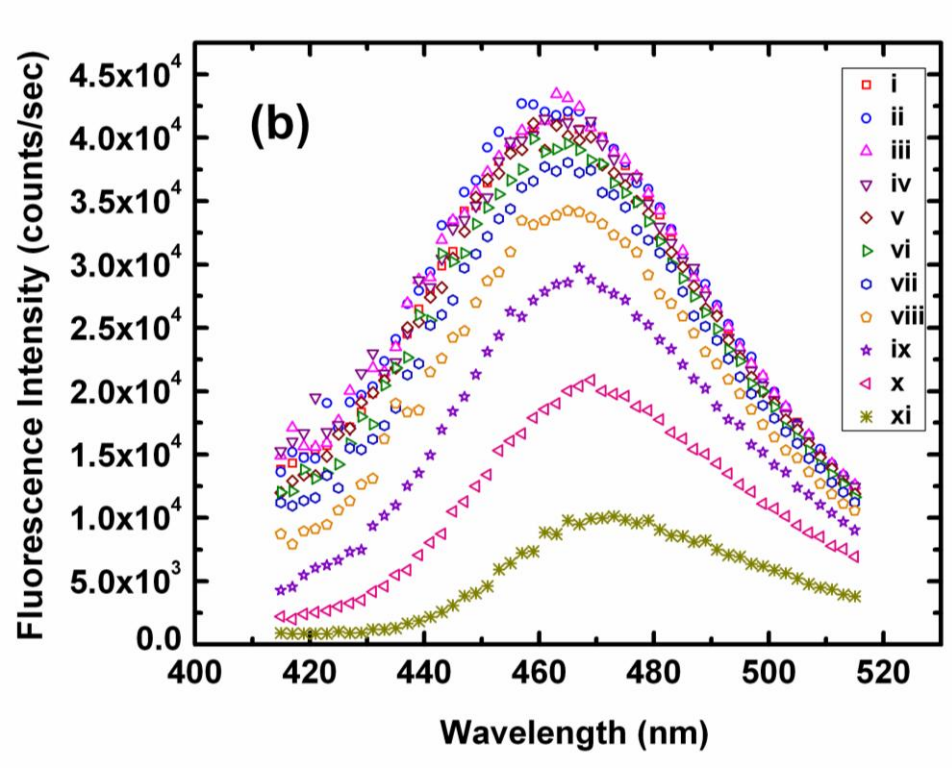

Figure 4-4: (a) Fluorescence of coumarin1 at varying paraoxon concentrations in the absence of OPH. 20mM CHES buffer, pH 9.0. [Coumarin1] = 2.33×10^{-8} M. PX concentration from 0.4×10^{-6} to 0.173×10^{-3} M; coumarin1 was excited at 343 nm. (i) C1, (ii) 0.4µM, (iii) 0.7µM, (iv) 1.8µM, (v) 3.5µM, (vi) 7µM, (vii) 18µM, (viii) 35µM, (ix) 87µM, and (x) 173µM. (b) Fluorescence of coumarin1 at varying paraoxon concentrations in the presence of OPH. 20mM CHES buffer, pH 9.0. [Coumarin1] = 2.33×10^{-8} M. PX concentration from 0.4×10^{-6} to 0.173×10^{-3} M; coumarin1 was excited at 343 nm. Coumarin1:OPH = 1:1. (i) C1, (ii) C1 +WT, (iii) 0.4µM, (iv) 0.7µM, (v) 1.8µM, (vi) 3.5µM, (vii) 7µM, (viii) 18µM, (ix) 35µM, (x) 87µM, and (xi) 173µM.

Relative fluorescence intensity change, RFI was calculated as:

$$RFI = \frac{FI_0 - FI_n}{FI_0}, where n = 1,2,3....n$$

RFI represents the ratio of change of fluorescence in the presence of paraoxon to the fluorescence in the absence of paraoxon. Approximately 15% change in the RFI was observed in the absence of OPH, while in the presence of OPH 80% RFI was observed in the fluorescence intensity of coumarin1 at the highest concentration of PX. The changes in the absence of OPH are likely due to auto hydrolysis of PX. A calibration curve for paraoxon is presented in Figure 5-5 in which the mean relative fluorescence intensity (RFI) is plotted against the paraoxon concentration. The minimum paraoxon detected was 0.7 µM, which corresponds to less than 2% fluorescence quenching. Good linearity was observed at paraoxon concentrations up to 8µM. Experiments were performed to determine if there were any changes in fluorescence intensity associated with diethyl phosphate (DeP), the second product of paraoxon degradation. The calibration curve was repeated, with addition of varying concentrations of DeP. No changes in fluorescence were observed for DeP (Data not shown).

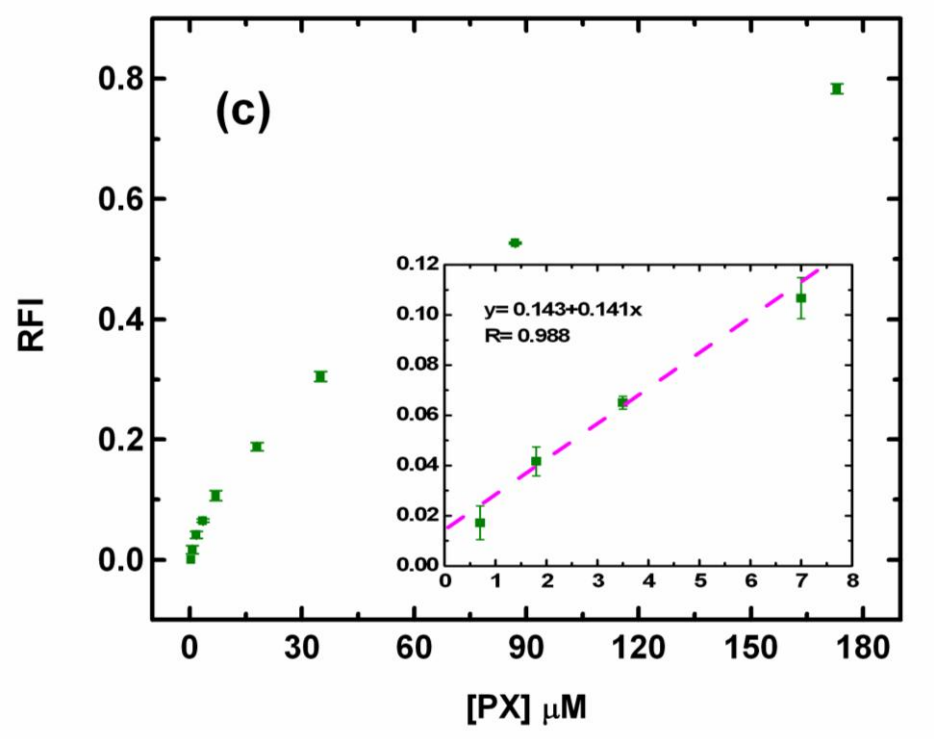

Figure 4-5: Calibration curve with paraoxon. Mean relative fluorescence intensity change (RFI) is plotted as a function of added paraoxon (PX) concentration. 20mM CHES buffer, pH 9.0, coumarin1 concentration 2.33×10^{-8} M, 1:1 coumarin1: OPH

4.3.3. Analytical procedure and evaluation

The principle of this method was validated with parathion, a *p*-nitrophenyl substituent organophosphorus compound. The detection methodology was as described for the paraoxon studies, fluorescence intensities at varying concentrations of parathion were measured and a calibration curve generated from the measurements. The minimum parathion concentration detected was 0.7μM, and linearity (Y = 0.0069 + 0.00209X, R = 0.98575) was observed at concentrations up to 143 μM. These results provided evidence that this detection method will work for other nitrophenyl substituent organophosphates. To determine if the detection was selective toward nitrophenyl substituent

organophosphates as it is designed to be, non-*p*NP producing OPs like malathion and DFP were tested. Using the same detection methodology, the fluorescence intensity was measured (Figure 4-6a and b) and the relative fluorescence intensities were calculated. No evidence of quenching was observed at 7µM DFP and 7µM malathion but at the same concentration, PX gave around 11% quenching in fluorescence.

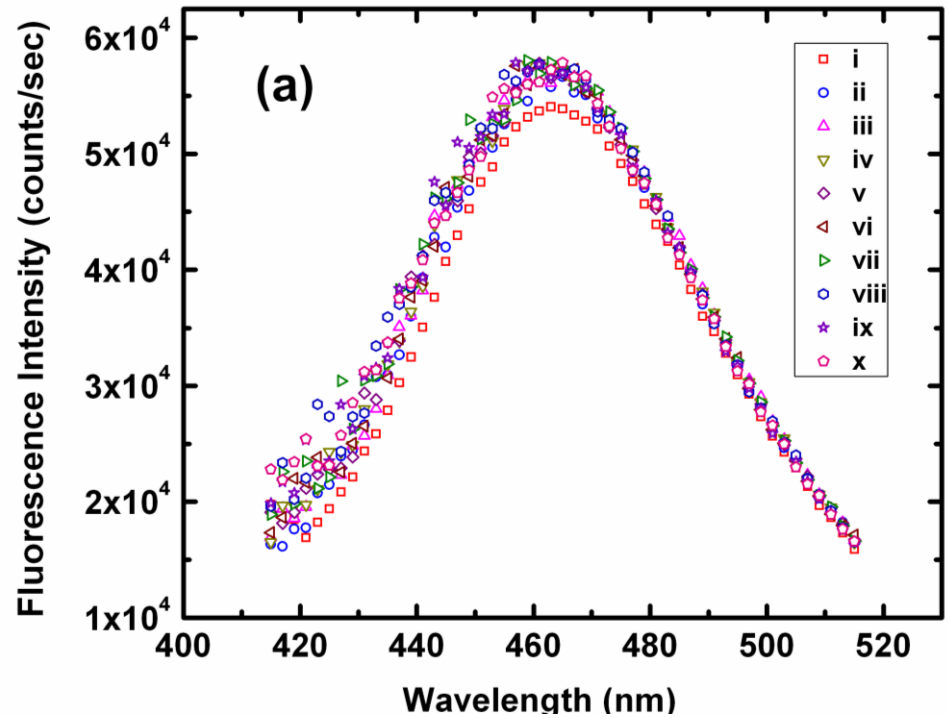

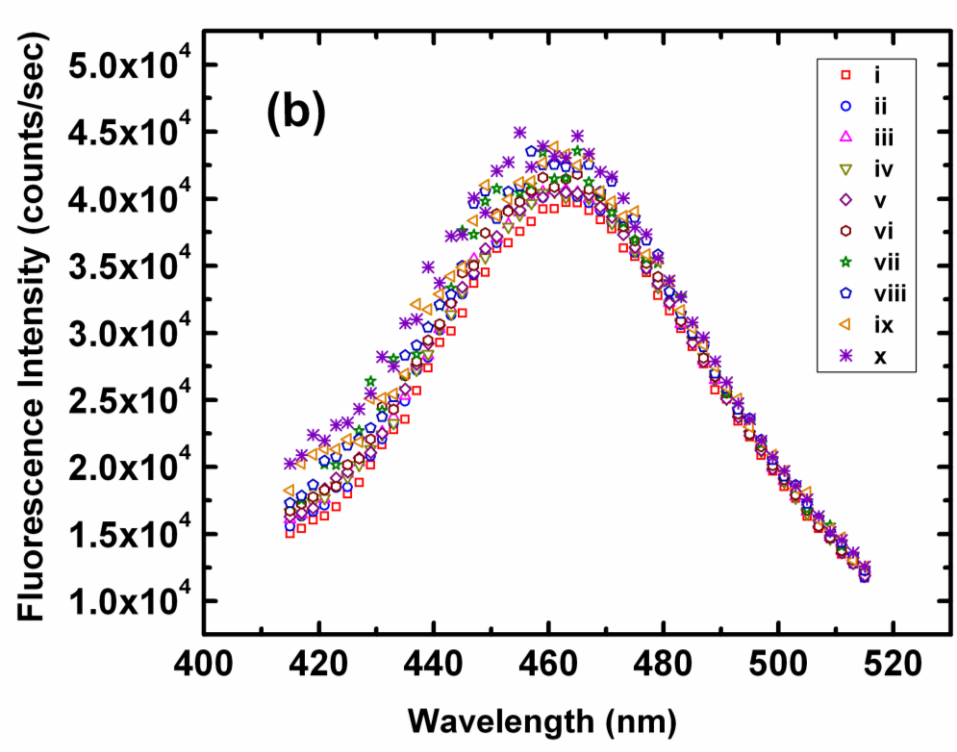

Figure 4-6: Selectivity of the methodology. (a) Fluorescence of coumarin1 at diisopropyl fluorophosphate (DFP) concentrations from 1.65×10^{-6} to 0.165×10^{-3} M. (i) C1, (ii) C1 +WT, (iii) 1.65µM, (iv) 3.3µM, (v) 6.6µM, (vi) 16.5µM, (vii) 33µM, (viii) 49.6µM, (ix) 82.8µM, and (x) 165µM. (b) Fluorescence of coumarin1 at varying malathion concentrations from 0.4×10^{-6} to 0.087×10^{-3} M. (i) C1, (ii) C1 +WT, (iii) 0.4µM, (iv) 0.7µM, (v) 1.8µM, (vi) 3.5µM, (vii) 7µM, (viii) 18µM, (ix) 35µM, and (x) 87µM. Both OPs were tested in the presence of OPH–coumarin1, in 20mM CHES buffer, pH 9.0. [Coumarin1] = 2.33×10^{-8} M. Coumarin1 was excited at 343 nm. Coumarin1: OPH = 1:1

4.4. CONCLUSION

The results presented here report the development of an alternative method for the detection of *p*-nitrophenyl-substituted organophosphates using the fluorescence changes

of a competitive inhibitor, coumarin1. Coumarin1 in the presence of *p*-nitrophenol leads to fluorescence quenching which is suspected to be due to fluorescence resonance energy transfer (FRET). The energy transfer efficiency for the coumarin1 and *p*NP pair for the ratio of 1:1 concentration was found to be 50% [14]. This approach allows for the development of a simple, cost effective and easy methodology for detection of *p*-nitrophenol and, by coupling with OPH, for detection of *p*NP-substituent organophosphates. It has been illustrated that this concept can be developed as a biosensor of paraoxon and parathion, it can also be applied to other nitrophenyl substituted OP pesticides like methyl parathion and fenitrothion. Further studies are underway to better characterize the critical components for sensitivity that include type of coumarin, binding characteristics of coumarin to the enzyme, and surface attachment methods.

4.5. REFERENCES

1. United States Environmental Protection Agency, R.E.D. Fact Sheet, Paranitrophenol.
2. P. Mulchandani, C.M. Hangarter, Y. Lei, W. Chen, and A. Mulchandani, Amperometric Microbial Biosensor for P-Nitrophenol Using Moraxella Sp.-Modified Carbon Paste Electrode, Biosensors & Bioelectronics 21 (2005) pp. 523-527.
3. Y. Kalender, M. Uzunhisarcikli, A. Ogutcu, F. Acikgoz, and S. Kalender, Effects of Diazinon on Pseudocholinesterase Activity and Haematological Indices in

Rats: The Protective Role of Vitamin E, Environmental Toxicology and Pharmacology 22 (2006) pp. 46-51.

4. T.K. D. Donaldson, A. Grube, *Pesticides Industry Sales and Usage, 2000 and 2001 Market Estimates*. 2004, U.S. Environmental Protection Agency.

5. Y. Lei, P. Mulchandani, W. Chen, and A. Mulchandani, Direct Determination of P-Nitrophenyl Substituent Organophosphorus Nerve Agents Using a Recombinant Pseudomonas Putida Js444-Modified Clark Oxygen Electrode, Journal of Agricultural and Food Chemistry 53 (2005) pp. 524-527.

6. M. Tegtmeier and W. Legrum, 7-Aminocoumarins Are Substrates of Cytochrome P450-Isozymes, Archiv Der Pharmazie 331 (1998) pp. 143-148.

7. J. Orbulescu, C.A. Constantine, V.K. Rastogi, S.S. Shah, J.J. DeFrank, and R.M. Leblanc, Detection of Organophosphorus Compounds by Covalently Immobilized Organophosphorus Hydrolase, Analytical Chemistry 78 (2006) pp. 7016-7021.

8. C.S. McDaniel, L.L. Harper, and J.R. Wild, Cloning and Sequencing of a Plasmid-Borne Gene (Opd) Encoding a Phosphotriesterase, Journal of Bacteriology 170 (1988) pp. 2306-2311.

9. K. Lai, N.J. Stolowich, and J.R. Wild, Characterization of P-S Bond Hydrolysis in Organophosphorothioate Pesticides by Organophosphorus Hydrolase, Archives of Biochemistry and Biophysics 318 (1995) pp. 59-64.

10. D.P. Dumas, J.R. Wild, and F.M. Raushel, Diisopropylfluorophosphate Hydrolysis by a Phosphotriesterase from Pseudomonas-Diminuta, Biotechnology and Applied Biochemistry 11 (1989) pp. 235-243.

11. D.P. Dumas, H.D. Durst, W.G. Landis, F.M. Raushel, and J.R. Wild, Inactivation of Organophosphorus Nerve Agents by the Phosphotriesterase from Pseudomonas-Diminuta, Archives of Biochemistry and Biophysics 277 (1990) pp. 155-159.

12. B.D. Di Sioudi, C.E. Miller, K.H. Lai, J.K. Grimsley, and J.R. Wild, Rational Design of Organophosphorus Hydrolase for Altered Substrate Specificities, Chemico-Biological Interactions 120 (1999) pp. 211-223.

13. J.K. Grimsley, J.M. Scholtz, C.N. Pace, and J.R. Wild, Organophosphorus Hydrolase Is a Remarkably Stable Enzyme That Unfolds through a Homodimeric Intermediate, Biochemistry 36 (1997) pp. 14366-14374.

14. A. Mallick, B. Haldar, S. Sengupta, and N. Chattopadhyay, 7-Hydroxy-4-Methyl-8-(4'-Methylpiperazine-1'-Yl)Methyl Coumarin: An Efficient Probe for Fluorescence Resonance Energy Transfer to a Bioactive Indoloquinolizine System, Journal of Luminescence 118 (2006) pp. 165-172.

5. ENZYME-ENCAPSULATED SILICA MONOLAYERS FOR RAPID FUNCTIONALIZATION OF A GOLD SURFACE

5.1 INTRODUCTION

We developed a simple and rapid method for the deposition of amorphous silica onto a gold surface. The method is based on the ability of lysozyme to mediate the formation of silica nanoparticles. A monolayer of lysozyme is deposited via non-specific binding to gold. The lysozyme then mediates the self-assembled formation of a silica monolayer. The silica formation described herein occurs on a surface plasmon resonance (SPR) gold surface and is characterized by SPR spectroscopy. The silica layer significantly increases the surface area compared to the gold substrate and is directly compatible with a detection system. The maximum surface concentration of lysozyme was found to be a monolayer of 2.6 ng/mm^2 which allowed the deposition of a silica layer of a further 2 ng/mm^2. For additional surface functionalization, the silica was also demonstrated to be a suitable matrix for immobilization of biomolecules. The encapsulation of organophosphate hydrolase (OPH) was demonstrated as a model system. The silica forms at ambient conditions in a reaction that allows the encapsulation of enzymes directly during silica formation. OPH was successfully encapsulated within the silica particles and a detection limit for the substrate, paraoxon, using the surface-encapsulated enzyme was found to be 20µM.

Immobilization of enzymes on solid substrates, such as silicon [1, 2], polymers [3] and glass [4] is of great interest for a variety of applications including biocatalysis, biosensors and formation of protein arrays for biological screening. Often, the platform is merely an inactive support for the biomolecule. Recent interest however, has advanced to attaching biomolecules directly to a transducer surface to allow *in situ* and real-time detection of enzymatic activity [5, 6].

Surface plasmon resonance (SPR) is a versatile analytical method for real-time monitoring of interactions at a solid/liquid transducer surface. SPR uses the principle of total internal reflectance occurring at the interface between materials with differing refractive indices. An evanescent wave penetrates the interface (modified with a thin layer of gold) and couples with surface plasmons (oscillating free electrons). The interaction causes a change in reflectivity and a concurrent change in resonance angle, which correlates to the refractive index (RI) of the adjacent medium. The RI is therefore directly related to changes in surface concentration of interacting ligands. The change in RI is continuously monitored to produce a sensorgram of refractive index unit (RIU) as a function of time [7-9]. SPR has proven to be particularly useful for the analysis of biological systems and can be used for example, to determine kinetic parameters and reaction characteristics [9, 10]. SPR has been recently used to study enzymatic reactions on various surfaces and microarrays. Kim et al. [11] for example, performed enzymatic reactions on surface bound substrates and measured adsorbed enzyme concentrations and substrate cleavage rates by the use of combined SPR and surface-plasmon enhanced fluorescence techniques. SPR has also been demonstrated as a method for determining

the kinetics of surface enzyme reactions based on Langmuir adsorption and Michaelis–Menten kinetics [12, 13]. SPR is adaptable to a wide range of biomolecular reactions as labelling of ligands or receptor molecules is not required. The use of SPR for biological systems however, generally requires the development of specific methods to attach biomolecules on the sensor surface and orient the molecules for optimal biological activity. Maintaining an interaction between biomolecules and the SPR waveguide surface generally requires covalent modification, which can change biological function and lower the catalytic activity as the orientation of the enzyme active site is hindered by attachment [14].

Recent studies have shown that silica formation can be catalyzed by simple peptides or proteins, such as lysozyme, in a silicification reaction analogous to the formation of silica in biological systems [15-18]. The lysozyme-precipitated silica nanoparticles proved suitable for immobilization of other enzymes. The silicification reaction yields a network of fused silica nanospheres, providing a high surface area for encapsulation and permitting high enzyme loading capacities [19]. We now report herein, a versatile method for immobilization of biomolecules directly onto a SPR transducer surface by encapsulating biomolecules within a lysozyme-mediated self-assembled layer of silica particles. The immobilization of lysozyme is based on non-specific physical adsorption of the protein to the gold SPR surface through a combination of electrostatic and surface interactions [20]. Non-specific binding will therefore result in the formation of a film of lysozyme upon the gold surface, which is then available to participate in the silicification reaction and direct the assembly of a layer of silica at the surface. Physical

adsorption generally causes little conformational change of the enzyme and no reagents or pretreatment and activation of the surface is required. A disadvantage is enzyme leaching during continuous use, as the binding is primarily due to weak hydrogen bonding and Van der Waals forces [21]. Previous literature reports however, indicate that lysozyme retains its tertiary structure when adsorbed to a hydrophilic interface, no significant denaturation occurs, and in addition, the binding is irreversible [22].

The fabrication of SPR chips, consisting of gold films coated with thin silicon dioxide layers has been recently reported [23]. The method however, involves vapor-deposited silica layers that showed a lack of stability in aqueous buffer solutions and is unsuitable for enzyme immobilization. A sol–gel technique has been successfully applied to generate stable gold/silica interfaces, which allowed further functionalization but preparation required multi-step attachment using biotin and streptavidin binding chemistries [24]. The lysozyme-mediated silica formation described herein provides a method for coating a gold surface with a thin layer of silica particles, greatly increasing the surface area of the transducer. In addition, the silica provides a matrix for the encapsulation of additional biomolecules, significantly enhancing the functionality of the resulting silica layers by directing the attachment of immobilized biomolecules directly at the gold surface.

5.2 EXPERIMENTAL

5.2.1 Enzymes and reagents

Potassium phosphate buffer (0.1N NaOH, 0.1M KH_2PO_4, pH 8) was used throughout unless otherwise stated. Paraoxon was obtained from ChemService, West Chester, PA. All other reagents and chemicals were of analytical grade and obtained from Sigma–Aldrich (St. Louis, MO). Silicic acid was prepared as described previously [19]. Organophosphorus Hydrolase (OPH) was generously provided by James Wild and his research group (Texas A&M University). The enzyme purification method has been described previously [25].

5.2.2 Formation of silica nanoparticles on the gold surface

The formation of silica particles was characterized by SPR using SPREETATM sensors (Texas Instruments) with two analysis channels. A gold surfaced SPR sensor module, and its supporting hardware and software (SPREETA, Texas Instruments) were coupled to a continuous-flow cell to allow contact with reaction solutions. Experimental setup and cleaning steps were performed as previously described [26]. The sensor was docked with the fluidics block and reference measurements were obtained with air and water as baseline measurements. An *in situ* washing step (0.12N NaOH, 1% Triton-X) was performed to ensure that the surface remained hydrophilic. A further baseline with phosphate buffer was taken as a reference measurement. Initially, lysozyme (1 mg/ml) was non-specifically adsorbed to the gold surface and any excess was removed by washing with phosphate buffer. Silicification was carried out *in situ* by introducing

TMOS (100mM tetramethyl orthosilicate in 1mM HCl) to the lysozyme-modified surface. This process was repeated with different lysozyme concentrations (5, 25 and 50 mg/ml) to determine the optimum enzyme concentration. All immobilization procedures were performed at room temperature (~22 ◦C). Immobilization steps were monitored by measuring the change in refractive index (RI) as a function of time followed by integration using SPREETA software. Net responses were calculated by comparison of 'working' and 'control' channels. Calculations and statistical analysis were performed with OriginPro 7.5 software (OriginLab Corporation, Massachusetts, USA).

5.2.3 Calculation of adlayer thickness and surface coverage

The adlayer thickness and surface coverage of each monolayer was calculated using the formula described by Jung et al [27, 28]; $d_a = (l_d/2)\times[(n_{eff} - n_b)/(n_a - n_b)]$, where d_a is the thickness of the adlayer, l_d the characteristic decay length of an evanescent wave at 307 nm, n_{eff} the effective RI of the adlayer (from the SPR signal), n_b the RI of the buffer (from reference reading), and n_a is the RI of the adlayer material assuming an RI of 1.57 for protein and an RI of 1.43 for biosilica [29].

5.2.4 Enzyme assay for immobilized organophosphate hydrolase activity

OPH was encapsulated within the silica matrix by adapting the method described above. The initial protein monolayer was established using a solution of 25 mg/ml lysozyme to coat the SPR surface. A solution of 100mM TMOS containing OPH was then passed over the surface for approximately 45 min to yield the silica layer and co-

encapsulate OPH during the silicification reaction. The SPR surface was rinsed thoroughly with buffer to remove any loosely associated enzyme and silica prior to further analysis. Enzyme activity was determined by measuring the hydrolysis of paraoxon as described previously [30]. Paraoxon (1–500 µM) was circulated across the surface at a flow rate of 100 µl/min for 2 min. Enzyme activity was determined by collecting 200 µl of the paraoxon hydrolysis product (*p*-nitrophenol). The absorbance of the hydrolysis product was measured at 405 nm using a UV–vis fiber optic spectrophotometer (Ocean Optics Inc., Dunedin, FL).

5.2.5 Scanning electron microscopy

For scanning electron microscopy imaging, glass slides coated with a chromium adhesion layer (~2 nm) followed by ~50 nm gold film were used. The gold slides were cleaned with freshly prepared piranha solution (3:1, H_2SO_4 and H_2O_2. *Caution*: Piranha solution is dangerous and should be handled with care) followed by thorough rinsing with DI water. The slides were then sonicated in acetone (5 min), rinsed with DI water, and sonicated in ethanol (5 min) before plasma cleaning in air (5 min). The slides were prepared as described above with a range of lysozyme concentrations, followed by silica formation in the presence of 100mMTMOS.The samples were then coated with a thin layer of gold (~10 nm) and imaged using a JEOL JSM 7000F field emission scanning electron microscope (JEOL USA, Inc., Peabody, MA).

5.3 RESULTS AND DISCUSSION

5.3.1 SPR analysis of lysozyme and silica nanocomposite films

SPR spectroscopy revealed rapid adsorption of lysozyme to the gold waveguide surface (Figure 5-1a). The change in surface density results in small changes in RI at the interface and a corresponding shift in the resonance angle. Upon introduction of lysozyme, an initial rapid signal increase was observed and was attributed to the change in the bulk refractive index of the circulating solution. The change in RI then increased gradually, corresponding to the adsorption of lysozyme to the gold surface. Surface saturation was indicated by a plateau in the RI signal. The decrease in the RI during the wash step was due to removal of unbound lysozyme. The RI signal change increased linearly with higher protein concentrations (Figure 5-1b). The lysozyme adlayer also thickened with increasing lysozyme concentration but showed a plateau at 25 and 50 mg/ml (Table 1), indicating that the gold surface was saturated at high protein concentrations. The surface coverage of lysozyme was calculated and revealed a maximum surface concentration of ~2.6 ng/mm2 (~1.10×10^{11} molecules/mm^2) and a maximum film thickness of ~2 nm (±0.047) (Table 1). The measured maximum coverage of lysozyme at saturation is in agreement with the theoretical surface density for a monolayer of lysozyme (1.8–2.7 ng/mm^2), based on a protein with a molecular mass of 14 kDa and dimensions of 4.5 nm×3.0 nm×3.0 nm [20, 21]. SEM images of the monolayer showed a glass-like film of lysozyme across the surface of the waveguide (Figure 5-2a).

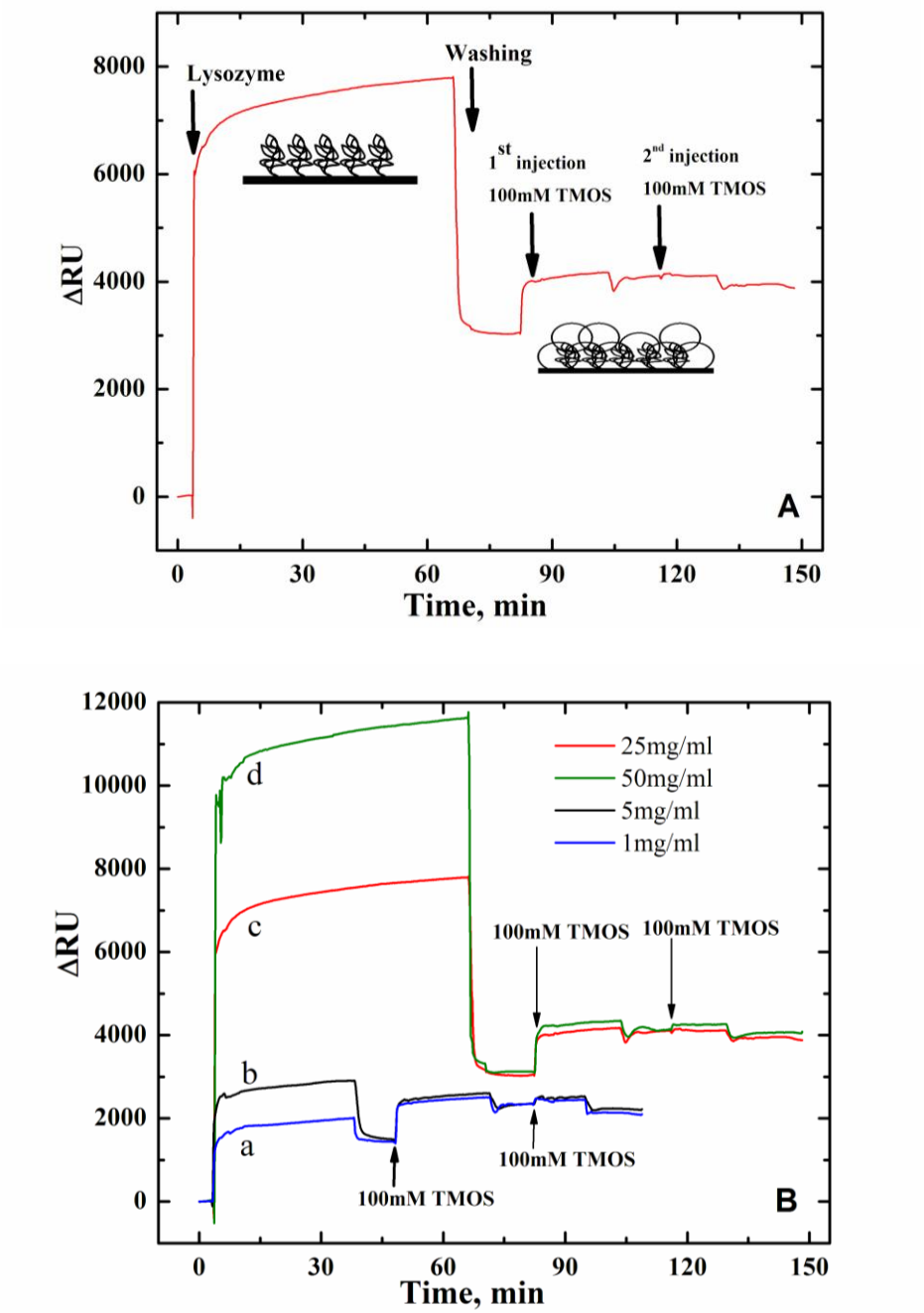

Figure 5-1: (a) SPR spectroscopy response showing the binding of lysozyme and formation of silica at the SPR surface. Sensorgram shows addition of 25 mg/ml lysozyme, followed by washing. 100mM TMOS was added as a precursor for silica formation. (b) Formation of lysozyme-mediated silica coating on gold. SPR response

of lysozyme deposited to the gold surface at a range of concentrations: 1 mg/ml (curve a), 5 mg/ml (curve b), 25 mg/ml (curve c) and 50 mg/ml (curve d). Addition of TMOS (100mM) is indicated by an arrow.

The bound lysozyme molecules mediated the formation of a silica adlayer *in situ*. Introduction of a solution of TMOS caused a rapid increase in RI, indicating changes in surface refraction consistent with the formation of a second distinct adlayer of silica (Figure 5-1b). The reaction was rapid and approximately 90% of silica formation occurred within the first minutes of contact. Washing the silica layer with buffer did not decrease the signal significantly, indicating that the silica was firmly attached to the surface. The change in the RI was used to calculate the deposition characteristics of the silica particles. The maximum thickness of the layer was calculated to be ~6.6 nm (Table 5-1).

[Lysozyme], mg/ml	Thickness of protein adlayer, d (nm)	Surface coverage (molecules/mm^2)	Thickness of silica adlayer, d (nm)
1	0.934	5.23E+10	3.74
5	0.978	5.47E+10	3.75
25	1.963	1.10E+11	6.56
50	2.029	1.14E+11	6.60

Table 5-1. Effect of lysozyme concentration on thickness of lysozyme and silica adlayers

The thickness of the silica layer did not increase following a second injection of TMOS suggesting that the surface was saturated with silica and conditions were not substrate limited. SEM analysis confirmed the formation of an interconnected, dense coating of silica nanospheres formed upon the gold surface. At low concentrations of

lysozyme, a scattered deposition of silica was observed with silica particles having an average size ~10 nm (Figure 5-2). When lysozyme was present in excess, however, dense coatings of interconnected aggregates of much larger silica particles (~230 nm) formed in addition to the initial monolayer of silica nanospheres (Figure 5-2c and d). In aqueous static suspensions, lysozyme forms silica spheres of approximately 570 nm diameter [15]. The reduction in size of the silica particles observed here is attributed the formation of the silica particles under continuous flow conditions. Silica spheres are the lowest free energy structure formed in a static environment, but application of a dynamic flow will affect the formation and aggregation of silica.

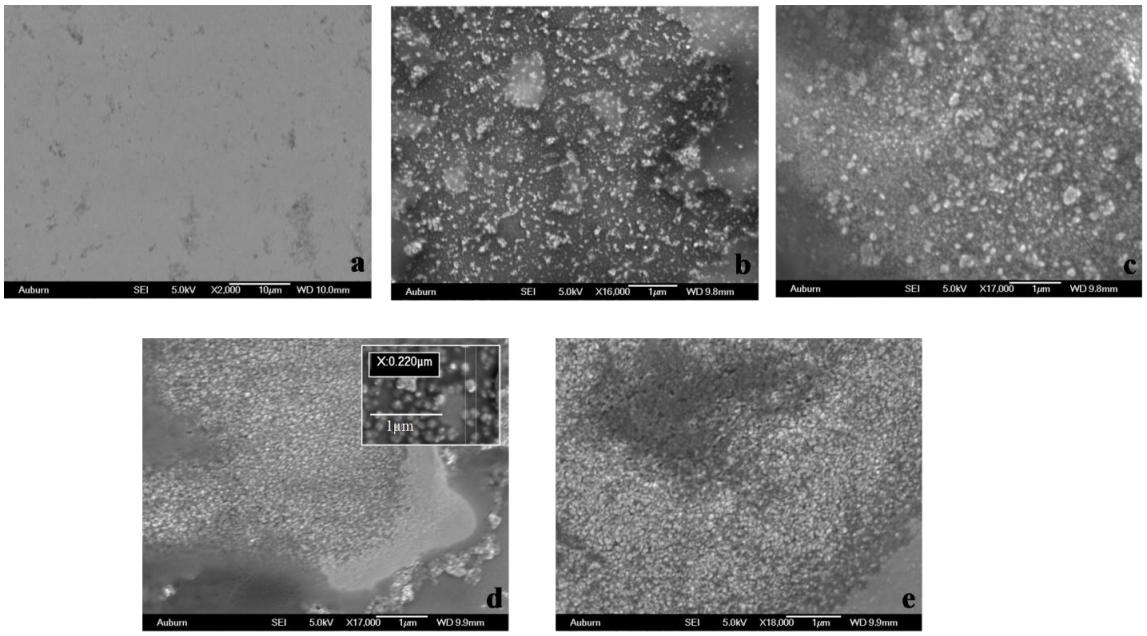

Figure 5-2: SEM images of silica-encapsulated OPH at the SPR surface. Gold surface modified with (a) lysozyme (25 mg/ml); (b) lysozyme (1 mg/ml) with 100mM TMOS; (c) lysozyme (5 mg/ml) with 100mM TMOS; (d) lysozyme (25 mg/ml) with 100mM TMOS; (e) lysozyme (25 mg/ml) with 100mM TMOS and OPH (0.1 mg/ml).

Even though the SEM shows the size of the nanoparticle as 230 nm the thickness measured by SPR for the silica layer is significantly less (~7 nm). The results are consistent with the immediate formation of a thin film of silica directly at the surface which provides a template for subsequent formation of larger silica particles, as observed for many silicification reactions [31]. The surface plasmon resonance phenomenon occurs at the metal–liquid interface and is highly sensitive to specific interactions at the interface which may be on the order of only a few nanometers. Although a generated evanescent wave can travel up to ~300 nm in the *z* direction [27], the medium beyond the interface will affect the observed RI. The inability to see the depth of the whole silica structure using SPR in the present work is in agreement with previous literature reports where silica layers of greater than 44 nm did not show significant SPR response [23].

The lysozyme is presumably attached at the surface in an orientation which does not diminish its ability to mediate silica formation. Variations in TMOS concentration may theoretically affect the thickness of the silica layer. Preliminary control experiments in static suspensions however, revealed that silica formation does not occur if the TMOS concentration is below 25mM (data not shown), accordingly, silica adlayer formation was not investigated at lower precursor concentrations. In control experiments, no formation of silica particles was observed in the absence of lysozyme. Bovine serum albumin (BSA) adsorbed to the gold surface but did not precipitate silica in the presence of TMOS, confirming that lysozyme is integral to the silica formation at the surface (data not shown).

5.3.2 Encapsulation of organophosphate hydrolase

The further biofunctionalization of the silica particles at the surface was investigated using organophosphate Hydrolase (OPH) as a model system. The gold surface was saturated with lysozyme as defined above and used to mediate the formation of silica particles containing various concentrations of OPH. The silica particles formed on the gold surface as described above and examination using SEM clearly showed that the surface was coated with a film of evenly distributed spheres (Figure 5-2e). The addition of OPH to the hydrolyzed TMOS solution did not result in any significant changes in the morphology of the silica surface (Figure 5-2d and e). OPH encapsulated within the silica coating maintains activity, confirmed by the hydrolysis of paraoxon and the activity of OPH correlates with protein concentrations used in the encapsulation step (Figure 5-3a). The kinetic parameters of the encapsulated enzyme were determined by contacting the encapsulated enzyme at the surface with paraoxon at a range of concentrations.

At low concentrations of paraoxon (20–100 μM), the silica-encapsulated OPH shows a linear response (Figure 5-3a) but enzyme activity becomes saturated at paraoxon concentrations above 300μM (Figure 5-3b). A reproducible detection limit of 20μM paraoxon was achieved with OPH concentrations greater than 0.05 mg/ml. A decrease in the concentration of encapsulated OPH resulted in a proportional reduction in detection sensitivity. The kinetic parameters of the encapsulated OPH (K_m = 0.09(±0.022)) were determined (Figure 5-3b) and are in good agreement with the kinetics of OPH in solution

[32] indicating that immobilization of OPH in silica does not significantly hinder the mass transport of substrate.

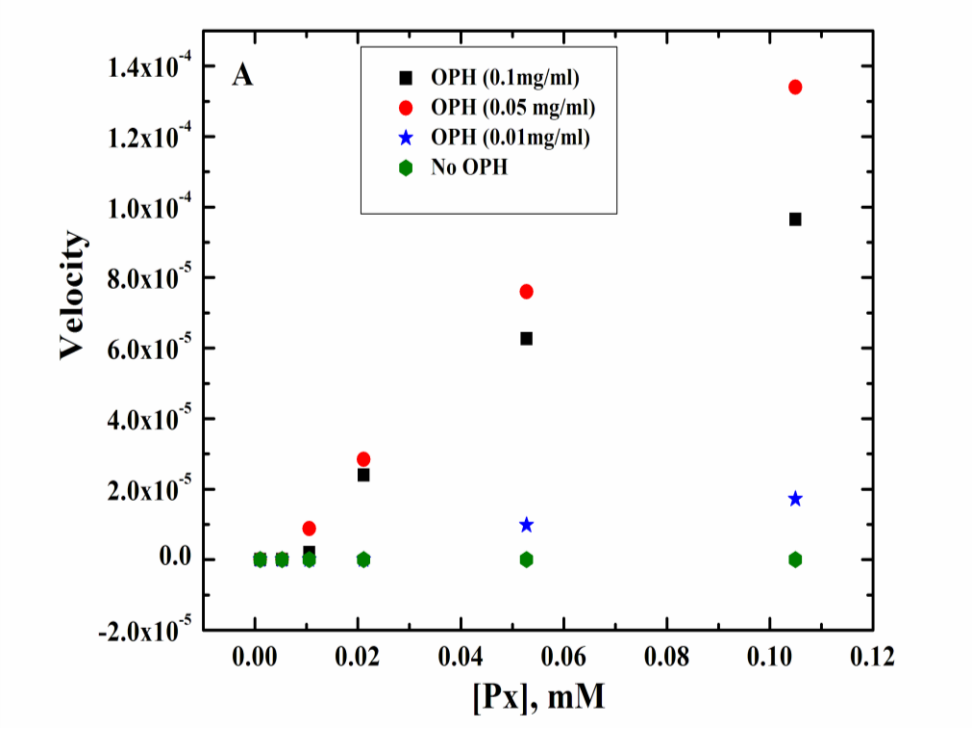

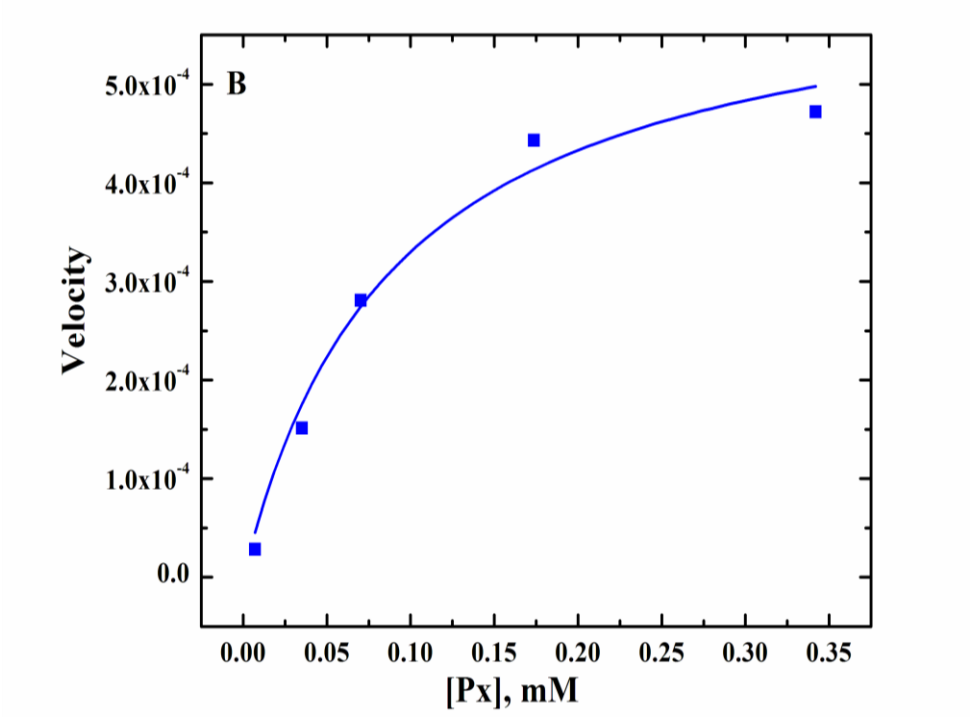

Figure 5-3: Paraoxon hydrolysis by silica-encapsulated organophosphate Hydrolase immobilized to the SPR surface. (a) Hydrolase activity in relation to OPH concentrations present during silicification step at a range of substrate concentrations. (b) Michaelis–Menten plot of immobilized OPH (0.5 mg/ml during silicification) to reveal maximal velocity of reaction.

5.4 CONCLUSION

The formation of silica using lysozyme precipitation provides a simple and rapid method for the deposition of silica films directly to a gold surface. The silica layer proved sufficiently stable under continuous flow conditions to allow measurement of enzyme kinetic parameters. The silica deposition and surface immobilization of OPH demonstrated in this study provides a model system with potential application to a range of formats. The surface encapsulated OPH could be reused continually for over 2 days, but lost activity gradually over the time period, concurrent with a loss of silica film thickness (data not shown). The immobilization efficiency and stability achieved were sufficient for demonstrating the concept, but further analysis of the silica coating is required to optimize the approach. The formation of a silica layer on the gold surface significantly increases the surface area at the transducer interface and potentially enhances the sensitivity of SPR spectroscopy applications [33]. The silica layer also proved suitable for encapsulation of OPH and the immobilized enzyme retained activity over a period of several hours, providing accurate and reproducible measurements of immobilized enzyme kinetics. The immobilization technique described provides a versatile method for enzyme encapsulation that selectively immobilizes proteins directly

on a transducer surface with no requirement for surface modification before immobilization. OPH is not directly tethered to the SPR surface, which may limit any restriction in the orientation of the active site, as often observed when enzymes are covalent attached to a surface.

The approach may lead to development of a versatile method for the immobilization of enzymes on an SPR transducer surface that might be applied to biosensors or protein microarrays [34-36]. In addition, the methodology developed for OPH immobilization on the gold surface may be applied to other electrochemical detection platforms.

5.5 REFERENCES

1. T. Laurell, J. Drott, and L. Rosengren, Silicon Wafer Integrated Enzyme Reactors, Biosensors and Bioelectronics 10 (1995) pp. 289-299.
2. A. Subramanian, S.J. Kennel, P.I. Oden, K.B. Jacobson, J. Woodward, and M.J. Doktycz, Comparison of Techniques for Enzyme Immobilization on Silicon Supports, Enzyme and Microbial Technology 24 (1999) pp. 26-34.
3. A. Vilkanauskyte, T. Erichsen, L. Marcinkeviciene, V. Laurinavicius, and W. Schuhmann, Reagentless Biosensors Based on Co-Entrapment of a Soluble Redox Polymer and an Enzyme within an Electrochemically Deposited Polymer Film, Biosensors and Bioelectronics 17 (2002) pp. 1025-1031.

4. R.H. Taylor, S.M. Fournier, B.L. Simons, H. Kaplan, and M.A. Hefford, Covalent Protein Immobilization on Glass Surfaces: Application to Alkaline Phosphatase, Journal of Biotechnology 118 (2005) pp. 265-269.

5. A.W. Flounders, A.K. Singh, J.V. Volponi, S.C. Carichner, K. Wally, A.S. Simonian, J.R. Wild, and J.S. Schoeniger, Development of Sensors for Direct Detection of Organophosphates.: Part Ii: Sol-Gel Modified Field Effect Transistor with Immobilized Organophosphate Hydrolase, Biosensors and Bioelectronics 14 (1999) pp. 715-722.

6. S.E. Letant, B.R. Hart, S.R. Kane, M.Z. Hadi, S.J. Shields, and J.G. Reynolds, Enzyme Immobilization on Porous Silicon Surfaces, Advanced Materials 16 (2004) pp. 689-693.

7. R.J. Green, R.A. Frazier, K.M. Shakesheff, M.C. Davies, C.J. Roberts, and S.J.B. Tendler, Surface Plasmon Resonance Analysis of Dynamic Biological Interactions with Biomaterials, Biomaterials 21 (2000) pp. 1823-1835.

8. J. Homola, S.S. Yee, and G. Gauglitz, Surface Plasmon Resonance Sensors: Review, Sensors and Actuators B: Chemical 54 (1999) pp. 3-15.

9. D.G. Myszka, Spr Biosensors as Biophysical Research Tools, Faseb Journal 14 (2000) pp. A1511-A1511.

10. Y.R. Kim, H.J. Paik, C.K. Ober, G.W. Coates, S.S. Mark, T.E. Ryan, and C.A. Batt, Real-Time Analysis of Enzymatic Surface-Initiated Polymerization Using Surface Plasmon Resonance (Spr), Macromolecular Bioscience 6 (2006) pp. 145-152.

11. J.-H. Kim, S. Roy, J.T. Kellis, A.J. Poulose, A.P. Gast, and C.R. Robertson, Protease Adsorption and Reaction on an Immobilized Substrate Surface, Langmuir 18 (2002) pp. 6312-6318.

12. H.J. Lee, A.W. Wark, and R.M. Corn, Creating Advanced Multifunctional Biosensors with Surface Enzymatic Transformations, Langmuir 22 (2006) pp. 5241-5250.

13. H.J. Lee, A.W. Wark, T.T. Goodrich, S. Fang, and R.M. Corn, Surface Enzyme Kinetics for Biopolymer Microarrays: A Combination of Langmuir and Michaelis-Menten Concepts, Langmuir 21 (2005) pp. 4050-4057.

14. C.D. Hodneland, Y.-S. Lee, D.-H. Min, and M. Mrksich, Supramolecular Chemistry and Self-Assembly Special Feature: Selective Immobilization of Proteins to Self-Assembled Monolayers Presenting Active Site-Directed Capture Ligands, Proceedings of the National Academy of Sciences 99 (2002) pp. 5048-5052.

15. H.R. Luckarift, M.B. Dickerson, K.H. Sandhage, and J.C. Spain, Rapid, Room-Temperature Synthesis of Antibacterial Bionanocomposites of Lysozyme with Amorphous Silica or Titania, Small 2 (2006) pp. 640-643.

16. J.N. Cha, K. Shimizu, Y. Zhou, S.C. Christiansen, B.F. Chmelka, G.D. Stucky, and D.E. Morse, Silicatein Filaments and Subunits from a Marine Sponge Direct the Polymerization of Silica and Silicones in Vitro, Proceedings of the National Academy of Sciences 96 (1999) pp. 361-365.

17. T. Coradin, P.J. Lopez, C. Gautier, and J. Livage, From Biogenic to Biomimetic Silica, Comptes Rendus Palevol 3 (2004) pp. 443-452.

18. N. Kroger, R. Deutzmann, and M. Sumper, Polycationic Peptides from Diatom Biosilica That Direct Silica Nanosphere Formation, Science 286 (1999) pp. 1129-1132.

19. H.R. Luckarift, J.C. Spain, R.R. Naik, and M.O. Stone, Enzyme Immobilization in a Biomimetic Silica Support, Nature Biotechnology 22 (2004) pp. 211-213.

20. J.M. Kleijn, D. Barten, and M.A. CohenStuart, Adsorption of Charged Macromolecules at a Gold Electrode, Langmuir 20 (2004) pp. 9703-9713.

21. C.A. Haynes and W. Norde, Globular Proteins at Solid/Liquid Interfaces, Colloids and Surfaces B: Biointerfaces 2 (1994) pp. 517-566.

22. T.J. Su, J.R. Lu, R.K. Thomas, Z.F. Cui, and J. Penfold, The Effect of Solution Ph on the Structure of Lysozyme Layers Adsorbed at the Silica-Water Interface Studied by Neutron Reflection, Langmuir 14 (1998) pp. 438-445.

23. S. Szunerits and R. Boukherroub, Electrochemical Investigation of Gold/Silica Thin Film Interfaces for Electrochemical Surface Plasmon Resonance Studies, Electrochemistry Communications 8 (2006) pp. 439-444.

24. D.K. Kambhampati, T.A.M. Jakob, J.W. Robertson, M. Cai, J.E. Pemberton, and W. Knoll, Novel Silicon Dioxide Sol-Gel Films for Potential Sensor Applications: A Surface Plasmon Resonance Study, Langmuir 17 (2001) pp. 1169-1175.

25. J.K. Grimsley, J.M. Scholtz, C.N. Pace, and J.R. Wild, Organophosphorus Hydrolase Is a Remarkably Stable Enzyme That Unfolds through a Homodimeric Intermediate, Biochemistry 36 (1997) pp. 14366-14374.

26. S. Balasubramanian, I.B. Sorokulova, V.J. Vodyanoy, and A.L. Simonian, Lytic Phage as a Specific and Selective Probe for Detection of Staphylococcus Aureus--a Surface Plasmon Resonance Spectroscopic Study, Biosensors and Bioelectronics 22 (2007) pp. 948-955.

27. L.S. Jung, C.T. Campbell, T.M. Chinowsky, M.N. Mar, and S.S. Yee, Quantitative Interpretation of the Response of Surface Plasmon Resonance Sensors to Adsorbed Films, Langmuir 14 (1998) pp. 5636-5648.

28. A.N. Naimushin, S.D. Soelberg, D.K. Nguyen, L. Dunlap, D. Bartholomew, J. Elkind, J. Melendez, and C.E. Furlong, Detection of Staphylococcus Aureus Enterotoxin B at Femtomolar Levels with a Miniature Integrated Two-Channel Surface Plasmon Resonance (Spr) Sensor, Biosensors and Bioelectronics 17 (2002) pp. 573-584.

29. J. Aizenberg, V.C. Sundar, A.D. Yablon, J.C. Weaver, and G. Chen, Biological Glass Fibers: Correlation between Optical and Structural Properties, Proceedings of the National Academy of Sciences of the United States of America 101 (2004) pp. 3358-3363.

30. B.D. Di Sioudi, C.E. Miller, K. Lai, J.K. Grimsley, and J.R. Wild, Rational Design of Organophosphorus Hydrolase for Altered Substrate Specificities, Chemico-Biological Interactions 119-120 (1999) pp. 211-223.

31. E.G. Vrieling, S. Hazelaar, W.W. Gieskes, Q. Sun, T.P. Beelen, and R.A.V. Santen, Silicon Biomineralization: Towards Mimicking Biogenic Silica Formation in Diatoms, Progress in Molecular and Subcellular Biology,Springer-Verlag, Berlin, 2003.

32. A.L. Simonian, A.W. Flounders, and J.R. Wild, Fet-Based Biosensors for the Direct Detection of Organophosphate Neurotoxins, Electroanalysis 16 (2004) pp. 1896-1906.

33. S. Oh, J. Moon, T. Kang, S. Hong, and J. Yi, Enhancement of Surface Plasmon Resonance (Spr) Signals Using Organic Functionalized Mesoporous Silica on a Gold Film, Sensors and Actuators B: Chemical 114 (2006) pp. 1096-1099.

34. T.-J. Lin, K.-T. Huang, and C.-Y. Liu, Determination of Organophosphorous Pesticides by a Novel Biosensor Based on Localized Surface Plasmon Resonance, Biosensors and Bioelectronics, Selected Papers from the 2nd International Meeting on Microsensors and Microsystems 22 (2006) pp. 513-518.

35. H. Huang and Y. Chen, Label-Free Reading of Microarray-Based Proteins with High Throughput Surface Plasmon Resonance Imaging, Biosensors and Bioelectronics 22 (2006) pp. 644-648.

36. M.-G. Kim, Y.-B. Shin, J.-M. Jung, H.-S. Ro, and B.H. Chung, Enhanced Sensitivity of Surface Plasmon Resonance (Spr) Immunoassays Using a Peroxidase-Catalyzed Precipitation Reaction and Its Application to a Protein Microarray, Journal of Immunological Methods 297 (2005) pp. 125-132.

6. SURFACE PLASMON RESONANCE INVESTIGATION OF SITE-ORIENTED PROTEIN BINDING ON THE GOLD SENSOR SURFACE

6.1 INTRODUCTION

Enzyme activity can be directly associated with sensor performance. If the active site is hindered, maximal enzyme activity cannot be attained. Therefore, oriented immobilization of enzymes plays a vital role when immobilizing enzymes onto solid supports. Oriented-immobilization provides insight into enzyme function and stability which are vital factors for enzyme-based biosensors [1-4]. Organophosphorus hydrolase (OPH) has been used extensively as a biocatalyst for development of biosensors to detect organophosphate neurotoxins [5-11]. For sensitive and specific detection of organophosphates, the binding and orientation of OPH on the sensor surface is of paramount importance. The current study investigates the relationship between the orientation of the OPH molecule on the sensor surface and its activity. To achieve this, linear peptides representing surface regions of OPH were used to create antipeptide antibodies which targeted different regions of OPH. One antibody (Ab#1) targets a region very near to the active site of the enzyme and the other two (Ab#2 and Ab#3) bind at regions away from the active site. It is predicted that binding near the active site would anchor the OPH molecule in a "face down" orientation, thus limiting active site access. Identifying the antipeptide antibodies which yield a surface with maximal activity allows

for evaluation of the impact that oriented immobilization may have on sensor sensitivity. Surface Plasmon Resonance was used to study the binding kinetics between OPH and the antibodies. All the experiments were performed using a commercially available SPR sensor (SPREETA™). The antibody (Ab#2) was investigated first since it allows better orientation of OPH for maximum accessibility to substrate. Rabbit anti-chicken IgG and Protein-G were utilized to properly bind the antibody on the gold surface. The dissociation constants of the OPH-antibody complexes were calculated. These studies have provided us with more detailed information on the orientation of immobilized OPH. In addition, it has enabled development of better surface immobilization of OPH on sensor surfaces for biosensor applications.

6.2 EXPERIMENTAL

6.2.1 Materials

Protein G was purchased from Pierce, Rockford, IL and BSA was obtained from Fisher Scientific, Suwanee, GA. The rabbit anti-chicken IgG was purchased from Jackson ImmunoResearch Laboratories, Inc., West Grove, PA. Purified OPH and the chicken anti-OPH were provided by J. Wild's group, Texas A&M University, College Station, TX. Paraoxon was purchased from ChemService, Inc., West Chester, PA. The buffer was prepared using water generated from Millipore Direct-Q Water system (Resistivity, 18 $M\Omega/cm^2$). All the samples were prepared in 0.01M PBS (0.138M NaCl, 0.0027M KCl) pH 7.4 buffer.

6.2.2 Antibody Binding Regions on OPH

Three different antibodies (Ab#1, Ab#2, and Ab#3) were made against OPH in chicken. The binding regions of these antibodies on OPH surface is shown in the Figure 6-1. The red region indicates the binding region of Ab#1 and the blue indicate the region where Ab#2 and Ab#3 bind. The yellow denotes the active site of the enzyme.

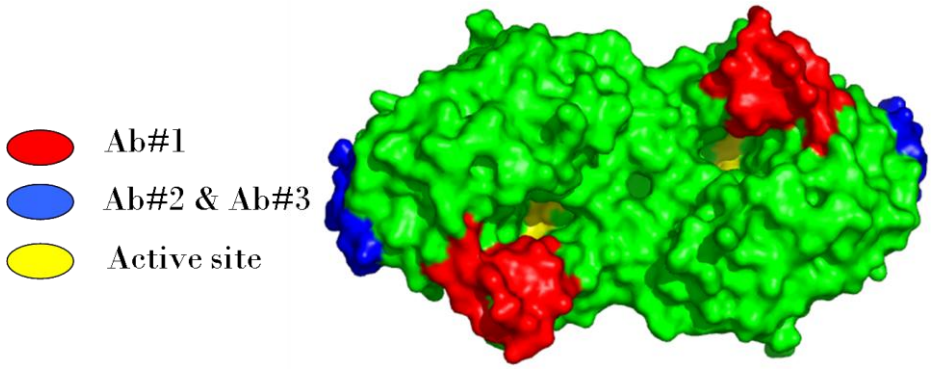

Figure 6-1: Antibody binding epitopes on OPH

Because Ab#1 binds very near to the active site of OPH, we suspect that when OPH is bound to any surface through this particular antibody, it anchors the molecule down i.e. it restricts the free entry of substrate to the active site. Therefore the activity of OPH would be expected to be less when compared to the binding through Ab#2 and Ab#3 which bind away from the active site rendering flexibility for the entry of the substrate (Figure 6-2).

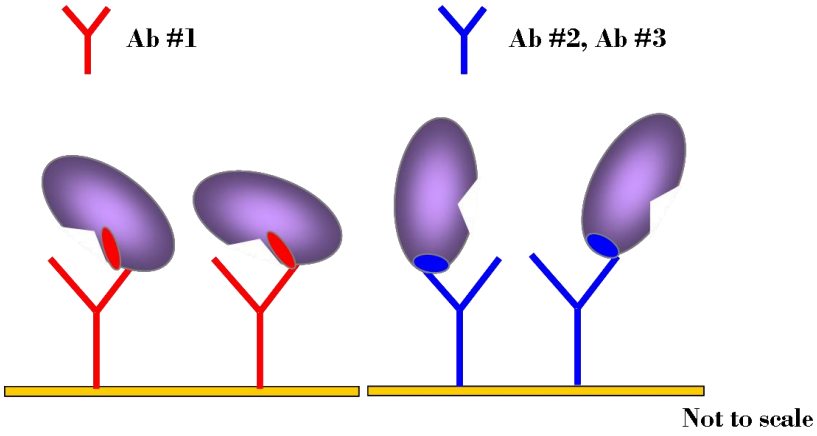

Figure 6-2: Effect of orientation of OPH on kinetic behavior

6.2.3 Binding constant calculation

Binding constants were accomplished using SPR on a Seattle instrument at room temperature. The following figure (Figure 6-3) shows the sequence of formation of the sensing layer on the SPREERA surface to determine the binding constant of the three antibodies towards OPH. Because these antibodies were made against chicken, Protein G could not be used directly to orient the antibodies on the surface. Therefore to accomplish this, secondary rabbit anti-chicken antibodies were used for proper orientation of the primary antibodies on the sensor surface. BSA was used for non-specific blocking.

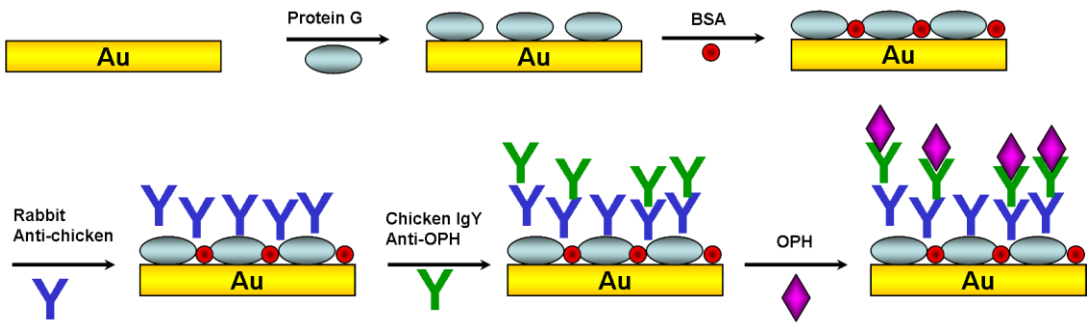

Figure 6-3: Sequence of binding layer construction on sensor surface

6.2.4 SPREETA Preparation

The sensor surface was cleaned with piranha solution followed by rinsing and sonication with Milli-Q water. The sensor was then initialized in air and water, followed by *in-situ* cleaning with NaOH-TritonX. After establishing a baseline with PBS, Protein G (0.1mg/ml) was non-specifically adsorbed on the gold surface. BSA (1 mg/ml) and PBS-Tween was used to block remaining sites, followed by specific immobilization of rabbit anti-chicken antibody. The primary antibody (Ab#1, Ab#2 or Ab#3) was introduced only in the working channel and PBS in the control channel. Varying concentrations of OPH (4.74E-11 - 2.8E-06 M) were introduced though both channels. Known concentrations of paraoxon were introduced to determine the activity of the immobilized OPH.

6.2.5 Calculation of adlayer thickness and surface coverage

The adlayer thickness and surface coverage of each monolayer was calculated using the formula described by [12, 13]; $d_a = (l_d/2)\times[(n_{eff} - n_b)/(n_a - n_b)]$, where d_a is the thickness of the adlayer, l_d the characteristic decay length of an evanescent wave at 307 nm, n_{eff} the effective RI of the adlayer (from the SPR signal), n_b the RI of the buffer (from reference reading), and n_a is the RI of the adlayer material assuming an RI of 1.57 for proteins. The surface coverage (g/mm^2) = $d_a\times$ density (~1.3×10^{-3} g/mm^3) and surface coverage (molecules/mm^2) = [surface coverage (g/mm^2) × Avagadro number]/ Mol. Wt.

6.2.6 Immobilized Enzyme Activity

Paraoxon, 0.0106-0.53 mM, was circulated across the surface at a flow rate of 105µl/min for 2 min. Activity was measured by collecting 200 µl of flow through, measuring the absorbance of *p*-nitrophenol thus formed at 405nm, after the two minute circulation. Absorbance change was recorded using a 2100 Ultrospec Pro UV-vis spectrophotometer.

6.3 RESULTS AND DISCUSSION

6.3.1 Binding constants

A 1:1 complex model was assumed for calculation of the dissociation constants for all three antibodies. Response curves for all antibodies were obtained and results presented in Table 6-1. The affinity of OPH towards Ab#2 was higher when compared to the other two antibodies.

Antibody	K_d, M	Orientation of OPH
Ab#1	9.97E-08	
Ab#2	1.15E-10	
Ab#3	2.64E-07	

Table 6-1: Dissociation constants for the OPH antibodies

6.3.2 Kinetics of immobilized OPH

From the real time sensorgram of the surface construction, the surface coverage of the antibodies and OPH was calculated (Table 6-2).

Antibody	Surface coverage, Ab's, molecules/mm^2	Surface coverage OPH, molecules/mm^2
Ab#1	1.37 E+09	2.25 E+09
Ab#2	1.61 E+09	3.12 E+09
Ab#3	1.07 E+09	7.99 E+08

Table 6-2: Surface coverage of OPH and Anti-OPH

OPH bound through Ab#1 covers the sensor surface resulting in only 72 % as many OPH molecules immobilized though Ab#2 on the surface. The Michaelis-Menton plot was constructed for the activity data and as expected the activity of OPH bound through Ab#2 and Ab#3 was higher when compared to Ab#1 (Figure 6-4). The specific activity per mm^2 of immobilized OPH is 7.5E-14, 1.1E-13 and 3.2E-13 μmol/sec for Ab#1, Ab#2 and Ab#3 respectively at a paraoxon concentration of 0.106 mM.

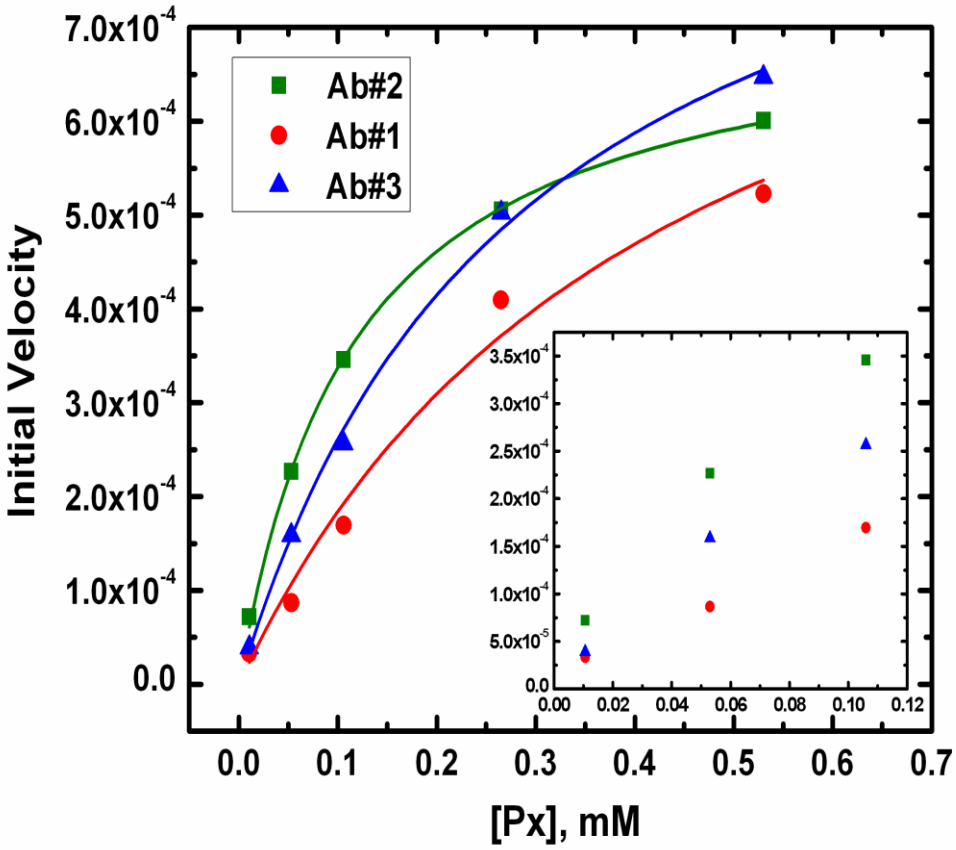

Figure 6-4: Activity of OPH immobilized through antipeptide antibodies

6.4 CONCLUSION

In this study, OPH was immobilized on the sensor surface through antipeptide antibodies and it was demonstrated that maximal activity of OPH can be obtained through site-specific orientation thereby yielding higher sensitivity of detection. The OPH antibodies created for this study were not stable for long periods of time and did not have very high affinity. Therefore, in the future improved sensor performance can be achieved by synthesizing higher affinity antipeptide antibodies.

6.5 REFERENCES

1. A.A. Karyakin, G.V. Presnova, M.Y. Rubtsova, and A.M. Egorov, Oriented Immobilization of Antibodies onto the Gold Surfaces Via Their Native Thiol Groups, Analytical Chemistry 72 (2000) pp. 3805-3811.
2. J.H. Kang, H.J. Choi, S.Y. Hwang, S.H. Han, J.Y. Jeon, and E.K. Lee, Improving Immunobinding Using Oriented Immobilization of an Oxidized Antibody, Journal of Chromatography A 1161 (2007) pp. 9-14.
3. J. Turkova, Oriented Immobilization of Biologically Active Proteins as a Tool for Revealing Protein Interactions and Function, Journal of Chromatography B 722 (1999) pp. 11-31.
4. S.V. Rao, K.W. Anderson, and L.G. Bachas, Oriented Immobilization of Proteins, Mikrochimica Acta 128 (1998) pp. 127-143.
5. S. Paliwal, M. Wales, T. Good, J. Grimsley, J. Wild, and A. Simonian, Fluorescence-Based Sensing of P-Nitrophenol and P-Nitrophenyl Substituent Organophosphates, Analytica Chimica Acta 596 (2007) pp. 9-15.
6. M. Ramanathan and A.L. Simonian, Array Biosensor Based on Enzyme Kinetics Monitoring by Fluorescence Spectroscopy: Application for Neurotoxins Detection, Biosensors & Bioelectronics 22 (2007) pp. 3001-3007.
7. R.P. Deo, J. Wang, I. Block, A. Mulchandani, K.A. Joshi, M. Trojanowicz, F. Scholz, W. Chen, and Y.H. Lin, Determination of Organophosphate Pesticides at a Carbon Nanotube/Organophosphorus Hydrolase Electrochemical Biosensor, Analytica Chimica Acta 530 (2005) pp. 185-189.

8. J. Kumar, S.K. Jha, and S.F. D'Souza, Optical Microbial Biosensor for Detection of Methyl Parathion Pesticide Using Flavobacterium Sp Whole Cells Adsorbed on Glass Fiber Filters as Disposable Biocomponent, Biosensors & Bioelectronics 21 (2006) pp. 2100-2105.

9. B.J. White and H.J. Harmon, Optical Solid-State Detection of Organophosphates Using Organophosphorus Hydrolase, Biosensors & Bioelectronics 20 (2005) pp. 1977-1983.

10. E.I. Rainina, E.N. Efremenco, S.D. Varfolomeyev, A.L. Simonian, and J.R. Wild, The Development of a New Biosensor Based on Recombinant E-Coli for the Direct Detection of Organophosphorus Neurotoxins, Biosensors & Bioelectronics 11 (1996) pp. 991-1000.

11. A.L. Simonian, T.A. Good, S.S. Wang, and J.R. Wild, Nanoparticle-Based Optical Biosensors for the Direct Detection of Organophosphate Chemical Warfare Agents and Pesticides, Analytica Chimica Acta 534 (2005) pp. 69-77.

12. L.S. Jung, C.T. Campbell, T.M. Chinowsky, M.N. Mar, and S.S. Yee, Quantitative Interpretation of the Response of Surface Plasmon Resonance Sensors to Adsorbed Films, Langmuir 14 (1998) pp. 5636-5648.

13. A.N. Naimushin, S.D. Soelberg, D.K. Nguyen, L. Dunlap, D. Bartholomew, J. Elkind, J. Melendez, and C.E. Furlong, Detection of Staphylococcus Aureus Enterotoxin B at Femtomolar Levels with a Miniature Integrated Two-Channel Surface Plasmon Resonance (Spr) Sensor, Biosensors and Bioelectronics 17 (2002) pp. 573-584.

7. ORIENTATION-SPECIFIC ATTACHMENT OF ORGANOPHOSPHORUS HYDROLASE ON BIOSENSOR SURFACES

7.1 INTRODUCTION

By choosing an appropriate enzyme with well defined interactions with organophosphorus compounds, decontamination and biosensor applications can be afforded both high specificity and high sensitivity. Organophosphorus hydrolase (OPH) is an enzyme capable of degrading a wide array of organophosphate pesticides and nerve agents [1-7] and this ability makes it ideal for many detection and decontamination purposes.

Several approaches are available when immobilizing enzymes in decontamination and detection applications, the simplest being a mixture. OPH has been successfully used to decontaminate surfaces when incorporated in fire fighting foams and latex paints [8, 9]. This strategy circumvents the problems of using caustic agents on large areas. Slightly more complicated, but still requiring no modification of the enzyme, is entrapment. Encapsulation of the enzyme in murine erythrocytes by hypotonic dialysis has been shown to be successful at degrading pesticides [10]. An optical technique utilizing poly(ethylene glycol) hydrogel-encapsulated OPH was able to detect paraoxon at levels as low as 16 nM (0.004 ppm) using pH sensitive seminapthofluorescein

(SNAFL) [11]. Cryoimmobilization of *E. coli* cells expressing OPH have been used to detect paraoxon as low as 1×10^3 nM (0.25 ppm) using a potentiometer biosensor [12].

Other slightly more sophisticated methods of immobilizing OPH, yet still non-covalent, include using self assembled chitosan/poly(thiophene-3-acetic acid) layers allowed for the detection of paraoxon at levels as low as 1.0 nM [13]. Concentrations as low as 0.028 nM (7 ppt) paraoxon have been detected using OPH-cellulose binding domain fusions proteins, and is reported to retain similar kinetic characteristics as the free enzyme when immobilized [14]. Although entrapment and non-covalent attachment offer ease of construction for decontamination or detection surfaces, the ideal surface would be durable and reusable. It is these features which make covalent attachment the most desirable. The studies mentioned above were predominantly non-covalent, relying on hydrophobic interactions, electrostatic attractions, or physical containment to immobilize an enzymatic fraction, whether whole cells or purified enzymes.

Covalent attachment relies on chemical modification of side chains exposed at the enzyme's surface. Cystamine-glutaraldehyde immobilization has been used in an amperometric detection system [15, 16], relying on the detection of pH change resulting from the release of protons when OPH hydrolyses substrates. OPH has been immobilized in photosensitive polyethylene glycol (PEG) gels, which employs both covalent attachment and physical entrapment [17]. The reversible inhibition of OPH has been utilized for the development of an optical sensor that detects substrate binding and not hydrolysis of target compounds [18]. In this system, purified enzyme is immobilized on a glass surface through glutaraldehyde activation of lysines. Introduction of a substrate

results in the competitive displacement of the porphyrin bound in the active site and the change in the porphyrin absorption spectrum was observed.

Immobilization strategies are as varied as the intended applications and all will have advantages and disadvantages that would preclude the use of a single technique. A recent extensive review details the use of OPH, as well as other enzymes, in biomaterials for detection and decontamination of chemical warfare agents [19]. To address the issue of efficiency of the immobilized enzyme, this study presents a method to further refine surface construction by the orientation-specific attachment of OPH. Such attachment should facilitate movement of substrates and products to and from the active site as well as prevent restriction of secondary structure near the active site.

7.2 EXPERIMENTAL

7.2.1 Variant design

To aid in the selection of residues for substitution, two methods were employed to calculate solvent accessibility of the lysine residues from the 1DPM PDB file. First, parameter optimized surfaces analysis (POPS) was used to calculate an approximation of area of the first solvation shell for each lysine residue [20]. Secondly, *pfis* calculations were performed to determine the degree of burial, specifically of the ζ-N, of each lysine residue [21].

7.2.2 Site directed mutagenesis

The pUC19 plasmid containing the wild type gene (pOP419) [7] was used as the template, and OPH mutation was made with the QuickChange™ site-directed

mutagenesis kit (Stratagene, LaJolla, CA). Non-homologous, non-overlapping primers were synthesized by Integrated DNA Technologies, Inc. (Coralville, IA) and used for the mutagenesis reactions. The primers used to construct the variant were 5' aaaggggtcgcgcagcctgtggtc 3', 5' gaccacaggctgcgcgacccctttca 3. The mutated plasmids were sequenced to ensure the fidelity of the PCR reactions. Electrophoretic separation and analysis was performed by the Gene Technology Laboratory of Texas A&M University, the resulting sequence data was analyzed with Vector NTI software (Stratagene, LaJolla, CA).

7.2.3 Enzyme purification & biotinylation

Enzymes were purified as previously described [22]. Purified enzymes were concentrated to greater than 1 mg/ml for storage at 4 °C in the final column buffer (10 mM KPO_4, 20 mM KCl, 50 µM $CoCl_2$, pH 8.3). Protein concentration was determined by using an extinction coefficient of 58,000 $M^{-1}cm^{-1}$, when measuring absorbance at 280 nm. Purity was verified by SDS-PAGE.

Enzymes WT and K175A (1 mg/ml) were incubated with equal concentrations of Biotin (Pierce, Rockford, IL) in 5% DMSO, 10 mM KPO_4 pH 8.3 overnight on a shaker at 4 ºC. Unbound biotin was removed by overnight dialysis against 500mL, 10 mM KPO_4 (pH 8.3) at 4 ºC.

7.2.4 Enzyme activity assay

Substrates used in this study were paraoxon and demeton-S (ChemService) and the free thiol reporter for the demeton-S assays was 2,2' Dithiodipyridine (2,2' TP).

Michaelis constants (K_M) and the catalytic rates (k_{cat}) for paraoxon and demeton-S were determined by performing enzymatic assays with varying concentrations of substrate and constant enzyme concentrations. The activity of the biotinylated enzymes was measured in a similar fashion with paraoxon as the substrate.

Paraoxon hydrolysis was followed by measuring the appearance of the *p*-nitrophenol anion at 400 nm (ε = 17, 000 $M^{-1}cm^{-1}$) in 20 mM CHES (pH 9.0) at 25 °C, and initial velocities were calculated and fit to the Michaelis-Menten equation, allowing for substrate inhibition (Eq 1).

$$v_o = \frac{V_{max} \times S}{K_M + (S \times (1 + \frac{S}{K_i}))} \quad (1)$$

Demeton-S hydrolysis was followed by the appearance of the 2,2' TP anion at 343 nm (ε = 7,060 $M^{-1}cm^{-1}$) in tripart buffer, pH 8.0 [23] and initial velocities were calculated and fit to the Michaelis-Menten (Eq 2).

$$v_o = \frac{V_{max} \times S}{K_M + S} \quad (2)$$

7.2.5 SPREETA preparation and sensing layer construction

The sensor surface was cleaned with piranha solution (3:1 mixture of sulfuric acid and 30% hydrogen peroxide, Note- Extreme caution has to be taken while handling piranha, it is a very strong oxidant and reacts violently with organic matter) followed by rinsing and sonication with Milli-Q water. The sensor was then initialized in air and water, followed by *in-situ* cleaning with NaOH-TritonX. After establishing a baseline with PBS, neutra-avidin (1mg/ml) was non-specifically adsorbed on the gold surface.

BSA (1 mg/ml) was used to block the remaining sites, followed by specific immobilization of biotinylated enzymes (WT, K175A – 1 mg/ml).

7.2.6 Calculation of surface coverage

The amount of enzyme covering the surface of the sensor was calculated using the equations described by (Eq. 3 and 4) [24, 25]. The thickness of the adsorbed layer (ad-layer) is calculated using;

$$d_a = (\frac{l_d}{2}) \times (\frac{n_{eff} - n_b}{n_a - n_b}) \qquad (3)$$

where d_a is the thickness of the ad-layer, l_d is the characteristic decay length of an evanescent wave at 307nm, n_{eff} is the effective RI of the ad-layer (from SPR signal), n_b is the RI of the buffer (1.333) and n_a is the RI of the proteins, 1.57. Surface coverage is calculated using the thickness and density of the protein;

$$surface\text{cov}erage(g/mm^2) = thickness(d_a) \times density(\sim 1.3 \times 10^{-3} g/mm^3)$$
$$surface\text{cov}erage(molecules/mm^2) = (\frac{surface\text{cov}erage(g/mm^2) \times avogadronumber}{mol.wt}) \qquad (4)$$

7.2.7 Immobilized enzyme activity

Paraoxon, 0.048-0.462 mM, was circulated across the surface using a flow rate of 100 µl/min for 2 min. Activity was determined by collecting 200 µl of the flow through and measuring the absorbance at 405 nm of the *p*-nitrophenol product.

7.3 RESULTS

7.3.1 Structural analysis

There are eight lysines per monomer in OPH. Of these, K169 is carboxylated and buried in the active site where it serves as a bridging ligand for the binuclear metal center. K82 is a surface residue; however, the ζ-N is only partially exposed. The remaining lysines are accessible and are the more probable attachment sites. Parameter optimized surfaces analysis (POPS) of the 1dpm PDB structure (Table 7-1) shows that K175 has 209.6 square angstroms of solvent accessible surface area (SASA) [20]. The percent burial of the ζ-N of K175 was calculated by *pfis* to be -8.2%, indicating a completely exposed side chain [21]. In cases of extremely exposed side chains in a protein, the algorithm can calculate negative values, which result from using the model tripeptide, Gly-X-Gly to represent a fully exposed side chain. Taken together, these data suggest that K175 should be the most likely residue for a biotinylation site, having a large amount of solvent exposed surface area and an exposed ζ-N, indicating the side chain is perpendicular to the enzyme surface.

Lys Residue	Hydrophobic	Hydrophilic	Total
77	94.4	54.9	149.3
82	48.2	13.5	61.7
169	11.8	10.4	22.2
175	142.4	67.2	209.6
185	33.2	36.3	69.5
285	37.2	29.6	66.8
294	102.4	63.0	165.4
339	42.7	58.4	101.2

Table 7-1: Solvent accessible surface area of OPH lysine residues in square angstroms

7.3.2 Enzyme activity in solution

The K175A variant is kinetically similar to wild type in solution assays, having a k_{cat} of 3100 s^{-1} and K_M of 0.05 mM giving a catalytic efficiency of 6.2 $\times 10^7$ compared to 1 $\times 10^8$ for the wild type. It is more susceptible to substrate inhibition, with a K_I of 6.1 mM versus 17 mM for the wild type. With demeton-S, K175A has a k_{cat} of 2 s^{-1} and K_M of 3.1 mM giving a catalytic efficiency of 558 compared to 870 for the wild type, which has a k_{cat} of 35 s^{-1} and a K_M of 0.04 mM.

7.3.3 Surface construction and immobilized activity

From the real time sensorgram of the surface construction (Figure 7-1), the surface coverage of the enzymes was calculated. K175A covers the sensor surface at $1.8\times10^{10} \pm 9.2\times10^8$ mm^{-2} and the WT covers the surface at a concentration of $2.16\times10^{10} \pm$

7.3×10^{8} mm^{-2}, resulting in only 83% as many K175A molecules immobilized on the surface. The specific activity per mm^2 of immobilized K175A is $5.22\times10^{-15} \pm 2.8\times10^{-16}$ $\mu mol\times s^{-1}$ and the WT is $4.30\times10^{-15} \pm 1.3\times10^{-16}$ $\mu mol\times s^{-1}$ at a paraoxon concentration of 0.05 mM.

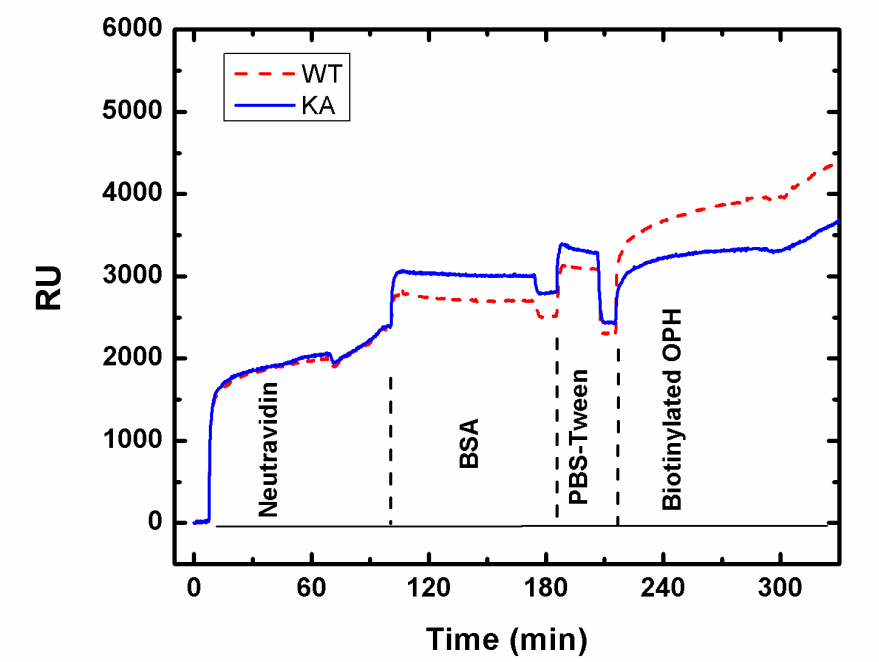

Figure 7-1: SPR sensorgram of surface assembly

7.3.4 Comparison of enzyme activity on surface and in solution

The activity of the biotinylated WT and K175A was measured both in solution and on the surface. The kinetic constants were determined using a Michaelis-Menton plot of initial reaction rates of free or immobilized enzyme (Table 7-2). The biotinylated WT has ~ 48% more activity in solution than K175A (Figure 7-2) while when attached to the surface, the activity of K175A was found to be 18% higher than the WT enzyme.

Kinetic Parameters	Solution		Surface	
	WT	KA	WT	KA
V_{max}	$0.00005\pm1.5\times10^{-6}$	$0.00003\pm1.4\times10^{-6}$	$0.00044\pm1.6\times10^{-4}$	$0.00055\pm1.6\times10^{-4}$
K_m	0.0434±0.005	0.0624±0.008	0.1854±0.094	0.2278±0.089
k_{cat}	206.9	108		
k_{cat}/K_m	4.8×10^{6}	1.7×10^{6}		

Table 7-2: Kinetic constants for the immobilized and bulk enzymes

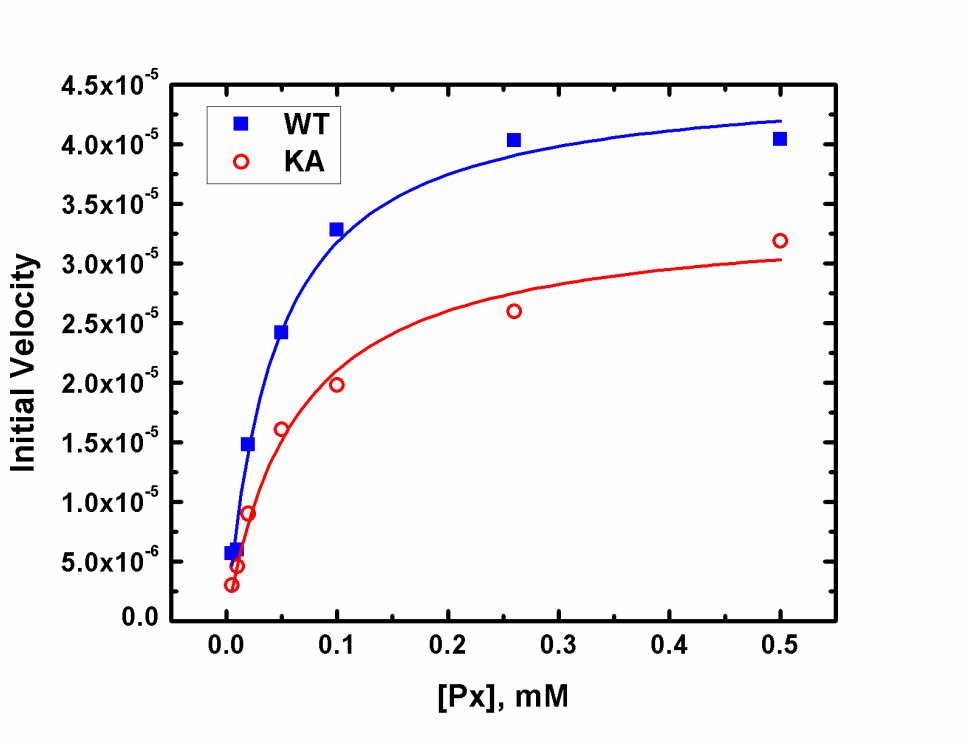

Figure 7-2: M-M plot for biotinylated WT and K175A in solution

A calibration graph (Figure 7-3) for the activity of the immobilized enzymes against the paraoxon concentration was obtained. A linear model was fit to the KA ($Y= 6.4\times10^{-16} + 9.2\times10^{-14} * X$, $R = 0.9979$) and WT ($Y = 6.9\times10^{-16} + 6.9\times10^{-14} * X$, $R =$

0.9996) data. This confirms the hypothesis that the removal of K175 lysine leads to increased accessibility of the substrate to and from the active site, thereby increasing the catalytic efficiency of the enzyme.

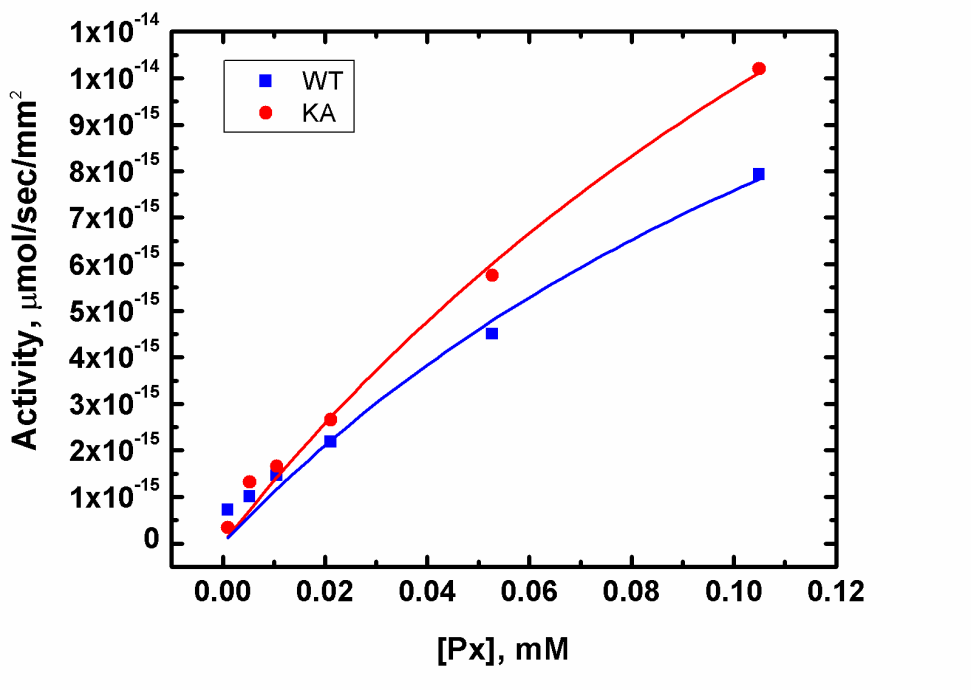

Figure 7-3: Activity of biotinylated WT and K175A on surface

7.4 DISCUSSION

Biotin forms an amide bond with the ζ-N of solvent exposed lysine side chains (Figure 8-4). Ordering the lysine residues based on solvent accessible surface areas and the degree of exposure of the ζ-N allows a comparison of the likelihood any given side chain will be biotinylated. The more solvent accessible surface area (SASA) and more exposed the ζ-N, the higher probability of biotinylation. The most exposed surface lysine in OPH is K175. Its proximity to the active site could conceivably inhibit the movement of substrates and products in and out of the active site if the enzyme were immobilized through this side chain in an essentially "face down" manner.

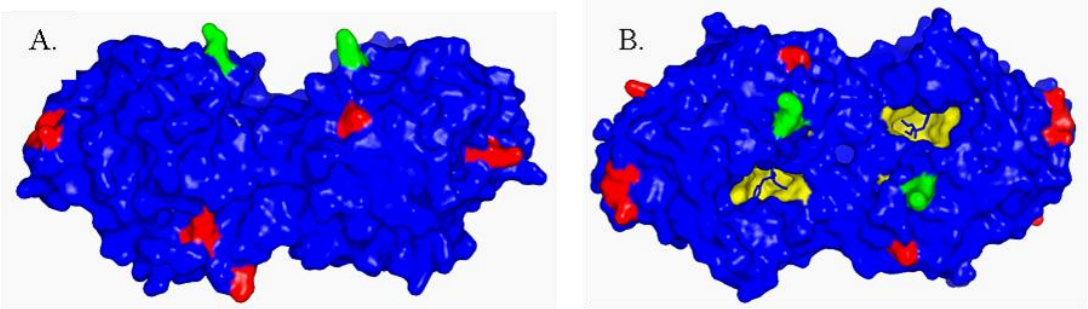

Figure 7-4: A. Solvent exposed lysine side chains of OPH. K175 is shown in green, others in red. B. The active site is shown in yellow to show the proximity to K175

The activity of K175A is 18% greater than that of the WT enzyme after immobilization on a surface, when the number of protein molecules per mm^2 is taken into account. The increased efficiency could be the result of orientation, whereby the active site is facing the bulk solvent. Alternatively, increased flexibility in the secondary structure near the active site, by not being immobilized through residue 175, could allow for a more efficient enzyme on a surface.

7.5 CONCLUSION

In conclusion, the orientation-specific attachment of an enzyme, Organophosphorus Hydrolase was studied for biosensor applications. A substitution in the wild-type enzyme led to a higher catalytic efficiency of the enzyme when surface attached, as determined by SPR. By selectively removing attachment sites, in this case a lysine, from the protein surface, the enzyme molecules can be site-specifically attached, and thus, the orientation of the protein molecules on the surface can be controlled. In addition, these studies highlight the loss of activity that is often observed with covalent modification.

7.6 REFERENCES

1. M.M. Benning, J.M. Kuo, F.M. Raushel, and H.M. Holden, Three-Dimensional Structure of Phosphotriesterase: An Enzyme Capable of Detoxifying Organophosphate Nerve Agents, Biochemistry 33 (1994) pp. 15001-15007.
2. M.M. Benning, S.-B. Hong, F.M. Raushel, and H.M. Holden, The Binding of Substrate Analogs to Phosphotriesterase, J. Biol. Chem. 275 (2000) pp. 30556-30560.
3. B.D. Di Sioudi, C.E. Miller, K. Lai, J.K. Grimsley, and J.R. Wild, Rational Design of Organophosphorus Hydrolase for Altered Substrate Specificities, Chemico-Biological Interactions 119-120 (1999) pp. 211-223.
4. M. Chen-Goodspeed, M. Sogorb, and F.M. Raushel, Determining Reactivity and Stereospecificity of Phosphotriesterase from Pseudonomas Diminuta by Site-Specific Mutagenesis, Faseb Journal 13 (1999) pp. A1446-A1446.
5. M. Chen-Goodspeed, M.A. Sogorb, F. Wu, S.-B. Hong, and F.M. Raushel, Structural Determinants of the Substrate and Stereochemical Specificity of Phosphotriesterase, Biochemistry 40 (2001) pp. 1325-1331.
6. S.B. Hong and F.M. Raushel, Control of Stereoselectivity in Phosphotriesterase, Protein Engineering 388 (2004) pp. 256-266.
7. K.H. Lai, K.I. Dave, and J.R. Wild, Bimetallic Binding Motifs in Organophosphorus Hydrolase Are Important for Catalysis and Structural Organization, Journal of Biological Chemistry 269 (1994) pp. 16579-16584.
8. K.E. LeJeune and A.J. Russell, Biocatalytic Nerve Agent Detoxification in Fire Fighting Foams, Biotechnology and Bioengineering 62 (1999) pp. 659-665.

9. C.S. McDaniel, J. McDaniel, M.E. Wales, and J.R. Wild, Enzyme-Based Additives for Paints and Coatings, Progress in Organic Coatings, Coatings Science International Conference Program 55 (2006) pp. 182-188.

10. L. Pei, G. Omburo, W.D. Mcguinn, I. Petrikovics, K. Dave, F.M. Raushel, J.R. Wild, J.R. Deloach, and J.L. Way, Encapsulation of Phosphotriesterase within Murine Erythrocytes, Toxicology and Applied Pharmacology 124 (1994) pp. 296-301.

11. R.J. Russell, M.V. Pishko, A.L. Simonian, and J.R. Wild, Poly(Ethylene Glycol) Hydrogel-Encapsulated Fluorophore-Enzyme Conjugates for Direct Detection of Organophosphorus Neurotoxins, Anal. Chem. 71 (1999) pp. 4909-4912.

12. E.I. Rainina, E.N. Efremenco, S.D. Varfolomeyev, A.L. Simonian, and J.R. Wild, The Development of a New Biosensor Based on Recombinant E. Coli for the Direct Detection of Organophosphorus Neurotoxins, Biosensors and Bioelectronics 11 (1996) pp. 991-1000.

13. C.A. Constantine, S.V. Mello, A. Dupont, X. Cao, D. Santos, O.N. Oliveira, F.T. Strixino, E.C. Pereira, T.-C. Cheng, J.J. Defrank, and R.M. Leblanc, Layer-by-Layer Self-Assembled Chitosan/Poly(Thiophene-3-Acetic Acid) and Organophosphorus Hydrolase Multilayers, J. Am. Chem. Soc. 125 (2003) pp. 1805-1809.

14. R.D. Richins, A. Mulchandani, and W. Chen, Expression, Immobilization, and Enzymatic Characterization of Cellulose-Binding Domain-Organophosphorus Hydrolase Fusion Enzymes, Biotechnology and Bioengineering 69 (2000) pp. 591-596.

15. J. Wang, R. Krause, K. Block, M. Musameh, A. Mulchandani, and M.J. Schöning, Flow Injection Amperometric Detection of Op Nerve Agents Based on an Organophosphorus-Hydrolase Biosensor Detector, Biosensors and Bioelectronics 18 (2003) pp. 255-260.

16. A.W. Flounders, A.K. Singh, J.V. Volponi, S.C. Carichner, K. Wally, A.S. Simonian, J.R. Wild, and J.S. Schoeniger, Development of Sensors for Direct Detection of Organophosphates.: Part Ii: Sol-Gel Modified Field Effect Transistor with Immobilized Organophosphate Hydrolase, Biosensors and Bioelectronics 14 (1999) pp. 715-722.

17. F.M. Andreopoulos, M.J. Roberts, M.D. Bentley, J.M. Harris, E.J. Beckman, and A.J. Russell, Photoimmobilization of Organophosphorus Hydrolase within a Peg-Based Hydrogel, Biotechnology and Bioengineering 65 (1999) pp. 579-588.

18. B.J. White and H.J. Harmon, Optical Solid-State Detection of Organophosphates Using Organophosphorus Hydrolase, Biosensors and Bioelectronics, Selected Papers from the Eighth World Congress on Biosensors, Part II 20 (2005) pp. 1977-1983.

19. A.J. Russell, J.A. Berberich, G.E. Drevon, and R.R. Koepsel, Biomaterials for Mediation of Chemical and Biological Warfare Agents, Annual Review of Biomedical Engineering 5 (2003) pp. 1-27.

20. F. Fraternali and L. Cavallo, Parameter Optimized Surfaces (Pops): Analysis of Key Interactions and Conformational Changes in the Ribosome, Nucleic Acids Research 30 (2002) pp. 2950-2960.

21. E.J. Hebert, A. Giletto, J. Sevcik, L. Urbanikova, K.S. Wilson, Z. Dauter, and C.N. Pace, Contribution of a Conserved Asparagine to the Conformational Stability of Ribonucleases Sa, Ba, and T1, Biochemistry 37 (1998) pp. 16192-16200.

22. J.K. Grimsley, J.M. Scholtz, C.N. Pace, and J.R. Wild, Organophosphorus Hydrolase Is a Remarkably Stable Enzyme That Unfolds through a Homodimeric Intermediate, Biochemistry 36 (1997) pp. 14366-14374.

23. B. Di Sioudi, J.K. Grimsley, K. Lai, and J.R. Wild, Modification of near Active Site Residues in Organophosphorus Hydrolase Reduces Metal Stoichiometry and Alters Substrate Specificity, Biochemistry 38 (1999) pp. 2866-2872.

24. L.S. Jung, C.T. Campbell, T.M. Chinowsky, M.N. Mar, and S.S. Yee, Quantitative Interpretation of the Response of Surface Plasmon Resonance Sensors to Adsorbed Films, Langmuir 14 (1998) pp. 5636-5648.

25. A.N. Naimushin, S.D. Soelberg, D.K. Nguyen, L. Dunlap, D. Bartholomew, J. Elkind, J. Melendez, and C.E. Furlong, Detection of Staphylococcus Aureus Enterotoxin B at Femtomolar Levels with a Miniature Integrated Two-Channel Surface Plasmon Resonance (Spr) Sensor, Biosensors and Bioelectronics 17 (2002) pp. 573-584.

8. COVALENT IMMOBILIZATION OF ORGANOPHOSPHORUS HYDROLASE ON CARBON NANOTUBES FOR ELECTROCHEMICAL BIOSENSOR APPLICATIONS

8.1 INTRODUCTION

Recent advances in the area of nanotechnology have provided a new platform for the development of novel biosensors using carbon nanotubes. Carbon nanotubes (CNTs) are thin cylinders of carbon tubes which were discovered in 1991 by S. Iijima. Since then they have been a subject of enormous interest. Based on their structural properties there are two types of carbon nanotubes: single-walled nanotubes (SWNTs) and multi-walled nanotubes (MWNTs). SWNTs consist of a single graphene sheet rolled into a seamless tube of typically 1-2 nm diameter and several microns in length. MWNTs consist of several graphite sheets rolled into concentric tubes, typically 2-50 nm diameter and with tube length extending up to several microns. Depending on the manner the graphene sheet is rolled up, the nanotubes are classified as either having a zigzag, armchair or a chiral structure.

CNTs have been synthesized using various techniques, the most common being arc discharge, laser ablation and chemical vapor deposition. An important aspect of large scale synthesis of CNTs is its purification. They contain amorphous carbon, metal residues and smaller fullerenes as impurities which interfere with the properties of CNTs. Several methods like acid treatment, oxidation, ultrasonication, ferromagnetic separation,

annealing and chromatographic separation have been used to remove the impurities without altering the structure of the nanotubes. These nanotubes display remarkable mechanical, chemical and electrical properties. Based on their helicity, these nanotubes can either be conducting, semi-conducting or insulating. CNTs offer several advantages for sensing applications: higher surface area [1] for immobilization and higher sensitivity. They have been used because of its strong electrocatalytic activity and the ability of reducing surface fouling effects on sensor surfaces [2, 3].

Both single-walled carbon nanotubes (SWNTs) and multi-walled carbon nanotubes (MWNTs) display unique properties and have been recognized as attractive building blocks for numerous technological innovations in the fields of molecular and opto electronics [4-6], field-emission devices [7], components in high-performance composites [8-10], sensors [11-13] and energy storage [14]. The application of carbon nanotubes (CNTs) greatly depend on the critical control of their chemistry. Partial oxidation, side-wall functionalization, filling of inter-tubular spacing with "guest" species, physical and chemical functionalization are some of the routes commonly employed to modify the chemical nature of CNTs. Dai and coworkers [15] first demonstrated that adsorption of gas molecules on SWNT induces a large change in their conduction. This has led to the construction of myriad of sensors using CNTs for NH_3, CO, CO_2, H_2O and C_2H_5OH detection. By specific functionalization of CNTs with metal nanoparticles and conjugated polymers, rational chemical sensing was achieved due to molecular selectivity.

CNT functionalization (both covalent and non-covalent) with biological molecules has not only overcome the lack of CNT solubility in aqueous solutions but also

enabled sensing of physiologically important biological material (DNA, proteins and carbohydrates). Favorable molecular interactions between these macromolecules and CNTs were subsequently utilized for successful separation of SWNTs based on chirality which is critical for exploitation of SWNTs unique properties. For biosensors, recent reports in literature have shown two different methods for the immobilization of biological species to nanotubes: covalent and non-covalent immobilization. A common technique to incorporate biomolecules is through covalent functionalization of the CNTs which enables chemical bonding between the CNTs and the material of interest. This has been achieved through different conjugation strategies with the use of proper coupling agents. Besteman *et al*. [16] have demonstrated the first biosensor based on individual SWNTs. In the paper they demonstrated that the immobilization of glucose oxidase on CNTs decreases the conductance, which can be attributed to a change in the total capacitance of the tube rather than a simple electrostatic interpretation. Lin *et al*. [17] described a glucose biosensor in which the enzyme glucose oxidase was covalently immobilized on CNTs via carbodiimide by forming amide linkages between amine residues and carboxylic acid groups on the CNTs tips. They illustrated that catalytic reduction of hydrogen peroxide liberated from the enzymatic reaction of glucose oxidase lead to the selective detection of glucose.

Here, we report electrochemical-based biosensing of organophosphates using covalently functionalized OPH on CNTs. CNTs were used both as a support for the immobilization of OPH and also for the amplification of the electrochemical signal of p-nitrophenol. Two different approaches for OPH immobilization are described. The first approach involves formation of a peptide bond via EDC/NHS by direct coupling of lysine

residues present on the surface of OPH with carboxylic groups, generated by acid oxidation of CNTs. .The second approach involves crosslinking OPH with the amine groups generated on CNTs through APTES via gluteraldehyde chemistry. Recently organophosphate detection using OPH modified-multi walled carbon nanotubes (MWNTs) was reported wherein, the enzyme was physically adsorbed on the nanotubes surface [18]. However, it a well-known fact that non-covalent adsorption of proteins may be susceptible to enzyme leaching, which could further lead to a drastic reduction in the sensor efficiency. In addition, we report the characterization and the catalytic study of the enzyme-immobilized nanotubes. Successful functionalization of CNTs was confirmed by scanning electron microscopy (SEM), transmission electron microscopy (TEM), Fourier transform infrared spectrometry (FT-IR) and Raman spectroscopy. Our results provide a general and direct pathway for fabrication of biosensor using nanoscale components with excellent stability and sensitivity.

8.2 EXPERIMENTAL

8.2.1 Materials

MWNTs (purity 95%, length 1-5 μm, diameter 30±10 nm) synthesized by CVD were purchased from Nanolabs and SWNTs were obtained from Rice University (purity >99.5%). Organophosphorus Hydrolase (OPH) was generously provided by J. Wild (Texas A&M University) and Nafion solution was obtained from D. Ivnitski, University of New Mexico, Albuquerque. Paraoxon was obtained from ChemService, West Chester, PA, 1-ethyl-3-(3-dimethylaminopropyl) carbodiimide (EDC) and 3-aminopropyltriethoxy silane (APTES) were from Sigma-Aldrich, *N*-hydroxysuccinimide (NHS) was obtained

from Acros-Organics. All other reagents and chemicals were of analytical grade and obtained from Sigma–Aldrich (St. Louis, MO). Water used for preparation of aqueous solutions was from a Millipore Direct-Q Water system (resistivity, 18 MΩ cm^{-2})

8.2.2 Oxidation of CNTs

A suspension of 5 mg of CNTs (MWNTs and SWNTs separately) was sonicated in a 1510 Branson Sonicator at room temperature for 9 hours in a mixture of 3:1 conc. H_2SO_4 and 70% HNO_3. The contents were allowed to cool and sufficient time was given to let the nanotubes to settle down. The supernatant was discarded and the filtrate was extensively washed with de-ionized water and filtered by centrifugation until the pH of the solution was near neutral. The filtrate was then freeze dried and a dark solid product was obtained. These oxidized CNTs were used for the immobilization of OPH.

8.2.3 Protein immobilization on CNTs by EDC-NHS chemistry

2 mg of freshly oxidized MWNTs and SWNTs were suspended in 5 mL of deionized water by sonicating the mixture for 1.5 h at room temperature. Then, 1 mL of 500 mM MES buffer solution, pH 6.1 and 2.3 ml of a 50 mg/mL aqueous solution of NHS were added to the above suspension. Under fast stirring, 1.2 mL of freshly prepared aqueous solution of EDC (10 mg/mL) was added immediately, and the mixture was stirred continually at room temperature for 0.5 h. The suspension was filtered through a 0.05μm hydrophilic polycarbonate membrane and then rinsed thoroughly with the buffer solution to remove excess EDC, NHS and the by-product urea.

The activated CNTs were then re-dispersed in 9 mL of buffer solution, and 1 mL of a 0.2 mg/mL OPH in 50 mM phosphate buffer solution, pH 7.4. After incubating the mixture on a platform shaker at 4°C for 9.5 h, the nanotube suspension was centrifuged at 13200 rpm and rinsed with buffer several times to remove any unbound protein. The enzyme–nanotube conjugate was finally suspended in 20mM CHES buffer solution, pH 9.0. A part of the sample was freeze dried for characterization studies.

8.2.4 Protein immobilization on CNTs by APTES-GA chemistry

2 mg of oxidized MWNT were suspended in 10% APTES by heating the solution to 60°C for 6 h followed by stirring at room temperature for 3 h. APTES modified MWNTs were recovered by centrifugation and rinsed thoroughly with water. In the next step, 5mL of 10% aqueous solution of gluteraldehyde was added to the above MWNT-APTES suspension and the solution was sonicated for 0.5 h followed by stirring at room temperature for 2 h. The suspended nanotubes were rinsed extensively with copious amount of water. 0.2 mg/mL of OPH was added to the nanotubes suspension and the solution was gently stirred in a platform shaker overnight at 4°C. Loosely bound OPH was removed by centrifugation followed by rinsing with CHES. The conjugate was finally suspended in CHES buffer solution.

8.2.5 Characterization of protein immobilized CNT's

8.2.5.1 FT-IR

The spectra of all samples were obtained using potassium bromide (KBr) pellets in the range 500 – 4000 cm^{-1} using a Shimadzu (Thermo-Electron Corp., Waltham, MA) FT-IR spectrophotometer at room temperature.

8.2.5.2 TEM

Samples were prepared by placing a drop of CNTs suspension solution on 200 mesh formvar-coated nickel grids and air dried overnight before analysis. Images were recorded by a Zeiss EM 10 transmission electron microscope operating at 60kV.

8.2.5.3 SEM

Samples were prepared by dropping a small amount of CNT solution on a mica substrate and allowed to air dry overnight. The samples were then coated with a thin layer of gold (~10 nm) and imaged using a JEOL JSM 7000F field emission scanning electron microscope equipped with an energy dispersive X-ray analyzer (JEOL USA).

8.2.5.4 Raman Spectroscopy

Raman scattering studies were carried out with Renishaw-inVia Reflex (50x objective) with two excitation wavelengths at 514 nm (Argon Ion laser) and 785nm (Diode laser). Samples for the analysis were prepared by spreading freeze dried powder of CNT products on a double sided tape which was mounted on a glass slide. In order to

firmly attach the nanotubes in the form of a film, a clean glass cover-slip was pressed over it for 30 seconds.

8.2.5.5 Measurement of the catalytic activity of immobilized enzyme

Catalytic activity of the immobilized OPH on CNTs was determined spectrophotometrically by monitoring p-nitrophenol formation due to enzyme hydrolysis of substrate paraoxon. The kinetic constants were determined by performing enzymatic assays with varying concentrations of substrate and constant enzyme concentrations. The kinetic assay was carried out at room temperature using 20 mM CHES (pH 9.0) buffer solution. The hydrolysis product, p-nitrophenol (ε = 17,000 M^{-1} cm^{-1}) was monitored calorimetrically at 405 nm using Ultrospec 2100 Pro UV-Vis Spectrophotometer, Amersham Biosciences. The initial velocities were calculated and fit to the Michaelis-Menten equation.

8.2.5.6 Preparation of Electrode surface

The glassy carbon electrode (BAS, Ø = 1.6mm) was polished with 0.10 and 0.05 µm alumina slurry respectively and then ultrasonically cleaned in water for 15 min. 20 µL of the CNT suspension was cast on the cleaned electrode surface. After the solvent water was evaporated, 0.5% of Nafion solution was cast onto the modified electrode surface. The modified electrode was then dried to evaporate solvent and stored at refrigerated conditions until use. Amperometric measurements were performed using a BAS CV-50W (Bioanalytical Systems, USA). All experiments were conducted in a three electrode system containing a platinum wire auxiliary electrode, a CNT-modified glassy

carbon working electrode and a saturated Ag/AgCl reference electrode. The buffer solution was 10mM PBS which was deoxygenated with highly pure nitrogen for 5 minutes before any electrochemical measurements. All the electrochemical measurements were performed at room temperature.

8.3 RESULTS AND DISCUSSION

8.3.1 Characterization of protein immobilized CNT's

Figure 8-1 describes the step-by-step procedure used to covalently anchor OPH to CNTs. Each modification step is characterized using FT-IR to probe the vibrational changes during adsorption of proteins. Figure 8-2 shows the FT-IR spectrum of the oxidized MWNTs, SWNTs and OPH-modified CNTs. It is well-known that oxidation of CNTs by H_2SO_4 and HNO_3 results in the formation of hydrophilic groups, -COOH, -C=O and -OH. The spectra for the purified CNTs showed a peak at 1708 and 2933 cm^{-1}, which indicates the presence of the carboxylic groups and symmetric stretching of $-CH_2$ groups and increase of 3434 cm^{-1} peak clearly confirms introduction of more –OH groups after acid reflux. Following covalent immobilization of OPH, a strong band at 1210 cm^{-1} arises which is primarily due to in-plane N-H bend of secondary amide. Also, a characteristic carbonyl stretch of amide I band is observed at 1631 cm^{-1} arising from the backbone peptide bonds in enzymes. The bands at 1460 and 1390 cm^{-1} are assigned to the CH_2 deformation and to vibrations of the amino acid side chains, respectively. The OPH immobilized on the both cases was further evident from the disappearance of the carboxyl peak at 1708 cm^{-1} because of the formation of the peptide bond.

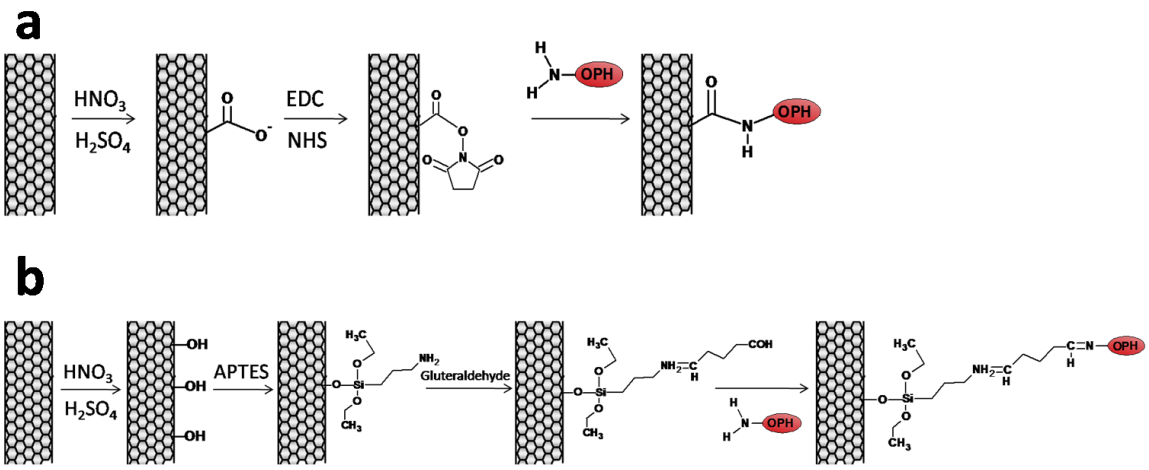

Figure 8-1: Covalent Immobilization of OPH on CNTs using A) EDC/NHS and B) APTES/GA

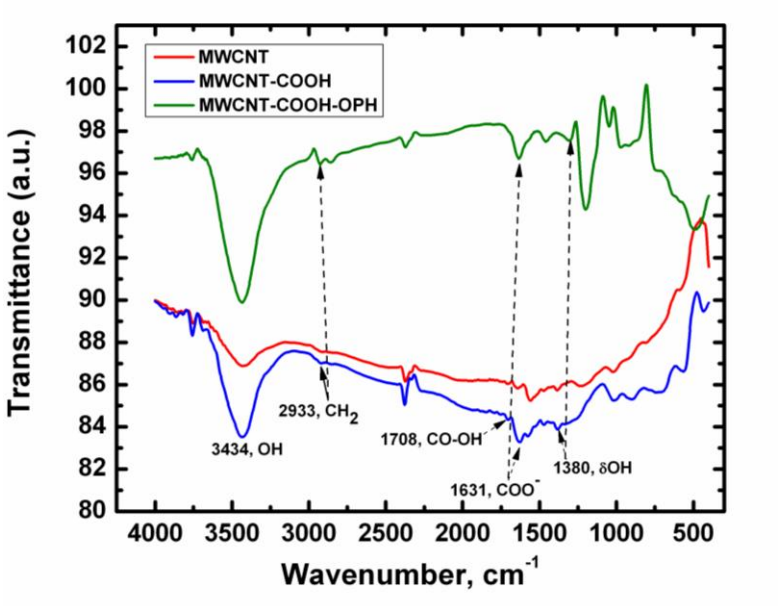

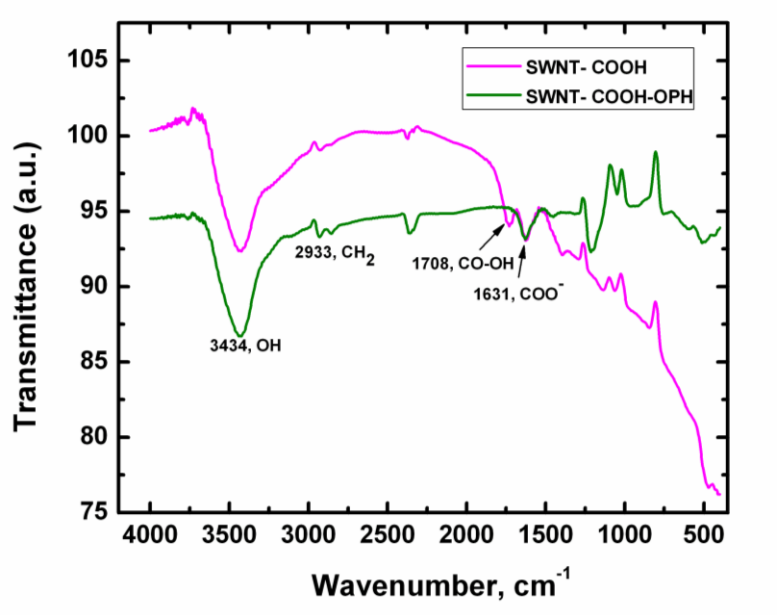

Figure 8-2: FT-IR spectra of the pristine, oxidized and OPH-functionalized MWNTs and SWNTs

8.3.1.1 TEM and SEM

Figure 8-3 shows the transmission electron microscopy characterization of oxidized and OPH-functionalized nanotubes. It is seen in Figure 8-3A that MWNT end tips which are evidently darker in comparison to the main body of the tubes. This clear appearance of the tips confirms the reduction in the length of MWNTs during acid-based oxidation process. Similar observations are noticed in case of oxidized SWNTs (Figure 8-3C) in which the short tubes are even more prominent. Figure 8-3B and 8-3D shows images of OPH functionalized MWNTs and SWNTs respectively. In case of OPH-MWNTs, an amorphous deposition on the sides and ends of MWNTs is clearly present. This is due to successful functionalization of OPH on the defect sites of MWNTs. However in case of OPH-SWNTs a network of SWNTs coated with a thin amorphous phase was observed. This may be due to strong interaction of the enzyme with overall

SWNTs surface. It is important to note that solubility of OPH-SWNTs in aqueous phase was found to be less than MWNTs. We believe that OPH interacted strongly with SWNTs where SWNTs formed a network with enzyme, which led to precipitation from the dispersion. It is also likely that SWNTs might have worked as a cross linker for proteins which possibly helped to form such kind of networks. This was further supported by our TEM measurement; it must be mentioned that imaging of OPH-SWNTs at the same resolution as that of OPH-MWNTs was very difficult. The thick protein coating hindered transmission of electrons from the SWNTs surface making it difficult to image at higher resolutions. Similar results were obtained from SEM (Figure 8-4A) provided evidence of a thick enzyme coating or crystallization of OPH on the surface of SWNTs which was entirely absent on oxidized SWNTs. However, in case of MWNTs thick deposition of OPH at different spots on the nanotubes are noticed (Figure 8-4B), which corroborates with the results obtained from TEM.

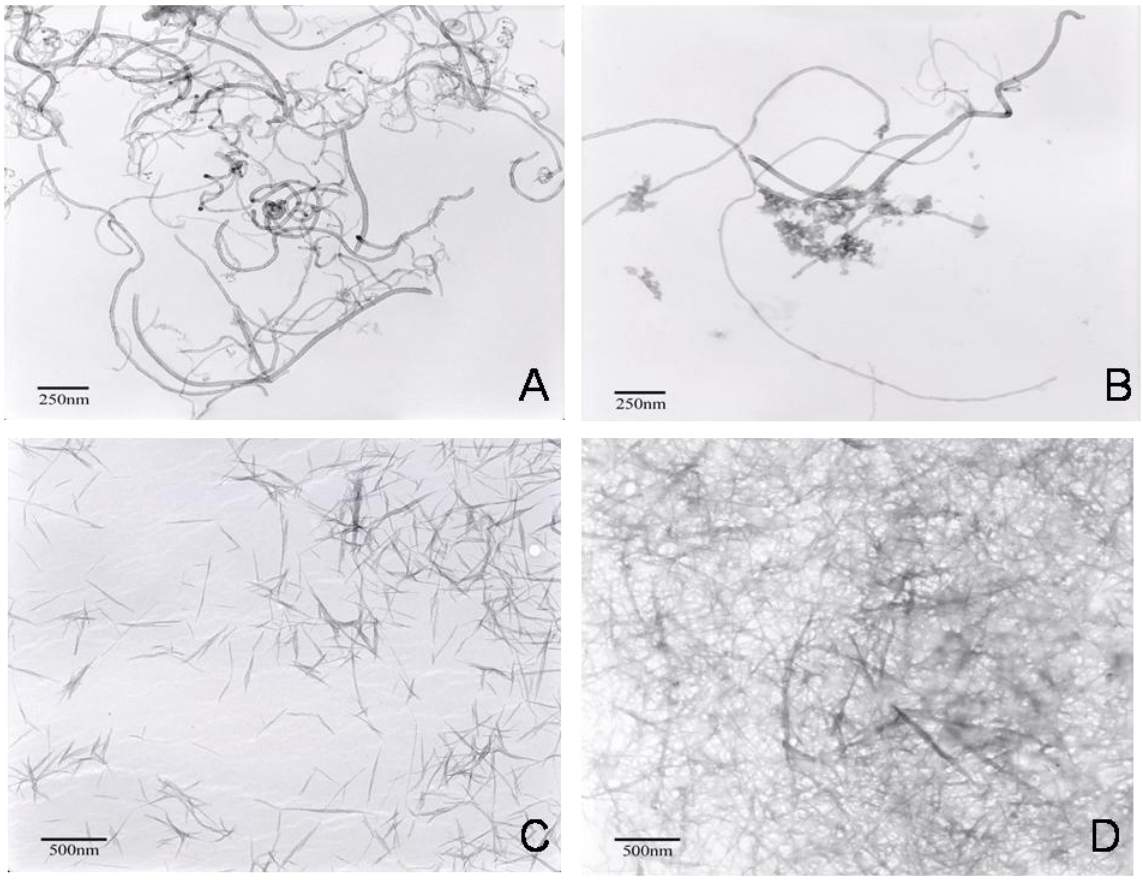

Figure 8-3: TEM images of A) oxidized MWNT; B) OPH-functionalized MWNT; C) oxidized SWNT; and D) OPH-functionalized SWNT

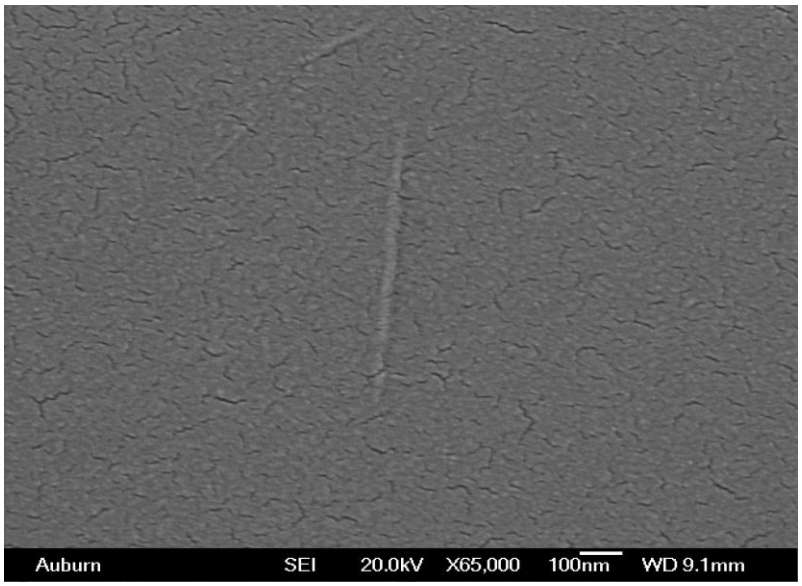

Figure 8-4 A: SEM images of oxidized and OPH-modified SWNT

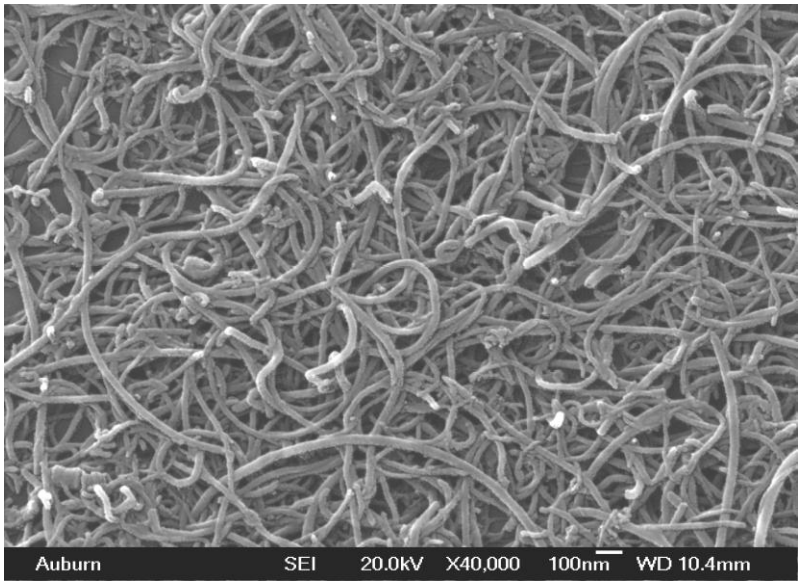

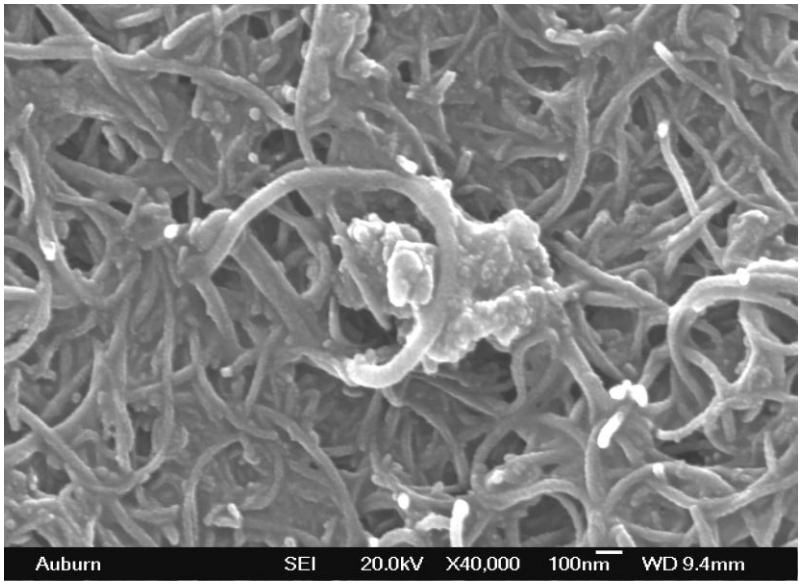

Figure 8-4 B: SEM images of oxidized and OPH-modified MWNT

8.3.1.2 Raman Spectroscopy

In order to testify the formation of covalent bond between the nanotubes and OPH, the Raman spectra of SWNTs with and without OPH were obtained. The characteristic peaks of the Raman spectra for these samples are the D and G bands which refer to the disorder mode ~1300 cm^{-1} and the tangential mode ~1600 cm^{-1}. It is clearly seen in Figure 8-5 that D/G ratio of OPH-SWNTs slightly increased compared to that of oxidized SWNT. This is due to covalent attachment of the OPH on the surface of SWNTs. It is also very likely that due to different active functional group on the surface of OPH may irreversibly bind on SWNTs surface which assisted further for successful functionalization.

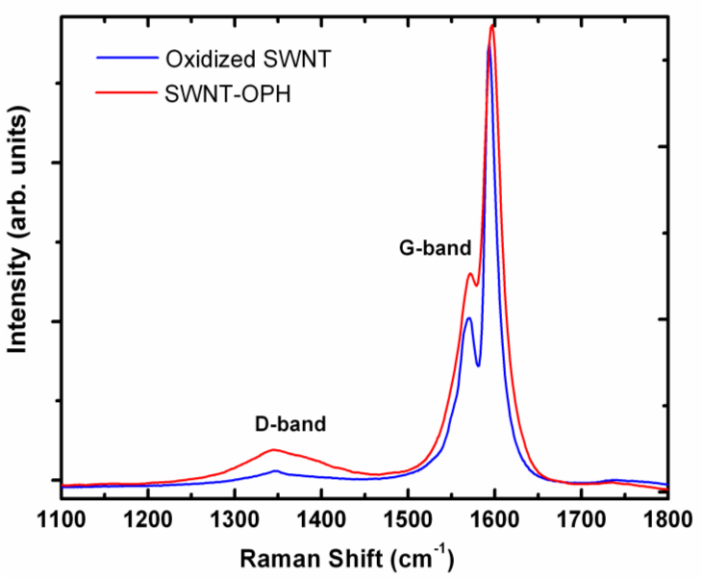

Figure 8-5: Raman spectrum of oxidized SWNT and SWNT-OPH showing D-band and G-band using 514 laser

8.3.1.3 Measurement of the catalytic activity of immobilized enzyme

The catalytic activities of OPH conjugated to surface of CNTs were measured spectrometrically. Figure 8-6 shows the immobilized OPH activity which is measured by monitoring the absorbance of *p*-nitrophenol formation at 405nm. SWNTs modified with OPH displayed the highest activity, which we suspect is due to higher OPH loading on the nanotubes. The higher enzyme loading might be attributed to the presence of increased number of carboxylic groups generated on SWNT due to acid treatment. Within MWNT, OPH conjugation through EDC/NHS chemistry demonstrated better activity compared to immobilization through APTES-GA. Table 8-1 summarizes the kinetic constants calculated for the enzyme-modified CNTs.

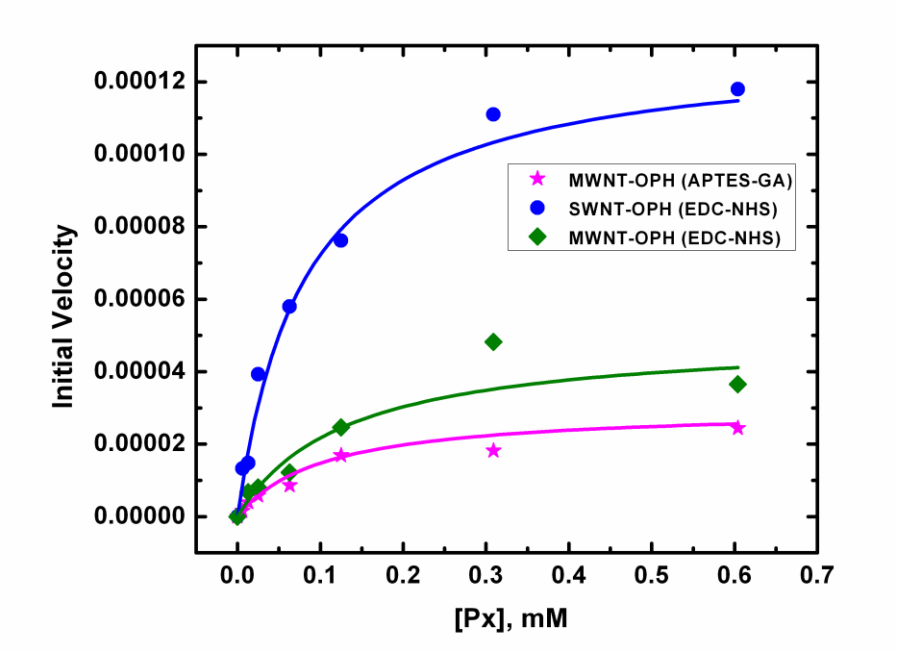

Figure 8-6: Activity of OPH immobilized on SWNT and MWNT

	SWNT (EDC-NHS)	MWNT (EDC-NHS)	MWNT (APTES-GA)	OPH in solution
V_{max}, µmoles/sec	0.00013	0.00005	0.00003	0.00111
k_m, mM	0.07993	0.13019	0.10348	0.05996

Table 8-1: Kinetic constants for catalytic activity of OPH

8.3.2 Flow Injection Amperometric Detection of Paraoxon with SWNTs-OPH and MWNTs-OPH Biosensor

Figure 8-7A shows the typical current versus time plot for detection of paraoxon using both biosensors at 0.5 and 4.5 µM. We found that the SWNT biosensor appears to be the most useful since it offers the highest sensitivity resulting from a high current and a high signal/noise ratio. Similar results were found by Mita *et al.* [19] in the study of different CNT tyrosinase-modified electrodes to determine bisphenol. The most efficient

biosensors were those constructed by using the following technique for the carbon paste modified with SWNTs. Figure 8-7B shows flow-injection calibration data for paraoxon over the concentration ranges 0.5-8.5 μM, and insert show that current increases proportionally to the concentration to yield highly linear calibration plots obtained for SWNTs-OPH. Detection limits of 2.3 μmol L^{-1} paraoxon can be estimated on the basis of the signal-to-noise characteristics of these data (S/N = 3).The stability of the system was examined over a 30-day period (using the same surfaces, with intermittent storage at 4 °C). As expected, the paraoxon sensors exhibited a negligible decrease (of about 8%) of its sensitivity to 0.5 and 4.5 μM paraoxon during that period. Good reproducibility by the enzyme electrode means that the biosensor can be used in on-line determination of paraoxon. The increase of the signal obtained with SWNTs is combined with excellent sensitivity. These results combine with the activity of immobilized enzymes (Figure 8-7) give a good indication that SWNTs have more OPH binding potential at higher current.

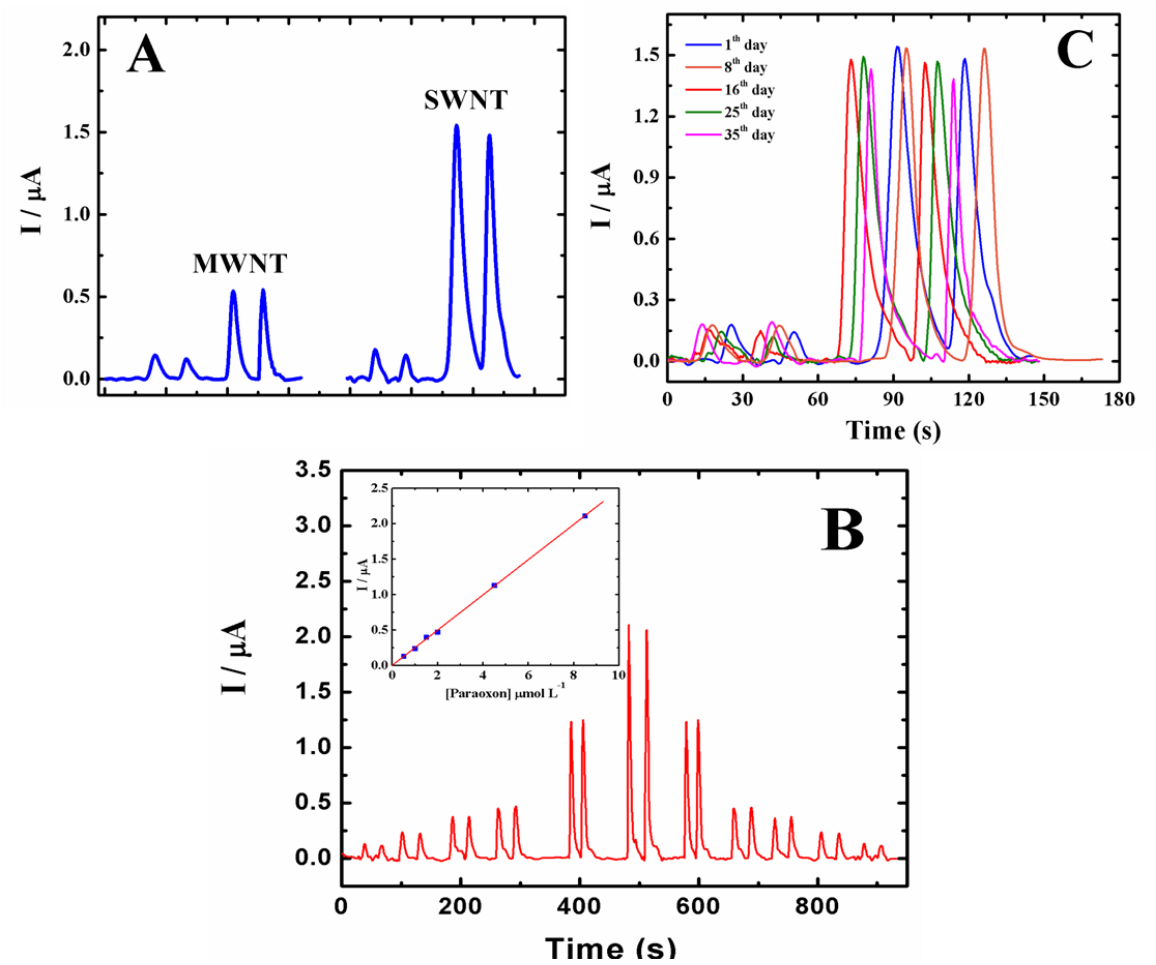

Figure 8-7 A) Comparison between OPH immobilized on MWNT and SWNT for paraoxon detection; B) Flow-injection (FI) on OPH-SWNT electrode with sequential injection of Paraoxon from 0.5µM to 8.5µM (inset: Calibration plot from FI-analysis showing a linear response for paraoxon detection); C) The operational stability of OPH-SWNT modified electrode over 35 day period

8.4 CONCLUSION

In this work, we have presented a simple and economical amperometric biosensor based on carbon nanotubes modified with covalently attached OPH for organophosphate detection. The characterization techniques confirmed the successful immobilization of

OPH on the CNT surface. Covalent functionalization seemed to be a better choice for enzyme immobilization to achieve improved sensor characteristics. Our studies with OPH have shown that a significant degree of enzymatic activity is retained after immobilization. The OPH-CNT solutions showed stable behavior in buffer solutions. The sensor exhibited, high sensitivity and good reproducibility, and was able to efficiently preserve the enzyme activity and did not show any evidence of enzyme leaking over time.

8.5 REFERENCES

1. X.Z. Wang, M.G. Li, Y.W. Chen, R.M. Cheng, S.M. Huang, L.K. Pan, and Z. Sun, Electrosorption of Nacl Solutions with Carbon Nanotubes and Nanofibers Composite Film Electrodes, Electrochemical and Solid State Letters 9 (2006) pp. E23-E26.
2. J. Wang, Carbon-Nanotube Based Electrochemical Biosensors: A Review, Electroanalysis 17 (2005) pp. 7-14.
3. X. Yao, H.X. Wu, J. Wang, S. Qu, and G. Chen, Carbon Nanotube/Poly(Methyl Methacrylate) (Cnt/Pmma) Composite Electrode Fabricated by in Situ Polymerization for Microchip Capillary Electrophoresis, Chemistry-a European Journal 13 (2007) pp. 846-853.
4. P. Avouris, Carbon Nanotube Electronics, Chemical Physics 281 (2002) pp. 429-445.
5. P. Avouris, Carbon Nanotube Electronics and Optoelectronics, Mrs Bulletin 29 (2004) pp. 403-410.

6. P.L. McEuen, M.S. Fuhrer, and H.K. Park, Single-Walled Carbon Nanotube Electronics, Ieee Transactions on Nanotechnology 1 (2002) pp. 78-85.

7. J.-M. Bonard, H. Kind, T. Stöckli, and L.-O. Nilsson, Field Emission from Carbon Nanotubes: The First Five Years, Solid-State Electronics 45 (2001) pp. 893-914.

8. R.H. Baughman, A.A. Zakhidov, and W.A. de Heer, Carbon Nanotubes - the Route toward Applications, Science 297 (2002) pp. 787-792.

9. M. Endo, M.S. Strano, and P.M. Ajayan, *Potential Applications of Carbon Nanotubes*, in *Carbon Nanotubes*. 2008. p. 13-61.

10. L.T. Qu, Q. Peng, L.M. Dai, G.M. Spinks, G.G. Wallace, and R.H. Baughman, Carbon Nanotube Electroactive Polymer Materials: Opportunities and Challenges, Mrs Bulletin 33 (2008) pp. 215-224.

11. J.J. Gooding, Biosensor Technology for Detecting Biological Warfare Agents: Recent Progress and Future Trends, Analytica Chimica Acta 559 (2006) pp. 137-151.

12. K.A. Williams, P.T.M. Veenhuizen, B.G. de la Torre, R. Eritja, and C. Dekker, Nanotechnology - Carbon Nanotubes with DNA Recognition, Nature 420 (2002) pp. 761-761.

13. W.R. Yang, P. Thordarson, J.J. Gooding, S.P. Ringer, and F. Braet, Carbon Nanotubes for Biological and Biomedical Applications, Nanotechnology 18 (2007)

14. C. Liu and H.M. Cheng, Carbon Nanotubes for Clean Energy Applications, Journal of Physics D-Applied Physics 38 (2005) pp. R231-R252.

15. J. Kong, N.R. Franklin, C.W. Zhou, M.G. Chapline, S. Peng, K.J. Cho, and H.J. Dai, Nanotube Molecular Wires as Chemical Sensors, Science 287 (2000) pp. 622-625.

16. K. Besteman, J.O. Lee, F.G.M. Wiertz, H.A. Heering, and C. Dekker, Enzyme-Coated Carbon Nanotubes as Single-Molecule Biosensors, Nano Letters 3 (2003) pp. 727-730.

17. Y.H. Lin, F. Lu, Y. Tu, and Z.F. Ren, Glucose Biosensors Based on Carbon Nanotube Nanoelectrode Ensembles, Nano Letters 4 (2004) pp. 191-195.

18. R.P. Deo, J. Wang, I. Block, A. Mulchandani, K.A. Joshi, M. Trojanowicz, F. Scholz, W. Chen, and Y. Lin, Determination of Organophosphate Pesticides at a Carbon Nanotube/Organophosphorus Hydrolase Electrochemical Biosensor, Analytica Chimica Acta 530 (2005) pp. 185-189.

19. D.G. Mita, A. Attanasio, F. Arduini, N. Diano, V. Grano, U. Bencivenga, S. Rossi, A. Amine, and D. Moscone, Enzymatic Determination of Bpa by Means of Tyrosinase Immobilized on Different Carbon Carriers, Biosensors and Bioelectronics 23 (2007) pp. 60-65.

9. FINAL CONCLUSIONS

The studies presented in this dissertation have demonstrated the successful development of rapid and specific detection platforms for detection of neurotoxic organophosphates. Also, various strategies for the optimization of factors affecting immobilized enzyme activity and stability have been described.

In the past few years, considerable interest has been shown towards environmental contamination with organophosphate (OP) insecticides. Terrorist attacks using these toxic nerve agents has demanded the development of accurate, specific and sensitive detections systems for field detection and discrimination of these neurotoxic agents. The analysis of OP neurotoxins typically requires sophisticated equipment, extensive sample preparation that is labor-intensive and prolonged processing time to validate the results. Therefore, with the described studies in this dissertation, we have attempted to develop simple, sensitive and rapid, optical and electrochemical biosensor assays for the direct detection of organophosphates. The biorecognition element for all the studies is an enzyme, organophosphate hydrolase (OPH). Different strategies were used for anchoring the enzyme to the sensor surfaces on various detection platforms. In addition, some of the systems described herein can be used to provide continual remote monitoring and spectral fluorescent notification.

A fluorescence-based approach for the direct detection of OPs was described. OPH was immobilized using a very simple procedure and any non-specific adsorption

was prevented using BSA. The rational design of the sensor system allowed qualitative detection of paraoxon at a limit of 0.05 µM. Although slight modifications to the excitation source of the fluorimeter could lead to better sensor sensitivity, this detection platform can be potentially used for remote monitoring. A very simple method for the detection of *p*-nitrophenol, an active ingredient found as an environmental contaminant in fresh water, was developed. The detection was based on the fluorescence changes of coumarin1, which is structurally very similar to some of the OPs. The fluorescence quenching in the presence of OPH was suspected to be due to fluorescence resonance energy transfer (FRET). The lowest concentration of paraoxon detected was 0.7µM. While the detection of paraoxon and parathion was demonstrated, this method could be applicable to any *p*-nitrophenyl substituent OPs.

An important aspect for any biosensor system is the biorecognition element, which in this research was an enzyme, OPH. Upon immobilization, the enzyme may be susceptible to leaking; therefore it is vital to provide sufficient stability during the immobilization process. To achieve this purpose, OPH was encapsulated *in situ* using silica nanoparticles. The silica layer not only provided protection to the enzyme but also helped retain immobilized enzyme activity over a period of several hours. The immobilization technique described was very simple as OPH was directly tethered on the transducer surface with no requirement for surface modification before immobilization. Also, to increase the sensitivity of detection, OPH was immobilized through site-specific antibodies. Maximal activity of OPH was obtained through oriented immobilization. In addition, to increase the efficiency of the immobilized enzyme, a method to further refine surface construction by the orientation specific attachment of OPH was developed. This

attachment facilitated the free movement of substrates and products to and from the active site. SPR was used to determine the higher catalytic efficiency of the modified enzyme when attached to the gold surface.

Finally, the covalent immobilization of OPH on carbon nanotubes has enabled simple, sensitive and rapid detection of organophosphates. Physical adsorption of enzymes on surfaces can lead to leaching of enzymes under continuous flow conditions, which could further decrease the sensitivity of detection. Therefore, covalent functionalization seemed to be a better choice for enzyme immobilization. The sensor thus created exhibited good stability and reproducibility, while efficiently preserving the enzyme activity. The unique properties of CNTs have enabled the design of this electrochemical biosensor with improved analytical performance with respect to conventional biosensor systems.

10.FUTURE WORK

As we move into the next millennium there is an increasing need for miniature and portable detection systems which are capable of deployment for field applications. Multi-analyte sensing using an array of enzymes specific towards different classes of neurotoxins will be vital for next generation sensors. The sensor systems described in this study with a few modifications would enable development of highly sensitive systems. The Analyte 2000 is a small and portable instrument designed for fluorescence detection of biomolecules. Slight alteration in the excitation light source to match the reporting fluorophore and minor modifications to the surface chemistry would enable achievement of lower detection limits.

To prevent reduction of enzyme activity and to protect the enzyme from harsh environmental conditions, OPH was encapsulated in silica nanoparticles, formed by the silicification reaction using lysozyme as described in Chapter 5. But due to non-covalent adsorption of the lysozyme, loss of enzymatic activity was observed in the first few hours. This was a direct result of the loss of silica from surface (Figure 10-1).

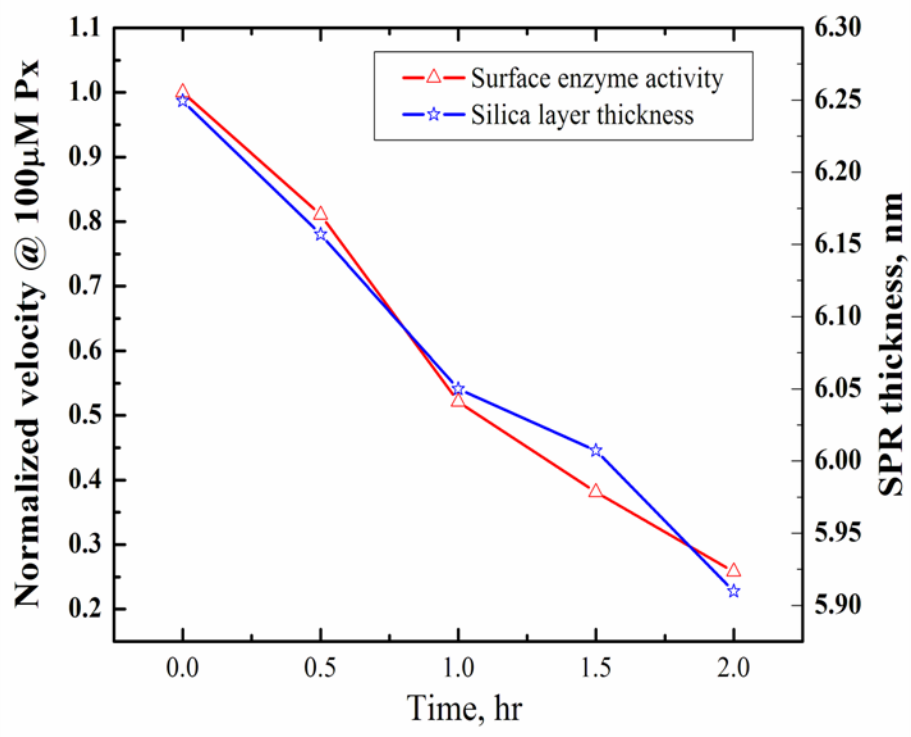

Figure 10-1: Stability of encapsulated OPH

In order to optimize the deposition of silica on the gold surface, to minimize any loss under continuous flow conditions and to retain enzymatic activity for longer periods of time, lysozyme needs to be covalently attached to the surface. One way to achieve this could be by chemical modification of the sensor surface with carboxyl-terminated self-assembled monolayers (SAMs) (Figure 10-2).

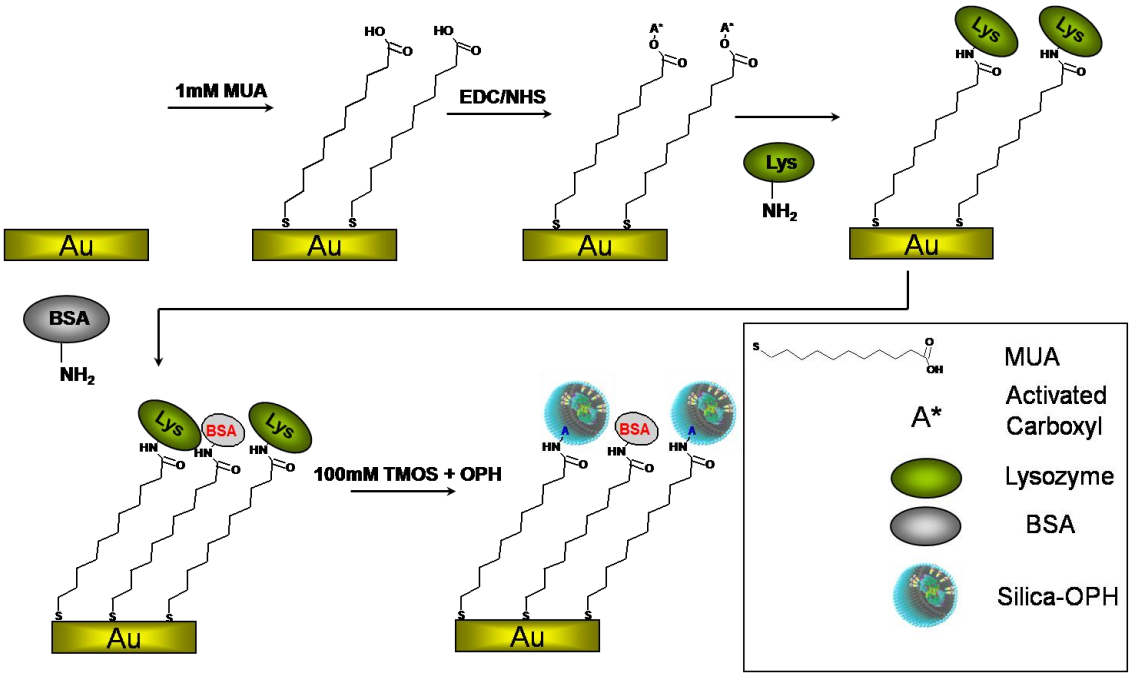

Figure 10-2: Chemical functionalization of silica-encapsulated OPH on gold surface

The benefit of using SAMs is that surfaces created from such thiols are stable for period of days to weeks. Also, synthesis of different variants of OPH with specificities towards different organophosphates will allow for better sensor characteristics. Production of stable and specific antipeptide antibodies towards different regions of OPH would help accomplish site-oriented binding of OPH. This would in turn facilitate free movement of substrates and products to and from the active site as well achievement of maximal OPH activity.